SURFCOAT KOREA 2019

SURFCOAT KOREA 2019

GRAPHENE KOREA 2019

Book of Abstracts

March 27th – 29th, 2019
Songdo Convensia, Incheon, Korea

Organizers

SETCOR Conferences & Exhibitions

MESSE ESANG

SurfCoat Korea 2019 Conference Program

27 - 29 March 2019 | Seoul, Republic of Korea

March 27, 2019		
09:00-10:00	**Registration + Welcoming coffee**	
SurfCoat Korea 2019 / Graphene Korea 2019 Joint Session I		
Conference Room 116/117		
Session Chairs: **Prof. Sang Ouk Kim, KAIST, Rep. of Korea** **Prof. Agnes Granier, CNRS-University of Nantes, France** **Prof. Holger Kersten, Kiel University, Germany**		
10:00-10:30	The GRAPHENE SHIFT is already ongoing **J. Hoon Lee**	**Mr. Joung Hoon Lee**, Standard Graphene Inc., **Rep. of Korea**
10:30-11:00	Graphene and Carbon Nanotube (CNT) Commercialization: Past, Present and Future **R. Collins** and K. Ghaffarzadeh	**Dr. Richard Collins**, IDTechEx- Cambridge, **UK**
11:00-11:30	Industrial deposition methods and applications of carbon based coatings **J. Vetter**, J. Karner , M. Kirk , F. Meunier , S. Krassnitzer , H. Eberle , M. Grischke, W. Kalss, J. Becker and A. Zedda	**Dr. Jörg Vetter,** Oerlikon Balzers Coating, **Germany**
11:30-11:45	Functionalized graphene as structural fortifier for polymers and coatings **C. Xia** and B. Zhmud	**Dr. Chao Xia**, Applied Nano Surfaces Sweden AB, **Sweden**
11:45-12:00	Chemically Induced Transformation of CVD-Grown Bilayer Graphene into Single Layer Diamond **P.V. Bakharev**, M. Huang, M. Saxena, S. W. Lee, S. H. Joo, S.O. Park, J. Dong, D. Camacho-Mojica, S. Jin, Y. Kwon, M. Biswal, F.Ding, S.K. Kwak, Z. Lee and R.S. Ruoff	**Dr. Pavel V. Bakharev**, Institute for Basic Science-Ulsan, **Rep. of Korea**
12:00-12:15	Graphene Growth on Cu Foil by Direct-Liquid-Injection Chemical Vapor Deposition with Cyclohexane Precursor in N2 Ambient **T. Intaro**, T. Taychatanapat, N. Nuntawong, S. Koh and S. Sanorpim	**Mr. Taworn Intaro**, Chulalongkorn University, **Thailand**
12:15-12:30	Scaling up single-crystal graphene by CVD of ethanol and methane **A. Capasso**, C.D. Liao, B. Sompalle, M.F. Cerqueira, J. Borme, G. Faggio, G. Messina, N. Lisi, G.H. Lee and P. Alpuim	**Dr. Andrea Capasso**, International Iberian Nanotechnology Laboratory, **Portugal**
12:00-14:00	**Lunch Break / Posters Session I - Room 118**	
SurfCoat Korea 2019 **Session I.A: Plasma Coatings deposition and processing**		
Conference Room 117		
Session Chairs: **Prof. Tiberiu Minea, CNRS- Paris-Saclay University, France** **Prof. Koji Sugioka, RIKEN Center for Advanced Photonics, Japan**		
14:00-14:30	Magnetron Sputtering: The Special Role of Localized Electron Heating and Supply of Neutrals **A. Anders**	**Prof. André Anders**, Leibniz Institute of Surface Engineering (IOM), **Germany**
14:30-15:00	Application of Plasma Monitoring and Diagnostic Techniques for the Reactive high-power Impulse Magnetron Sputtering **J-W. Lee**	**Prof. Jyh-Wei Lee**, Ming Chi University of Technology, **Taiwan**
15:00-15:30	Ionized PVD and Hybrid Processes **H. Barankova** and L. Bardos	**Prof. Hana Barankova**, Uppsala University, **Sweden**
15:30-16:00	Determination of momentum and energy fluxes in plasma surface processing **H. Kersten**, T. Trottenberg, A. Spethmann, M. Klette and L. Hansen	**Prof. Holger Kersten**, Kiel University, **Germany**

16:00-16:30	Coffee Break / Posters Session I	
Session Chairs: **Prof Jyh-Wei Lee, Ming Chi University of Technology, Taiwan** **Prof André Anders, Leibniz Institute of Surface Engineering (IOM), Germany**		
16:30-17:00	Tailored Growth Process of Ultra-Thin Films by Magnetron Plasma **T. Minea**, F. Cemin, M. Rudolph and D. Lundin	**Prof. Tiberiu Minea**, CNRS-Paris-Saclay University, **France**
17:00-17:30	Control of the deposition temperature and nanostructure of silicon and titanium oxide thin films in PECVD routes **A. Granier**, D. Li, M. Richard-Plouet, S. Bulou, P. Choquet and A. Goullet	**Prof. Agnes Granier**, CNRS-University of Nantes, **France**
17:30-18:00	Femtosecond Laser 3D Processing for Fabrication of Functional Micro- and Nano-Systems **K. Sugioka**	**Prof. Koji Sugioka**, RIKEN Center for Advanced Photonics, **Japan**
18:00-18:15	Fabrication and performance analysis of protective coating deposited on nickel alloy used in nuclear reactor **Y.Liu**, M.Zheng, X.Wang, H.Li, Y.Lu and H.Xia	**Dr. Yanhong Liu**, State Power Investment Corporation S&T Research Institute, **China**
18:15-18:30	Product Orientated Optimization of Coating Processes by Acoustic Levitation D. L. Wong, A. Reinbeck, S. C. Müller, H.-U. Moritz and W. Pauer	**Ms Doris Locsin Wong**, University of Hamburg, **Germany**
18:30-18:45	Influence of processing conditions on deposit layer formation by barrel nitriding treatment on aluminum alloy **K. Nambu**, K. Sayo and M. Okumiya	**Dr. Koichiro Nambu**, Toyota Technological Institute**, Japan**

18:30 – 21:00	Social Activity: SongDo Night Tour

March 28, 2019		
SurfCoat Korea 2019 **Session II A : Functional/ Multi-functional, composite/ hybrid, graded and multilayers coatings**		
Conference Room 117		
Session Chairs: **Prof. Hana Barankova, Uppsala University, Sweden** **Prof. Ulrich Schmid, TU Wien Institute of Sensor and Actuator Systems, Austria** **Prof. Andreas Gerdes, Karlsruhe Institute of Technology, Germany** **Prof Jyh-Wei Lee, Ming Chi University of Technology, Taiwan**		
09:30-10:00	Siloxane Based Flexible Hard Coating for Foldable Smartphone Cover Window Film **B-S. Bae**, G-M. Choi and J. Ko	**Prof. Byeong-Soo Bae**, KAIST, **Rep of Korea**
10:00-10:15	Silver nanowire/graphene-based Thin Film for Transparent Electrode and Thermal Heater Applications J. W. Shin, * **E. Jeong** and Y-H. Choa	**Ms. Jeong Eunhye**, Hanyang University, **Rep. of Korea**
10:15-10:30	Corona discharge mitigation of HV transmission lines by surface modification N. K. Tnyshtykbayev, **N. Zhakiyev**, J. Norem and Z. Insepov	**Dr. Nurkhat Zhakiyev**, Nazarbayev University, **Kazakhstan**
10:30-11:00	**Coffee Break / Posters Session II**	
SurfCoat Korea 2019 **Session II B : Surfaces and coatings characterization and properties**		
11:00-11:15	Roughness influence on self-adaptation and self-healing of DLC-MoS2 wear protective, low-friction coatings on 3D printed polymers **J.M. Lackner**, W. Waldhauser, L. Major, M. Kot and P. Angerer	**Dr. Juergen M. Lackner**, Joanneum Research Forschungsgesellschaft mbH, **Austria**
11:15-11:30	Wear Resistance of Electrodeposited Ni-P and Ni-B-TiO2 Sol-enhanced Nano-composite Coatings **S. Sheikholeslami**, W. Gao and Y. Wang	**Mr. Sina Sheikholeslami**, The University of Auckland, **New Zealand**
11:30-11:45	Synergistic Effect of Different Nanocontainers For Self-healing Corrosion Protection Coatings On AA2024-T4 **S. Manasa**, K.V. Gobi and R. Subasri	**Ms. Manasa Samavedam**, International Advanced Research Centre for Powder Metallurgy and New Materials (ARCI), **India.**
11:45-12:00	Barrier Coatings in Food Packaging Applications **M. Bendig**, H.-U. Moritz and W. Pauer	**Ms. Mareike Bendig**, University of Hamburg, **Germany**
12:00-12:15	Scanning Droplet Adhesion Microscopy **M. Vuckovac**, V. Liimatainen, V. Jokinen, V. Sariola, M.J. Hokkanen, Q. Zhou and R.H. A. Ras	**Dr. Maja Vuckovac**, Aalto University, **Finland**
12:00-13:45	**Lunch Break / Posters Session II - Room 118**	

13:45 – 14:00	**Group Photo**

SurfCoat Korea 2019 Session II C : Surface engineering / coatings in sustainable energy, conversion, optical, electric, photovoltaic and magnetic applications		
Session chairs: Prof. Karin Stana Kleinschek, University of Maribor, Slovenia Prof André Anders, Leibniz Institute of Surface Engineering (IOM), Germany Prof. Alessandro Pezzella,University of Naples Federico II, Italy		
14:00-14:30	Advanced Aluminium Nitride Thin Films for Piezoelectric MEMS **U. Schmid** and M. Schneider	**Prof. Ulrich Schmid**, TU Wien Institute of Sensor and Actuator Systems, **Austria**
14:30-14:45	Challenges on Adhesion in the Aqueous Processing of Cathodes for Lithium Ion Batteries **W. Bauer**, U. Kaufmann, M. Müller, L. Pfaffmann	**Dr. Werner Bauer**, Karlsruhe Institut of Technology, **Germany**
14:45-15:00	Oxide Surfaces, Interfaces and Thin Films: Electrochemical Studies Relevant to Perovskite Photovoltaics **L. Kavan**	**Prof. Ladislav Kavan,** J. Heyrovsky Institute of Physical Chemistry, **Czech Rep.**

SurfCoat Korea 2019 Session II D : Bio-interfaces/ Biomedical/ Bioactive surfaces and coatings		
15:00-15:30	Surface and material science of biopolymers and their potential application in biomedicine T. Mohan, M. Bračič, R. Kargl, T. Heinze and **K. Stana Kleinschek**	**Prof. Karin Stana Kleinschek**, University of Maribor, **Slovenia**
15:30-16:00	A Multiphysics Modelling of Magnetic-Sensitive Hydrogels **H. Li**	**Prof. Hua Li**, Nanyang Technological University, **Singapore**
16:00-16:30	**Coffee Break / Posters Session II**	
16:30-17:00	Bioinspired Melanin Coatings in Bioelectronics: the case of Eumelanin/PEDOT(PSS) blend for ITO-free electrodes **A. Pezzella**	**Prof. Alessandro Pezzella,** University of Naples Federico II, **Italy**
17:00-17:15	Derivatization of biopolymers for functional coatings A. Bratuša, L. Jurko, K. Stana Kleinschek and **R. Kargl**	**Dr. Rupert Kargl**, University of Maribor, **Slovenia**
17;15-17:30	Biopolymer-based coatings on the plasmochemical activated surface of NiTi alloy **P. Jabłoński**, W. Niemiec, Ł. Kaczmarek, M. Hebda, H. Krawiec and K. Kyzioł	**Mr. Piotr Jabłoński**, AGH University of Science and Technology, **Poland**
17:30-17:45	TiO_2/CaP as a bioactive coating produced by using plasma electrolytic oxidation technique **A. Zakaria**, M. Hamdi and M. Todoh	**Mrs. Siti Hidayatul A.B Zakaria**, Hokkaido University, **Japan**
17:45-18:00	Enhancement of Adhesion of γ-Al_2O_3 with Stainless Steel Catalytic Supports **M. Abbas**, M-W. Moon, J.Y. Byun and S. H. Kim	**Mr. Muzafar Abbas,** University of Science and Technology- Daejeon, **Rep. of Korea**

19:00 – 21:00	**Social Activity: The conference Cocktail Reception**

March 29, 2019 SurfCoat Korea 2019 Session III: Coatings for energy and environmental applications		
Conference Room 117		
Session chairs: **Prof. Hana Barankova, Uppsala University, Sweden** **Prof. Rimantas Ramanauskas, Center for Physical Sciences and Technology, Lithuania**		
09:00-09:30	Active Corrosion Protection of Metals by Ce-containing Conversion Coatings **R. Ramanauskas**, O. Girciene, L. Gudaviciute, S. Butkute, A. Kirdiekiene, I. Morkvenaite-Vilkonciene, J. Juodkazyte and A. Selskis	**Prof. Rimantas Ramanauskas**, Center for Physical Sciences and Technology, **Lithuania**
09:30-10:00	Prevention in Construction – from the molecule to the building **A. Gerdes**	**Prof. Andreas Gerdes**, Karlsruhe Institute of Technology, **Germany**
10:00-10:30	**Coffee Break**	
10:30-11:00	Insight into the structure-property relationship of the protective coatings at the atomic level **Z. Zhang**	**Dr. Zaoli Zhang**, Erich Schmid Institute of Materials Science, Austrian Academy of Sciences, **Austria**
11:00-11:15	Hybrid Organic-Inorganic Coatings of Double Layered Hydroxide on Aluminum Alloy for Enhanced Alkaline Resistance S-T. Tsai, W.C. ChangJean, P-H. Chao and **T-C. Tsai**	**Prof. Tseng-Chang Tsai**, National University of Kaohsiung, **Taiwan**
11:15-12:15	Getting published: The publication process in a peer-reviewed journal, and insight-views about the Dos and Don'ts for authors **A. Anders**	**Prof André Anders**, Leibniz Institute of Surface Engineering (IOM), **Germany** / Editor-in-Chief, Journal of Applied Physics, AIP Publishing, Melville, NY/ USA

13:30 – 18:00	**Social Activity: Visit to Ganghwa**

Posters Sessions

March 27, 2019
SurfCoat Korea 2019
Session I: Surface treatments and coatings deposition processes/Characterisation

Conference Room 118

N.	Poster Title	Author/Affiliation/Country
1.	In-situ thickness monitoring of dielectric layer growth using rotated silicon witness **L. Nozka**, P. Schovanek, M. Pech, D. Mandat and M. Hrabovsky	**Dr. Libor Nozka**, Palacky University, **Czech Republic**
2.	Characteristics of Ni/LPD-Al2O3/Sputtering-ZnO/Glass UV Photodetector C-C. Lin, **J-J. Huang** and D-S. Wuu	**Prof. Jung-Jie Huang**, Da-Yeh University, **Taiwan**
3.	Synthesis of N-heterocyclic complexes of Cr,Fe,Mn,Co and Ti conversion to nanoparticles and application for cyclohexane oxidation **Z. Alrufaydi**, SM. Ahmad and AT. Mubarak	**Mrs Zahrah Alrufaydi**, King Khalid University, **Saudi Arabia**
4.	Low cost metal-free reduction catalysts of violet phosphorus synthesized by High Energy Mechanical Milling **R.H. Jeong**, D.I. Kim, J.W. Lee, J-H. Yu, A. Ananth and J-H. Boo	**Mr. Rak Hyun Jeong**, Sungkyunkwan University,
5.	Particle Fabrication via Drying Droplet Method on a Super Hydrophobic Surface **H-J. Kim**, S-J. Kim, C.W. Park and H-M. Yang	**Dr. Hyung-Ju Kim**, Korea Atomic Energy Research Institute, **Rep.of Korea**
6.	On the method of laser surface micromachining to increase the adhesion properties of joints **G. Witkowski**, S. Tofil, K. Mulczyk and H. Danielewski	**Dr. Grzegorz Witkowski**, Kielce University of Technology, **Poland**
7.	Surface laser micromachining to increase the strength of joints in adhesive joints **Sz. Tofil**, G. Witkowski, K. Mulczyk and H. Danielewski	**Dr. Szymon Tofil**, Kielce University of Technology, **Poland**
8.	Newly Designed TiO2 Hollow Spheres and its Photocatalytic Properties C-N. Chen, **J-Y. Wang**, T -Y. Lin and J-J. Huang*	**Mr. Jui Yu Wang**, Da-Yeh University, **Taiwan**
9.	Micro-alloys precipitation in NiO- and CoO-bearing enamel coatings and their effect on adherence of enamel/steel **K. Chen**, M. Chen, S. Zhu and F, Wang	**Mr. Ken Chen**, University of Science and Technology of China, **China**
10.	Effects of Process Parameters on the Properties of Ga-doped SnOx Thin Films H. I. Bang, B. S. Bae and **E.-J. Yun**	**Prof. Eui-Jung Yun**, Hoseo University, **Rep.of Korea**
11.	Development and Evaluation of Self-polishing Copolymer (SPC) resins and antifouling paints based on silyl acrylate **R. Park** and H. Park	**Ms. Rahui Park**, Pusan National University, **Rep. of Korea**
12.	General Electrical Characteristics of an Impulse Magnetron Discharge in Target Material Vapor A.V. Kaziev, **K.A. Leonova**, M.M. Kharkov, A.V. Tumarkin, D.V. Kolodko and D.G. Ageychenkov	**Ms. Kseniya Leonova**, NRNU MEPhI, **Russia**
13	Highly stable robust superhydrophobic coating deposited on glass substrate using atmospheric pressure plasma jet **Md. M. Hossain**, Q. H.Trinh, D.B. Nguyen, M.S.P. Sudhakaran,Y. Sun Mok	**Mr. Md. Mokter Hossain**, Jeju National University, **Rep. of Korea**

Graphene Korea 2019 Preliminary Program

27 - 29 March 2019 | Seoul, Republic of Korea

March 27, 2019 SurfCoat Korea 2019 - Graphene Korea 2019 joint Session I		
Conference Room 116/117		
Session Chairs: **Prof. Sang Ouk Kim, KAIST, Rep. of Korea** **Prof. Agnes Granier, CNRS-University of Nantes, France** **Prof. Holger Kersten, Kiel University, Germany**		
09:00-10:00	**Registration + Welcoming coffee**	
10:00-10:30	The GRAPHENE SHIFT is already ongoing **J. Hoon Lee**	**Mr. Joung Hoon Lee**, Standard Graphene Inc., **Rep. of Korea**
10:30-11:00	Graphene and Carbon Nanotube (CNT) Commercialization: Past, Present and Future **R. Collins** and K. Ghaffarzadeh	**Dr. Richard Collins**, IDTechEx- Cambridge, **United Kingdom**
11:00-11:30	Industrial deposition methods and applications of carbon based coatings **J. Vetter**, J. Karner , M. Kirk , F. Meunier , S. Krassnitzer , H. Eberle , M. Grischke, W. Kalss, J. Becker and A. Zedda	**Dr. Jörg Vetter,** Oerlikon Balzers Coating, **Germany**
11:30-11:45	Functionalized graphene as structural fortifier for polymers and coatings **C. Xia** and B. Zhmud	**Dr. Chao Xia**, Applied Nano Surfaces Sweden AB, **Sweden**
11:45-12:00	Chemically Induced Transformation of CVD-Grown Bilayer Graphene into Single Layer Diamond **P.V. Bakharev**, M. Huang, M. Saxena, S. W. Lee, S. H. Joo, S.O. Park, J. Dong, D. Camacho-Mojica, S. Jin, Y. Kwon, M. Biswal, F.Ding, S.K. Kwak, Z. Lee and R.S. Ruoff	**Dr. Pavel V. Bakharev**, Institute for Basic Science-Ulsan, **Rep. of Korea**
12:00-12:15	Graphene Growth on Cu Foil by Direct-Liquid-Injection Chemical Vapor Deposition with Cyclohexane Precursor in N2 Ambient **T. Intaro**, T. Taychatanapat, N. Nuntawong, S. Koh and S. Sanorpim	**Mr. Taworn Intaro**, Chulalongkorn University, **Thailand**
12:15-12:30	Scaling up single-crystal graphene by CVD of ethanol and methane **A. Capasso**, C.D. Liao, B. Sompalle, M.F. Cerqueira, J. Borme, G. Faggio, G. Messina, N. Lisi, G.H. Lee and P. Alpuim	**Dr. Andrea Capasso**, International Iberian Nanotechnology Laboratory, **Portugal**
12:00-14:00	**Lunch Break / Posters Session I**	
Graphene Korea 2019 **Session I A : Graphene and 2D Materials, Growth, synthesis, modification and functionalization and Characterization**		
Conference Room 116		
Session Chairs: **Dr. Blanca Biel, University of Granada, Spain** **Prof. Feng Ding, Institute for Basic Science, Rep. of Korea** **Prof. Johnson Goh Kuan Eng, Agency for Science, Technology and Research (A*STAR), Singapore**		
14:00-14:30	Graphene Oxide Liquid Crystal **S.O. Kim**	**Prof. Sang Ouk Kim**, KAIST, **Rep. of Korea**
14:30-15:00	Strategies for the Synthesis of Wafer Scale Graphene Single Crystal **F. Ding**	**Prof. Feng Ding**, Institute for Basic Science, **Rep.of Korea**
15:00-15:30	Transfer-Free Large-Scale High-Quality Monolayer Graphene Synthesized at Lower Temperatures than Boiling Point of Water B-J. Park, Y. Han, J-S. Choi, H. Ha, H.Y. Kim, C. Jeon, J-H. Eom, G. Park, H-T. Jung, Y-H. Kim and **S-G. Yoon**	**Prof. Soon-Gil Yoon**, Chungnam National University, **Rep. of Korea**

15:30-16:00	Graphene anode for organic and perovskite light-emitting diodes **T-W. Lee**	**Prof. Tae-Woo Lee**, Seoul Nat. University, **Rep. of Korea**
16:00-16:30	**Coffee Break / Posters Session I**	
16:30-17:00	Point-like defects in transition metal dichalcogenides characterized by SPM simulations **B. Biel**, A. Gallardo and P. Pou	**Dr. Blanca Biel**, University of Granada, **Spain**
17:00-17:15	The structure of graphene folds in single crystal graphene film grown on a Cu (111) foil **D. Luo**, M. Choi, M. Wang, Y. Kwon, Z. Lee and R.S. Ruoff	**Dr. Da Luo**, Institute for Basic Science- Ulsan, **Rep. of Korea**
17:00-17:30	Many-body quantum Monte Carlo study of 2D materials: Cohesion, band gap, and strain effect in phosphorene T. Frank, R. Derian, K. Toár, L. Mitas, J. Fabian and **I. Štich**	**Prof. Ivan Stich**, Slovak Academy of Sciences, **Slovakia**
17:30-17:45	A novel approach to grow the bulk TMDC with two-dimensional material properties **S.W. Tong***, H. Medina and D. Chi	**Dr. Shi Wun Tong**, Agency for Science Technology and Research, **Singapore**
17:45-18:00	Influence of Nano-confined Water on the Frictional Properties of Single-layer Graphene Coated Rough Silica Surface **H-C. Chiu** and E-D. Chu	**Dr. Hsiang-Chih Chiu,** National Taiwan Normal University, **Taiwan**
18:00-18:15	Similarities and differences of fractional end charges in graphene zigzag ribbon and polyacetylene **S.-R Eric Yang**	**Prof. Sung R.Eric Yang**, Korea University, **Rep. of Korea**
18:15-18:30	Single layer h-BN grown on curved Ni(111) crystal: oxidation and oxygen intercalation **A. A. Makarova**, L. Fernandez, D. Yu. Usachov, A. Fedorov, K. A. Bokai, D. A. Smirnov, C. Laubschat, D. V. Vyalikh, F. Schiller and J. E. Ortega	**Dr. Anna Makarova**, Dresden University of Technology, **Germany**
18:30-18:45	Development of Roll to Roll CVD system for mass production of high quality and large area Graphene **Y-S. Kim**, J. Sung, J.S. Moon, W.B. Park, J.Rho and M. Hee Jung	**Dr. Youn-Su Kim**, LG electronics, **Rep. of Korea**

18:30 – 21:00	**Social Activity: SongDo Night Tour**

March 28, 2019
Graphene Korea 2019
Session II A: Graphene for electronic, photovoltaic and magnetic applications

Conference Room 116

Session Chairs:
Dr. Elena Polyakova, National University of Singapore, Singapore
Prof. Philip Feng, Case Western Reserve University, USA
Dr. Mindaugas Lukosius, Institute for High Performance Microelectronics, Germany

09:00-09:30	Moiré superlattices and minibands for Dirac electrons in graphene heterostructures **V. Falko**	**Prof. Vladimir Falko**, University of Manchester, **UK**
09:30-10:00	Programmable van der Waals materials **A. Mishchenko**	**Dr. Artem Mishchenko**, Manchester University, **UK**
10:00-10:30	Critical Overview of Performance of 2D Materials and Composites **E. Polyakova**	**Dr. Elena Polyakova,** National University of Singapore, **Singapore**
10:30-11:00	**Coffee Break / Posters Session II - Room 118**	
11:00-11:30	Upcoming industrial applications of graphene oxide **R. Wendelbo**	**Dr. Rune Wendelbo**, Abalonyx AS/ Graphene Batteries AS, **Norway**
11:30-12:00	Emergence of Black Phosphorus as Anisotropic 2D Material for Electronics and Optoelectronics **K-W. Ang**	**Prof. Kah-Wee Ang**, National University of Singapore, **Singapore**
12:00-12:15	High Areal Loading and Stable Sulfur Cathode Enabled with RGO Coating for LiS Batteries A. Oguz Tezel, **R. Wendelbo** and S. Fotedar	**Dr. Ahmet Oguz Tezel**, Graphene Batteries AS, **Norway**
12:00-13:45	**Lunch Break / Posters Session II**	

13:45 – 14:00	**Group Photo**

Session Chairs:
Prof. Won-Chun Oh, Hanseo University, Rep. of Korea
Dr. Artem Mishchenko, Manchester University, UK

14:00-14:30	Growth of Single-Crystalline Nanobelts Composed of Transition Metal Ditellurides for Future Electronic & Energy Applications **S-Y. Kwon**	**Prof. Soon-Yong Kwon,** Ulsan National Institute of Science and Technology, **Rep. of Korea**
14:30-15:00	Towards the integration of 200 mm graphene into microelectronics **M. Lukosius**	**Dr. Mindaugas Lukosius,** Institute for High Performance Microelectronics, **Germany**
15:00-15:30	Atom-by-atom engineering of Kekule lattices: the boundary of topological insulators **C. Morais Smith**	**Prof. Cristiane Morais Smith**, University of Utrecht, The **Netherlands**
15:30-16:00	Highly Tunable and Glowing Graphene Nanoelectromechanical Systems (NEMS) **P. Feng**	**Prof. Philip Feng**, Case Western Reserve University, **USA**
16:00-16:30	**Coffee Break / Posters Session II - Room 118**	
16:30-17:00	Finding Chiral Valleys in 2D Semiconductors **K. E. Johnson Goh**	**Prof. Johnson Goh Kuan Eng**, Agency for Science, Technology and Research, **Singapore**
17:00-17:30	Charge density wave and superconducting order in TiSe2 driven by excitonic condensation and its fluctuations **V.M. Pereira**	**Prof. Vitor M. Pereira**, National University of Singapore, **Singapore**

17:30-17:45	Graphene Fibers for Energy Applications **S. Padmajan Sasikala** and S.O. Kim,	**Dr. Suchithra Padmajan Sasikala**, KAIST, **Rep. of Korea**
17:45-18:00	2D Metal Chalcogenide Nanopatterning by Block Copolymer Lithography **T. Yun**, G.S. Lee, J.G. Kim and S. O. Kim	**Dr. Taeyeong Yun**, KAIST, **Rep. of Korea**

19:00 – 21:00	**Social Activity: The conference Cocktail Reception**

March 29, 2019 Graphene Korea 2019 Session III: Application of Graphene in Energy/ Health and biomedical		
Conference Room 116		
Session chairs: **Prof. Vitor M. Pereira, National University of Singapore, Singapore** **Prof. Ho Won Jang, Seoul National University, Rep. of Korea** **Dr. Elena Polyakova, National University of Singapore, Singapore**		
09:00-09:30	Flexible graphene-based gas sensors of low power consumption **H.W.Jang**	**Prof. Ho Won Jang**, Seoul National Univ., **Rep. of Korea**
09:30-09:45	Photoluminescence properties of monolayer monolayer transition metal dichalcogenides in an aqueous solution **W. Zhang**, K. Matsuda, and Y. Miyauchi	**Mr. Wenjin Zhang**, Kyoto University, **Japan**
09:45-10:00	Competing energy scale in Bilayer Graphene Quantum Point Contacts **Y. Lee**, A. Knothe, H. Overweg, P. Rickhaus, M. Eich, A. Kurzmman, K. Watanabe, T. Taniguchi, V. I. Fal'ko, T. Ihn and K. Ensslin	**Dr. Yongjin Lee**, ETH Zurich, **Switzerland**
10:00-10:15	Tuning the performance of graphene-field-effect-transistors using Self-Assembled Monolayers S. Ramadan, **Y. Zhang**, D. K. Hong Tsang, O. Shaforost, C.Watts, I. E. Dunlop, P.K. Petrov and N. Klein	**Mr. Yuanzhou Zhang**, Imperial College London, **UK**
10:15-10:30	Development and fabrication of graphene oxide membranes for water desalination Z.Balgin, **Z.Yelemessova**, Z.Yermogambetov, K.Tynyshtykbayev, and Z.Insepov	**Mrs. Zarina Yelemessova**, Nazarbayev University, **Kazakhstan**
10:30-11:00	**Coffee Break - Room 118**	
11:00-11:30	Prospective Study of Graphene Combined Semiconductor and its Potential Application **W-C. Oh**	**Prof. Won-Chun Oh**, Hanseo University, **Rep. of Korea**
11:30-11:45	Characterization of Hybrid MnO2/RGO/PANI Supercapacitor with Green Reducing Agent S.I. Khairul, **M.N.M.Ansari**, S.Z.Omar, P.J.Ker, M.N.Saifuddin, A.Q. Al-Amin and H.Hasmaizan	**Dr. Mohamed Ansari Mohamed Nainar**, Tenaga National University, **Malaysia**
11:45-12:00	Dielectric properties of semiconductor armchair graphene nanoribbon arrays **C. Vacacela Gomez**, A. Sindona, M. Pisarra, T. Tene and M. Guevara	**Dr. Cristian Vacacela Gomez**, Polytechnic School of Chimborazo, **Ecuador**
12:00-12:15	Chemically Functionalised Graphene Biosensor for the Label-free Sensing of Exosomes **D. Kwong Hong Tsang**,T. J. Lieberthal, C. Watts, I. E. Dunlop,S. Ramadan and N. Klein	**Ms. Deana K.H. Tsang**, Imperial College London, **UK**

13:30 – 18:00	**Social Activity: Visit to Ganghwa**

Posters Sessions

March 28, 2019
SurfCoat Korea 2019 / Graphene Korea 2019
Joint Session II: Surfaces and Coatings applications/ Graphene synthesis and applications

Conference Room 118

N.	Poster Title	Author/Affiliation/Country
1.	Growth of MnSi1.7 Thermoelectric Coating on Si Substrate by Pack Cementation A. Teknetzi, E. Tarani, D. Kourtidou, D. Karfaridis, E. Pavlidou, K. Chrissafis, G. Vourlias and **E. K. Polychroniadis**	**Prof. Efstathios Polychroniadis**, Aristotle University of Thessaloniki, **Greece**
2.	Electron Beam annealing method for realization of High Mobility Oxide Semiconductor Thin-film transistor **Y-J. Cha**, M.U. Cho and J. S. kwak*	**Dr. Yu-Jung Cha**, Sunchon National University, **Rep. of Korea**
3.	Anti-corrosion and Anti-oxidation Effects of Aluminum Metal Substrate by Inorganic-Organic Binder / Graphene NanoComposite Film Coating **H. Kim**, H. Lee, H-B. Cho and Y-H. Choa	**Mr. Han Kim**, Hanyang University, **Rep. of Korea**
4.	A Synergistic Combination of Au-coated Ag Nanowire and WO3 Nanofiber for Enhanced Electrochromic Application **Y-B. Oh**, J. Lee, H-B. Cho and Y-H. Choa	**Mr. Yeong-Been Oh**, Hanyang University, **Rep. of Korea**
5.	Preparation of one dimensional Co3O2-NiO@AgNWs nanowire for the thin film electrodes of supercapacitor J-Y. Lin, **Y-X. Zhang**, Y-Q. Wu and J-J. Huang	**Ms. Yu-Xuan Zhang**, National Yunlin University of Science and Technology, **Taiwan**
6.	Low–temperature Encapsulating perovskite solar cells by RF Sputtering **M. Kim**, S. Kim, H. Rui and C. Wung Bark	**Mr. Maro Kim**, Gachon University, **Rep. of Korea**
7.	Molybdenum Disulfide/Carbon Hybrid Thin Films as High-Performance cathode for Reverse Electrodialysis **N. Jeong**, H. Kim, J. Choi, J. Nam, K. Hwang, S. Yang, J. Han, E. Jwa and S. Park	**Dr. Namjo Jeong**, Korea Institute of Energy Research, **Rep. of Korea**
8.	Adlayer-free, single crystal graphene grown on large-area Cu (111) foil **M. Wang**, D. Luo, Y. Kwon and R.S. Ruoff	**Ms. Meihui Wang**, Institute for Basic Science-Ulsan, **Rep. of Korea**
9.	Crystalline and Uniform ZrO2 by Atomic Layer Deposition on Atmospheric Plasma Treated Graphene **J.W. Shin**, M.H. Kang, S. Oh, B. C. Yang, D. Go, T. H. Lee and J. An	**Mr. Jeong Woo Shin**, Seoul National University of Science and Technology, **Rep. of Korea**
10.	Temperature Dependence of optical properties of WS2 by Spectroscopic Ellipsometry **H. T. Nguyen**, T. J. Kim, H. G. Park, V. L. Le, X. A. Nguyen, W. Lee, D. H. Koo, C.-H. Lee and Y. D. Kim	**Mr. Hoang Tung Nguyen**, Kyung Hee University, **Rep. of Korea**
11.	A Graphene-Gated Carbon Nanotube Electron Emitter for Digital X-ray Tubes with High-Spatial Resolution **H. Jeon**, E. Go, J.-W. Lee, Y. Ahn, S. Park, J.-W. Kim, J.-T. Kang, J.-W. Jeong, K.N. Yun, J.-W. Yeon, S. Kim and Y.-H. Song	**Ms. Jeon Hyojin**, University of Science & Technology- Daejeon, **Rep. of Korea**
12.	Comparison of Cytotoxicity of Black Phosphorus Particles against Three Different Types of Fibroblastic Cells **S.J. Song**, Y.B. Lee, M.S. Kang, Y.C. Shin, H.U. Lee and D.W. Han	**Ms. Sujin Song**, Pusan National University, **Rep. of Korea**
13.	Structure-directing effect of single crystal graphene film on polymer carbonization and graphitization **B.V. Cunning**, B. Wang, T.J. Shin and R.S. Ruoff	**Dr. Benjamin V. Cunning**, Institute for Basic Science, **Rep. of Korea**
14	Mass produced high quality and large area CVD Graphene using Roll to Roll process **J. Sung**, Y-S. Kim, J.S. Moon, W.B. Park, J. Rho and M.H. Jung	**Dr. Jinwoo Sung**, LG electronics, Materials and Production Engineering Research Institute, **Rep. of Korea**

SurfCoat Korea 2019 / Graphene Korea 2019 Joint Session I

Graphene and Carbon Nanotube (CNT) Commercialization: Past, Present and Future

R. Collins,[1*] K. Ghaffarzadeh,[1]

[1] IDTechEx, Cambridge, UK

Abstract:
Graphene offers tremendous opportunity. Indeed, we forecast that it will become a *ca.* $300m market by 2027.[1] Despite this, many graphene companies are in that crucial step where they finally have to convert their numerous leads into sales. Many struggle to diversify away from small volume sales to the researcher community and the nominal global production capacity is still hugely underutilised. Nonetheless, the industry is accumulating experience, is finding the best applications to focus on, and is demonstrating tangible commercial progress. In fact, several companies have already secured several sales in tens to hundreds of tonne scale. IDTechEx expect 2019 will be the start of the tipping point, where the hype turns to commercial reality.
In this talk, we outline the past, present and future of graphene whilst considering trends in production capacity, price, revenues, and applications.
Graphene commercialization, in many ways, is following in the footsteps of CNTs. This technology too experienced a hype cycle but now is making a steady but fairly quiet commercial progress. Indeed, it has entered the phase of rapid volume growth partially thanks to its falling price over the past few years. In this talk, we will consider the past, present and future of CNTs in terms of the evolution of industry production capacity, price, revenues, and applications.
This talk will cover:
- Diversity of graphene products
- Price disparity
- Global production capacity
- The rise of China as the main territory
- Graphene application pipeline
- Investment, revenue and valuation trends
- MWCNT types and cost evolution
- History of MWCNT production capacity
- MWCNT application pipeline
- Market forecasts

Keywords: Market forecast, technology benchmarking, player and application analysis.

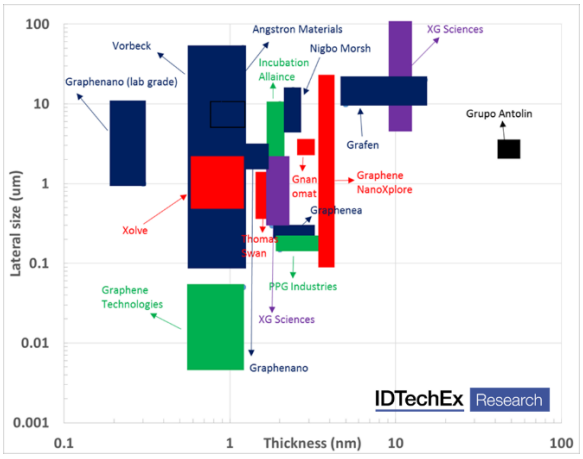

Figure 1: Analysis displaying the range of graphene commercially available.

References:

1. Ghaffarzadeh, K. (2018) Graphene, 2D Materials and Carbon nanotubes: Markets, technologies and Opportunities 2018-2028

Industrial deposition methods and applications of carbo based coatings

J. Vetter [1], J. Karner [2], M. Kirk [3], F. Meunier [4], S. Krassnitzer [2], H. Eberle [2], M. Grischke [2], W. Kalss [2], J. Becker [1], A. Zedda [2]

[1]Oerlikon Balzers, Germany
[2]Oerlikon Balzers, Liechtenstein
[3]Oerlikon Balzers, USA
[4]Oerlikon Balzers, France

Abstract:
The attractive properties of carbon based hard coatings include high hardness, chemical inertness, tunable electrical resistivity and optical properties, biocompatibility, excellent tribological behavior in many engineering applications, show a high potential for use in anti-corrosion and electrochemical applications, have a potential for sensory applications and for fuel cell applications. The main coating type in use are amorphous carbon coatings consisting of a disordered network of carbon atoms with sp^3 and sp^2 coordinated bonds. The family of amorphous carbon films is called diamond like carbon: DLC. However also diamond coatings with nearly 100% sp^3 carbon bond hybridization are in application. The main industrial deposition methods to generate amorphous carbon based coatings are the PACVD process, the vacuum arc evaporation (including filtered arc), the magnetron sputtering including the newer development of HiPIMS (e.g. s3P). The diamond coatings are deposited by a special PACVD process or by a hot filament process.
Tailored batch coating systems with different sizes are used both for large scale and small lot applications.
Modern coating systems are self-contained systems with components that are optimally matched to one another. These systems must fulfil the following criteria in order to comply with the market's increasing demands with respect to costs and quality:

- Short cycle times
- High productivity and operational economy
- High flexibility
- Low maintenance and spare parts costs (design to cost)
- High production reliability
- Fully automatic operation
- CE conformity and high occupational safety standards

The fundamental difference between machine types depends on the planned use and the flexibility required. From small batch machines to specialized systems with automatic robotic loading. Selected industrial coatings systems will be briefly described and typical applications of the carbon based coatings including a-C:H, a-C:H:X, a-C, ta-C and diamond are presented.

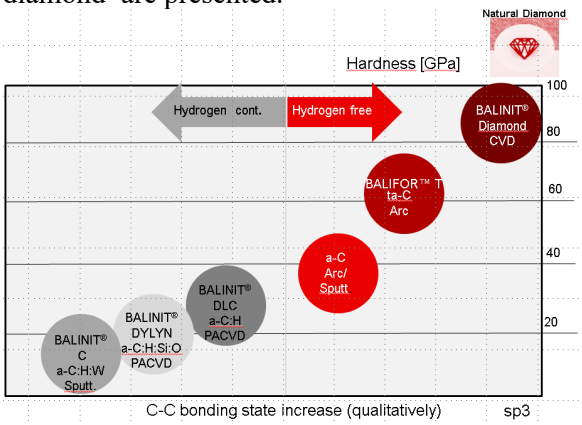

Figure 1: Main industrial applied carbon based coatings

References:

1. Vetter, J., 60 Years of DLC coatings: Historical highlights and technical review of cathodic arc processes to synthesize various DLC types, and their evolution for industrial applications, *Surf. Coat. Technol.* 257 (2014)213-240
2. Vetter, J., Berger, M., Derflinger V., Krassnitzer, S., Plasma- Assisted Coating Processes, https://www.oerlikon.com/balzers/com/en/portfolio/surface-technologies/plasma-assisted-coating-processes-new-pvd-and-cvd-book/

Functionalized graphene as structural fortifier for polymers and coatings

Chao Xia[1], Boris Zhmud[1]
[1] Applied Nano Surfaces Sweden AB, Uppsala, Sweden

Abstract:
Functionalized graphene is of great interest to polymer and coatings industry. Internationally, a huge research effort has been undertaken in developing new graphene-enhanced products. This presentation describes the so-called "reactive filler" concept whereby functionalized graphene is proposed to be used as composite cross-linker in polymer-bonded solid lubricant coatings in order to improve the mechanical strength and abrasion resistance of the latter. Several synthetic methods to graft oxirane, isocyanate, amine and polyol groups to graphene sheets are presented. Functionalized graphene fillers are evaluated in terms of dispersibility and compatibility with water-borne one-component epoxy and polyurethane coating formulations. The tribological properties of graphene-fortified coatings are studied as well. The use of graphene showes a tenfold increase in the mechanical strength and abrasion-resistance of polymer-bonded solid lubricant coatings. And these benefits can be further boosted by using chemically functionalized graphene sheets which will chemically cross-link with the polymer binder.

Keywords: graphene, waterborne, low friction coating.

Chemically Induced Transformation of CVD-Grown Bilayer Graphene into Single Layer Diamond

Pavel V. Bakharev[1], Ming Huang[1,2], Manav Saxena[1], Suk Woo Lee[2], Se Hun Joo[3], Sung O Park[3], Jichen Dong[1], Dulce Camacho-Mojica[1], Sunghwan Jin[1], Youngwoo Kwon[1], Mandakini Biswal[1], Feng Ding[1], Sang Kyu Kwak[1,3], Zonghoon Lee[1,2] & Rodney S. Ruoff[1,2,3,4]

[1] Center for Multidimensional Carbon Materials (CMCM), Institute for Basic Science (IBS), Ulsan 44919, Republic of Korea
[2] School of Materials Science and Engineering, Ulsan National Institute of Science and Technology (UNIST), Ulsan 44919, Republic of Korea
[3]School of Energy and Chemical Engineering, Ulsan National Institute of Science and Technology (UNIST), Ulsan 44919, Republic of Korea
[4]Department of Chemistry, Ulsan National Institute of Science and Technology (UNIST), Ulsan 44919, Republic of Korea

Abstract:
In this work, we report on the first experimental observation of the fluorine chemisorption induced sp^2 to sp^3 phase transition of large-area bilayer graphene to diamond-like film under moderate conditions (near-room temperature and at a low pressure (less than one atmosphere and the structure is stable at 1 atm)). The synthesis of a novel ultra-thin diamond-like material, namely fluorinated diamond monolayer ('*F-diamane*'), has been achieved in two ways. The first is the fluorination of bilayer graphene on single crystal metal (CuNi(111) alloy) foil, on which the bilayer graphene was grown by chemical vapor deposition (CVD). The other is fluorination of the same type of CVD bilayer graphene film transferred onto TEM (transmission electron microscopy) gold grids to obtain *F-diamane* film "suspended" on a chemically inert support. Our spectroscopic, transmission electron microscopy, and density functional studies unequivocally show that the fluorine chemisorption on CVD-grown bilayer graphene under certain conditions results in formation of F-diamane.

Keywords: bilayer graphene, single layer diamond, diamane, sp^2 to sp^3 phase transition, CVD, single crystal CuNi(111) alloy

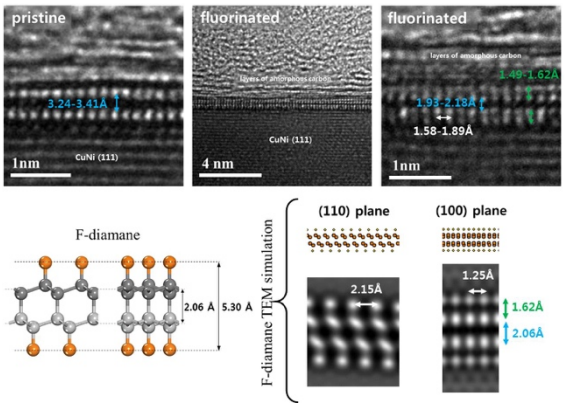

Figure 1: High resolution cross-sectional transmission electron micrographs of as-grown (pristine) BLG (top left image) and Sample A (top right images). Simulated HR-TEM images of DFT-optimized F-diamane (bottom images).

Acknowledgement
This work was supported by IBS-R019-D1

Graphene Growth on Cu Foil by Direct-Liquid-Injection Chemical Vapor Deposition with Cyclohexane Precursor in N_2 Ambient

T. Intaro[1,*], T. Taychatanapat[1], N. Nuntawong[2], S. Koh[3], and S. Sanorpim[1,*]

[1]Chulalongkorn University, Department of Physics, Bangkok, Thailand
[2]National Electronics and Computer Technology Center (NECTEC), Pathumthani, Thailand
[3]Aoyama Gakuin University, College of Science and Engineering, Sagamihara, Kanagawa, Japan

Abstract:
Controlling a liquid precursor flow rate is inherently difficult for chemical vapor deposition (CVD). As a result, CVD graphene grown by the liquid precursor shows non-controllable nucleation and nonuniform thickness. To solve this problem, we employ direct-liquid-injection chemical vapor deposition (DLI-CVD) which can control the flow rate of liquid precursors more accurately. In addition, we offer a safer process in which hydrogen gas is not required. Here, we use a low-cost cyclohexane (C_6H_{12}) and N_2 as a carbon precursor and carrier gas at the flow rate of 0.1-0.5 g/min and 300 sccm respectively. Graphene is grown on Cu foil substrate at 890 to 980 ºC for 10 min in the total pressure of 2 mbar. The graphene samples are then characterized by optical microscopy, Raman spectroscopy, and Hall measurement in order to study the structural and electrical properties. Raman spectra of the samples exhibit characteristic peaks of graphene with small D peak demonstrating the high quality of graphene grown by DLI-CVD. In addition, we perform the Raman mapping of our samples (Figure 1) in which a ratio of 2D and G peak intensities (I_{2D}/I_G) and D and G peak intensities (I_D/I_G) are plotted as a function of positions. We observe that the value of the ratio I_{2D}/I_G is typically greater than 2, indicating that our graphene is a uniform monolayer. On the other hand, the Raman mapping of the ratio I_D/I_G exhibits a high quality graphene layer. Hall measurement on graphene samples shows that the resistivity, carrier density, and carrier mobility are 2,300 Ω/sq, $5.7x10^{12}$ cm^{-2}, and 470 cm^2/Vs, respectively. The low carrier mobility is likely from impurities introduced during transfer process and device fabrication. Our results demonstartae a successful growth of large-area and high quality monolayered graphene using Cyclohexane precursor in N_2 ambient under certain growth conditions.

Keywords: graphene, direct-liquid-injection, CVD, Cu foil, Cyclohexane, N_2 Ambient.

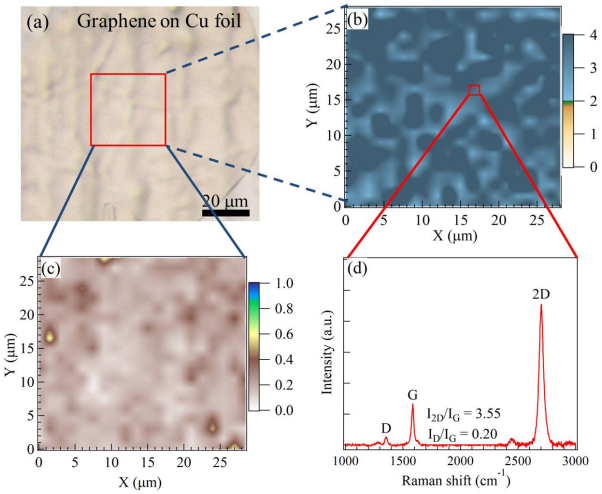

Figure 1: (a) Optical image of graphene on Cu foil. Raman mapping of (b) I_{2D}/I_G and (c) I_D/I_G rations taken inside the red-square and (d) Raman spectrum showing a uniform monolayer and low defect graphene.

References:

1. Gan, W., Han, N., Yang, C., Wu, P., Liu, Q., Zhu, W., Chen, S., Wu, C., Habib, M., Sang, Y., Muhammad, Z., Zhao, J., and Song, L. (2017) A ternary alloy substrate to synthesize monolayer graphene with liquid carbon precursor, *ACS Nano,* 11, 1371−1379.
2. Ferrari, A.C., Meyer, J.C., Scardaci, V., Casiraghi, C., Lazzeri, M., Mauri, F., Piscanec, S., Jiang, D., Novoselov, K.S., Roth, S., and Geim, A.K. (2006) Raman Spectrum of Graphene and Graphene Layers, *Phys. Rev. Lett.,* 97, 187401-187404.

Scaling up single-crystal graphene by CVD of ethanol and methane

A. Capasso,[1,*] C.D. Liao,[1] B. Sompalle,[1,2] M.F. Cerqueira,[1,2] J. Borme,[1] G. Faggio,[3] G. Messina,[3] N. Lisi,[4] G.H. Lee,[5] P. Alpuim[1,2]

[1] International Iberian Nanotechnology Laboratory, 4715-330 Braga, Portugal
[2]CFUM-Center of Physics of the University of Minho, 4710-057 Braga, Portugal
[3]DIIES Department, University "Mediterranea", Via Graziella, Loc. Feo di Vito, Reggio Calabria 89122, Italy
[4]ENEA, DTE PCU IPSE, Casaccia Research Centre, Via Anguillarese 301, Rome 00123, Italy
[5]Department of Materials Science and Engineering, Yonsei University, Seoul 03722, Republic of Korea

Abstract:
Recent efforts in graphene research led to significant advancement in production and processing methods. Among others, chemical vapor deposition (CVD) of hydrocarbons (*e.g.*, methane [1]) or alcohols (*e.g.*, ethanol [2, 3]) on Cu foils is the most suitable technique for the production of real graphene (*i.e.*, one-atom-thick honeycomb carbon lattice) samples. CVD samples are, however, typically made of polycrystalline grains, and the presence of grain boundaries negatively affects the charge mobility and conductivity, as well as the mechanical strength. The CVD growth of isolated (*i.e.*, not merged in a film) graphene crystals with lateral size in the mm range and beyond is attractive for fundamental research, but also in view of industrial applications in microelectronics. Understanding the initial stages of the CVD growth is key to a full control on the whole process. It recently became clear that oxygen has a crucial role in the process, influencing both the nucleation rate and growth kinetics.
Various approaches were proposed to exploit the effect of oxygen on the CVD growth of graphene. Preoxidation of Cu foils appeared as an effective way to reduce the number of nucleation sites, thus obtaining sparse graphene nuclei that could proceed to grow into single crystals [1]. In methane-CVD, by preoxidizing the Cu foils at ~200 °C, the nucleation density can decrease to a few nuclei/cm^2, *i.e.*, five orders of magnitude smaller than that on untreated Cu foils [4]. The Cu preoxidation treatment has three main effects: i) induces the passivation of active nucleation sites on the Cu surface; ii) promotes the formation of oxygen-rich bulk Cu during the high-temperature heating in CVD; iii) eliminates adsorbed organic contaminants, possibly remaining after the substrate cleaning process.
All these effects contribute to the nucleation density reduction. As an alternative way of exploiting the oxygen effect, a minor but continuous oxygen feed can be provided during the growth process by using an oxide wafer (e.g., SiO_2, Al_2O_3) placed in the CVD chamber in proximity (or in contact) to the Cu foil substrate. Most of these "oxygen-aided" approaches are usually combined with some "volume confinement" strategies [5, 6]. To restrain the volume in the proximity of the substrate, researchers either i) folded the Cu foils in an enclosure, or ii) placed them within a height-confined box of inert material (e.g., graphite, alumina). By restraining the volume, the concentration of Cu atoms sublimating from the Cu foil during CVD increases, promoting re-deposition on the foil surface and thus reducing its roughness. Besides, the increased Cu vapor pressure within the confined volume aids the carbon precursor dehydrogenation, thus speeding up the grain growth [7, 8]. The combination of these two effects can lead to a fast growth of isolated graphene single-crystals up to cm-scale [5].
Here, we performed a systematic investigation into the effect of the different strategies meant to reduce the nucleation rate and accelerate the growth rate. We explored the growth of large, isolated graphene grains by CVD of 1) ethanol and 2) methane on Cu foils. In the 1st case (ethanol-CVD), we optimized the nucleation process on flat Cu foils, directly exposed to the ethanol gas atmosphere, to devise the exact growth mechanism and gain full control on the nucleation rate. We were able to decrease the nucleation density to less than 3 nuclei/mm^2 and obtain single-crystal grains with a lateral size above 0.5 mm (Figure 1a), by using preoxidized Cu foil substrates (250°C in air) and an ethanol vapor flow of

1.5×10^{-3} sccm (1070°C, 60 min) [9]. When transferred onto Si/SiO_2 substrates, these crystals showed field-effect mobility beyond 1300 cm^2/V s. In the 2nd case (methane-CVD), we treated the Cu foils in a $FeCl_3$/HCl solution before the pre-oxidation treatment at 200°C. The substrates were loaded into a confined graphite cavity (18×14×1.5cm), acting as sample holder within the tube furnace. A sapphire wafer placed above the Cu foils (at a distance of 0.5 mm) was used to provide a continuous oxygen supply throughout the whole CVD process. In these conditions, we grew isolated single-crystal grains with a lateral size above 1.2 mm (Figure 1b) at a methane flow of 1.5×10^{-3} sccm (1045°C, 70 min).

Overall, the controlled growth of mm-scale single-crystal graphene provides a step further towards industrial production. When grown in large numbers and with high reproducibility, graphene crystals could serve as building blocks for commercial electronic devices, or act as seeds for the production of continuous, single-crystal graphene films over arbitrarily large areas.

Keywords: CVD-growth, nanocarbon, two-dimensional material, isolated grain, microelectronics.

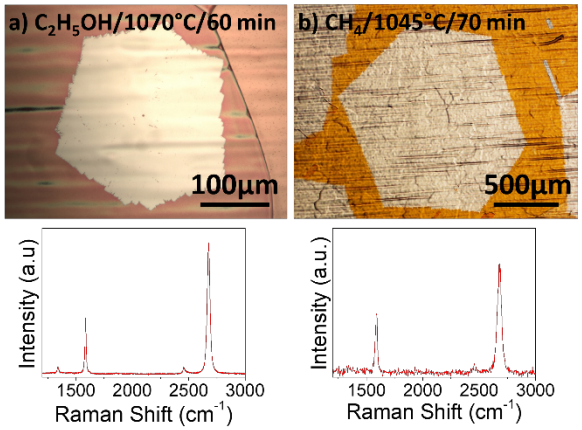

Figure 1: Optical images (top) and corresponding Raman spectra (bottom, after transfer on Si/SiO_2) of single-crystal graphene grown with 1.5×10^{-3} sccm of (a) ethanol and (b) methane.

References:

1. Hao, Y. et al. (2013) The Role of Surface Oxygen in the Growth of Large Single-Crystal Graphene on Copper, *Science*, 6159, 720–723.
2. Faggio, G., et al. (2013), High temperature growth of graphene films on copper foils by ethanol chemical vapour deposition, *Journal of Physycal Chemistry C*, 117, 21569-21576.
3. Lisi, N., et al. (2014), Rapid and highly efficient growth of graphene on copper by chemical vapor deposition of ethanol, *Thin Solid Films*, 571, 139-144.
4. Pham, P.H.Q., et al. (2016), Controlling Nucleation Density While Simultaneously Promoting Edge Growth Using Oxygen-Assisted Fast Synthesis of Isolated Large-Domain Graphene, *Chem. Mat.*, 28, 6511-6519.
5. Xu, X., et al. (2016), Ultrafast growth of single-crystal graphene assisted by a continuous oxygen supply, *Nat. Nanotechnol.*, 11, 930–935.
6. Chen, C.C., et al. (2015), Growth of Large-Area Graphene Single Crystals in Confined Reaction Space with Diffusion-Driven Chemical Vapor Deposition, *Chemistry of Materials*, 27, 6249-6258.
7. Teng, P.Y., et al. (2012), Remote Catalyzation for Direct Formation of Graphene Layers on Oxides, *Nano Letters*, 12, 1379-1384.
8. Kim, H., et al. (2016) Copper-Vapor-Assisted Chemical Vapor Deposition for High-Quality and Metal-Free Single-Layer Graphene on Amorphous SiO2 Substratexides, *ACS Nano*, 7, 6575-6582.
9. Gnisci, A., et al. (2018), Ethanol-CVD Growth of Sub-mm Single-Crystal Graphene on Flat Cu Surfaces, *J. Phys. Chem. C*, 122, 28830-28838.

SurfCoat Korea 2019
Session I A: Plasma Coatings deposition and processing

Magnetron Sputtering: The Special Role of Localized Electron Heating and Supply of Neutrals

André Anders,[1,2]

[1] Leibniz Institute of Surface Engineering (IOM), Leipzig, Germany
[2] Felix Bloch Institute, Leipzig University, Leipzig, Germany

Abstract:
Magnetron sputtering is a widely used technology well matured since its invention about half a century ago. Yet, we have learned a lot more about the underlying processes only in recent years, especially about the type of plasma instabilities that allow the devices to work. For a wide range of process conditions, magnetrons show spoke and breathing instabilities that help with ionization of neutrals and transport of particles, closing the electric circuit, and enabling / assisting film growth on substrates.
Among the newer findings is the localized nature of electron heating and supply of neutral atoms to the ionization region near the magnetron target. These factors, electron heating and supply of neutrals, are key to the rate of ionization, which is concentrated in moving ionization zones known as spokes [1, 2]. Recent theoretical [3], spectroscopic [4], and probe data [5] prove that most of the electrons' energy comes from the presheath and is provided by localized electric fields concentrated at the edge of spokes.
Most experimental work reported here was done at Lawrence Berkeley National Laboratory, Berkeley, CA, in collaboration with Yuchen Yang, Matjaz Panjan, and others, whose contributions are gratefully acknowledged.

Keywords: magnetron sputtering, plasma, electron heating, plasma diagnostics, plasma instabilities, spokes

References:

1. A. Anders, "Localized heating of electrons in ionization zones: Going beyond the Penning-Thornton paradigm in magnetron sputtering," *Appl. Phys. Lett.,* vol. 105, p. 244104, 2014.
2. A. Anders and Y. Yang, "Plasma studies of a linear magnetron operating in the range from DC to HiPIMS," *J. Appl. Phys.,* vol. 123, p. 043302, 2018.
3. C. Huo, D. Lundin, M. A. Raadu, A. Anders, J. T. Gudmundsson, and N. Brenning, "On sheath energization and Ohmic heating in sputtering magnetrons," *Plasma Sources Sci. Technol.,* vol. 22, p. 045005, 2013.
4. J. Andersson, P. Ni, and A. Anders, "Spectroscopic imaging of self-organization in high power impulse magnetron sputtering plasmas," *Appl. Phys. Lett.,* vol. 103, p. 054104, 2013.
5. M. Panjan and A. Anders, "Plasma potential of a moving ionization zone in DC magnetron sputtering," *J. Appl. Phys.,* vol. 121, p. 063302, 2017.

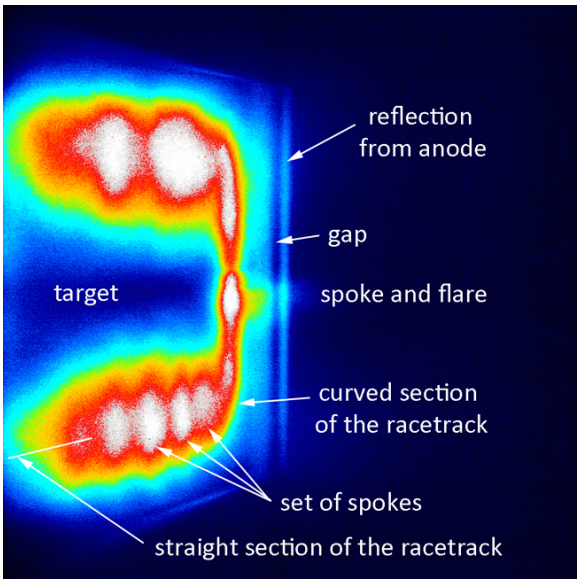

Figure 1: Oblique angle view on one end of a linear magnetron: intensity of emitted light in the visible spectrum is shown in false color, 3 ns image from a fast camera., Ti target in 0.3 Pa of argon, HiPIMS current of 900 A.

Application of Plasma Monitoring and Diagnostic Techniques for the Reactive High power Impulse Magnetron Sputtering

Jyh-Wei Lee,[1,2,3,*]

[1] Dept. of Materials Engineering, Ming Chi University of Technology, Taiwan
[2] Center for Thin Film Technologies and Applications, Ming Chi University of Technology, Taiwan
[3] College of Engineering, Chang Gung University, Taiwan

Abstract:
Reactive sputtering for coatings has been widely used in many industrial applications. The target poisoning issue is important for reactive sputtering when a compound thin film is deposited at the sputtering target surface causing a decreased deposition rate. High power impulse magnetron sputtering (HiPIMS) technique has been developed for more than 19 year, which opens a new era in the surface engineering and functional coating fabrication application. In terms of process control, reactive HiPIMS has greater challenges for selecting proper working conditions, such as duty cycle, frequency, reactive gas ratio and so on than these of non-reactive HiPIMS. The plasma monitoring and diagnostic techniques for understanding the plasma status and target poisoning ratio become very useful during the reactive HiPIMS. In general, the plasma sampling mass spectrometer (PSM), optical emission spectroscopy (OES) and plasma emission monitoring (PEM) techniques are frequently used in the reactive HiPIMS process. The time-averaged ion energy distribution function (IEDF) provided by PSM plasma ion analyzer can give information of ions arriving to the substrate during deposition. Meanwhile, the OES signal implies the poisoning of the target or the partial pressure of the reactive gas in the chamber. Through the rapid feedback control of piezoelectric valve by PEM system, the partial pressure, the inlet reactive gas rate into the sputtering system and the stoichiometry of thin film can be well controlled. In this work, the PSM, OES and PEM techniques were used to study the fabrication of TiN, ZrN, TiCrSiN, TiCrBN and Cr_xC_y hard coatings by reactive HiPIMS and reactive superimposed HiPIMS-MF systems. The PSM technique was employed to diagnose the influence of a radio frequency target power on the plasma status during the deposition of TiCrSiN hard coatings by a reactive hybrid HiPIMS-RF system. The PEM technique was adopted for growing TiN, ZrN, TiCrBN and CrxCy hard coatings at different target poisoning ratios by reactive superimposed HiPIMS-MF technique. Effects of different PEM controlled target poisoning ratios on the microstructure, chemical composition and mechanical properties of such hard coatings were discussed. The important key factors of plasma monitoring and diagnostic techniques for the deposition of hard coatings by reactive HiPIMS was highlighted in this work.

Keywords: Reactive high power impulse magnetron sputtering (HiPIMS), Plasma sampling mass spectrometer (PSM), Optical emission spectroscopy (OES), Plasma emission monitoring (PEM), TiN, ZrN, TiCrSiN, TiCrBN, Cr_xC_y

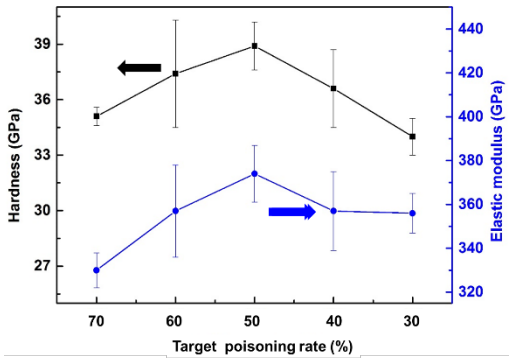

Figure 1: Hardness and elastic modulus of TiCrBN coatings grown under different target poisoning ratios.

References:

1. Anders. A. (2017), Tutorial: Reactive high power impulse magnetron sputtering (R-HiPIMS), *J. Appl. Phys.* 121,171101-34.

Ionized PVD and Hybrid Processes

H. Barankova,[1,2,*] L. Bardos,[1,2]

[1] Uppsala University, Angstrom Laboratory, Uppsala, Sweden
[2] BB Plasma Design AB, Uppsala, Sweden

Abstract:
Non-equilibrium plasma sources used for film deposition, in surface treatment or for plasma-chemical reactions need to provide stable and reproducible processes in order to achieve desirable properties of films, surfaces and reaction products. High and even tunable activation degree in the plasma is desirable so that enhanced properties of the deposited film and high deposition rates are achieved and tuning the film properties is possible.
Very efficient plasma sources that can be used directly for PVD, PE CVD or for hybrid combination of PVD and PE CVD are hollow cathodes. It has been shown for the reactive hollow cathode PVD, for example, that the deposition rate of TiN can substantially exceed the deposition rate of Ti, and similar effects have been shown also for AlN and CrN.
The paper shows different solutions of hollow cathode based plasma sources both for reduced and atmospheric pressures. The linear hollow cathodes in several arrangements for generation of plasma over large areas and suitable for further scale-up are presented. Examples of surface processing and coating by PVD, both by the Hollow Cathode Discharge and Hollow Cathode Arc, are given. A new type of planar magnetron in which the target is coupled with the hollow cathode magnetized by the magnetic field of the magnetron is described. Detailed principles of such arrangements are explained. Concept of a hybrid source combining the hollow cathode with the ECR, as well as cold atmospheric plasma sources Fused Hollow Cathode (FHC), and Hybrid Hollow Electrode Activated Discharge (H-HEAD) are discussed.

Keywords: ionized PVD, hybrid plasma source, hollow cathode, linear hollow cathode, hollow cathode arc, magnetized hollow cathode, reactive deposition in ionized magnetron, hollow cathode enhanced target, Fused Hollow Cathode

Determination of momentum and energy fluxes in plasma surface processing

H. Kersten*, T. Trottenberg, A. Spethmann, M. Klette, L. Hansen

Institute for Experimental and Applied Physics, Kiel University, Kiel, Germany

Abstract:
For an optimization of plasma-based processes as thin film deposition suitable diagnostics are required. In addition to well-established plasma diagnostic methods (e.g. optical emission spectroscopy, mass spectrometry, Langmuir probes, etc.) we perform examples of "non-conventional" low-cost diagnostics, which are applicable in technological plasma processes. Examples are the determination of energy fluxes by calorimetric probes and the measurement of momentum transfer due to sputtered particles by force probes. In particular, energy and momentum transfer transport through the plasma sheath (Fig.1) combined with the possibility to measure the effect of charge carriers as well as energetic neutrals are of interest.

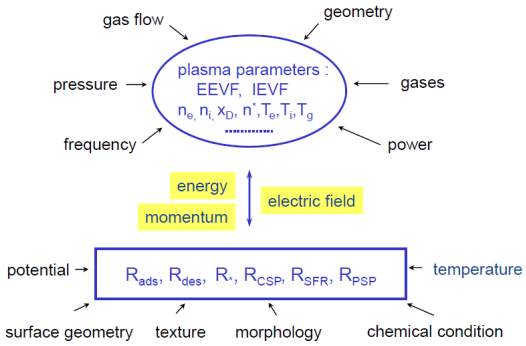

Figure 1: Interaction between process plasma and substrate surface via the sheath: the macroscopic parameters influence the internal properties of the plasma and the surface.

The total energy influx from plasma to a substrate can be measured by special calorimetric sensors [1]. One method is the passive thermal probe (PTP) based on the determination of the temporal slope of the substrate surface temperature (heating, cooling) in the course of the plasma process. By knowing the calibrated heat capacity of the sensor, the difference of the time derivatives yields the integral energy influx to the surface. Simultaneously, the electrical current to the substrate can be obtained and by variation of bias voltage the energetic contribution of charge carriers can be determined. By comparison with model assumptions on the involved plasma-surface mechanisms the different energetic contributions to the total energy influx can be separated [2].
Furthermore, for thin film deposition by sputtering it is essential to determine the sputtering yield as well as the angular distribution of sputtered atoms. In addition to model calculations (TRIM, TRIDYN etc.) an experimental determination of the related quantities is highly demanded. For this purpose, we developed interferometric force probes [3]. Such a quite sensitive probe bends a few µm due to momentum transfer by the bombarding and released particles, i.e. sputtered target atoms and recoiled ions. By knowing the material properties of the cantilever and by measuring its deflection, the transferred momentum, e.g. the force in µN range, can be determined experimentally. In the present study measurements are compared with TRIM simulations for different experimental discharge conditions.

Keywords: plasma process diagnostics, energy flux, momentum flux, force probe, thermal probe, thin film deposition, sputtering

References:

1. Kersten, H., Deutsch, H., Stefen, H., Kroesen G.M.W., Hippler, R., (2001) The energy balance at substrates during plasma processing, *Vacuum,* 63, 385-431.
2. Gauter, S., Haase, F., Kersten, H., (2019) Experimental unraveling the energy flux originating from a DC magnetron sputtering source, *Thin Solid Films*, 669, 8-18.
3. Trottenberg, T., Spethmann, A., Kersten, H., (2018) An interferometric force probe for beam diagnostics and the study of sputtering, *Eur. Phys. J. TI*, 5, 3.

Taylored Growth Process of Ultra-Thin Films by Magnetron Plasma

T. Minea*, F. Cemin, M. Rudolph, D. Lundin

[1]Laboratoire de Physique des Gaz et des Plasmas (LPGP), UMR 8578 CNRS, Université Paris-Sud, Université Paris-Saclay, 91405 Orsay, France
*Corresponding author: tiberiu.minea@u-psud.fr

Abstract:
The Ionized Physical Vapor Deposition (IPVD) technologies and particularly the High Power Impulse Magnetron Sputtering (HiPIMS) are beneficially explored for griwing ultra-thin fims. HiPIMS has emerged in last two decades as one of the most promising process leading to improved material properties in terms of density, adhesion, conductivity, structure, etc.
Most of the works reporting thin films grown by HiPIMS emphasize the positive role played by the ionized sputtered species that are the film precursors together with sputtered neutrals. Moreover, the flux ionized fraction of the precursors reacing the substrate was ofthen taken as the key parameter for improving the film quality. Here, is stressed out the key-role played by the precursors energy and not only by the flux fraction. Several recent optimized materials, metal (Cu) and compounds (TiO_2, TiN and TaNO) – demonstrate the coherence of this finding, especially for very thin coatings. The precursonr energy can be mastered by suitale biasing the substrate in HiPIMS, but also by enchancing the ion transport towards the substrate witout icreasing their energy in modified convention magnetron.
For metal films of copper, HiPIMS can be successfully used for epitaxial growth in one-step process (no pre-treatment) [1]. The electrical conductivity of ultra-thin films reaches half of the bulk value for (< 100 nm), as high as the filtered arc deposited films. These results are directly correlated with the crystalline orientation, the grain size and the plasma properties.
Second, HiPIMS can be tuned to grow pure anatase metastable phase of TiO_2 in reactive mode operation, when up to now only rutile has been reported by HiPIMS. Moreover, the deposition rate is highly increased compared to conventional direct current magnetron. The control of the impinging energy of ions drastically reduced the stress for the ultra-thi films or thicker. The same reduction of the stress has been recorded in the case of TiN, even if some other plasma parameters are different.
Finally, Ta_3N_5 can be sucessfully grown by the addition of an axial magnetic confinement of the plasma, in conventional magnetron, leading to ion production just in front of the substrate. Hence, this particular deposition process favorably increases the flux of low energy ions. Moreover, the surface of such prepared films is nanostructured [2].
In conclusion, the deep understanding of the plasma magnetron deposition process and the discrimination between the effect of precursor flux and the precursor energy contributing to the film growth has been exploited to optimize ultra-thin films for a large panel of energy relevant applications, *i.e.* ultra-thin conducting layers, photocatalysis, photoelectrolysis, hard and low friction, etc.

Keywords: HiPIMS; magnetron sputtering; thin films

References:

1. F. Cemin, D. Lundin, C. Furgeaud, A. Michel, G. Amiard, T. Minea, and G. Abadias, Scientific Reports 7 (2017) 1655; doi:10.1038/s41598-017-01755-8
2. M. Rudolph, A. Demeter, E. Foy, V. Tiron, L. Sirghi, T. Minea, B. Bouchet-Fabre, M.-C. Hugon, Thin Solid Films 636 (2017) 48; http://dx.doi.org/10.1016/j.tsf.2017.05.033

Control of the deposition temperature and nanostructure of silicon and titanium oxide thin films in PECVD routes

A. Granier,[1,*] D. Li,[1,3] M. Richard-Plouet,[1] S. Bulou,[2] P. Choquet,[2] A. Goullet[1]

[1] University of Nantes, CNRS, Institut des Matériaux Jean Rouxel, Nantes, France
[2] Materials Research and Technology Department, Luxembourg Institute of Science and Technology, Esch-sur-Alzette, Luxembourg.
[3] College of Mechanical Engineering, Yangzhou University, Yangzhou 225127, China

Abstract:
There is an increasing interest in developing surface treatment processes close to room temperature, for instance for flexible electronics. Pulsed Plasma Enhanced Chemical Vapor deposition (PECVD) is one route to simultaneously monitor the film properties, taking advantage of the out of equilibrium cold plasma, and to reduce the deposition temperature of thin films. Thin films generally deposited above 300°C were shown to be successfully deposited by PECVD on thermally sensitive substrates such as polymeric films. The challenge is to control the density and kinetics of active species (ions and radicals) impinging on the growing film so that thin films with the desired properties are obtained at much lower temperature than in conventional deposition routes requiring at least one step at high temperature.
The opportunities and challenges in the deposition of silicon and titanium oxide based films at low temperature by PECVD will be presented. The effect of the plasma parameters (pressure, positive ion energy, plasma pulsing…) on the film nanostructure and properties (optical, electrical and photocatalytic properties) will be investigated in detail. First, in the case of TiO_2 thin film deposition, different strategies leading to amorphous or cristallized films, according to the plasma conditions are discussed.
Radiofrequency inductively coupled plasmas (ICP) operated in contiunuous (CW) and pulse mode (at a frequency in between 200 Hz and 5 kHz) at low pressure were used. The film growth was monitored by in situ spectroscopic ellipsometry.The film nanostructure was characterized by Transmission Electron Microscopy, Raman spectroscopy, Selected Area Electron Diffraction (SAED) and X-Ray Diffraction.. The photocatalytic activity was studied by measuring methylene blue decomposition in aqueous solution under UV exposure.
The ICP plasma was previously shown to yield dense SiO_2 films at low temperature [1] and to allow the control of the crystalline phase (anatase and/or rutile) of TiO_2 thin films according to the ion energy [2]. It was furthermore recently shown that pulsing the ICP plasma allows the deposition of nanocrystallized anatase TiO_2 photocatalytic films on silicon and polymeric substrates at $T < 80°C$, whereas anatase is usually obtained above 300°C [3].
Finally, different approaches leading to the deposion of mixed titanium and silicon oxide films will be presented.

Keywords: Plasma Enhanced Chemical Vapor deposition, PECVD, pulsed plasma, titanium oxide, anatase.

References:

1. A. Bousquet, A. Granier, A. Goullet, J.P. Landesman, Influence of plasma pulsing on the deposition kinetics and film structure in low pressure oxygen/ hexamethyldisiloxane rf plasmas, *Thin Solid Films* 514, 45-51 (2006)
2. D. Li, M. Carette, A. Granier, J. P. Landesman, A. Goullet, Effect of ion bombardment on the structural and optical properties of TiO_2 thin films deposited from oxygen/ titanium tetraisopropoxide inductively coupled plasma, *Thin Solid Films* 589 (2015) 783.
3. D. Li, S. Bulou, N. Gautier, S. Elisabeth, A. Goullet, M. Richard-Plouet, P. Choquet, A. Granier, Nanostructure and photocatalytic properties of TiO_2 films deposited at low temperature by pulsed PECVD, *Applied Surface Science,* 466, 63-69 (2019)

Femtosecond Laser 3D Processing for Fabrication of Functional Micro- and Nano-Systems

Koji Sugioka

[1] RIKEN Center for Advanced Photonics, Wako, Saitama, Japan

Abstract:
The extremely high peak intensity associated with ultrashort pulse width of femtosecond laser allows us to induce nonlinear multiphoton absorption with materials that are transparent to the laser wavelength. More importantly, focusing the femtosecond laser beam inside the transparent materials confines the nonlinear interaction only within the focal volume, enabling three-dimensional (3D) micro- and nanofabrication. This 3D capability offers three different schemes, which involve undeformative, subtractive, and additive processing. The undeformative processing preforms internal refractive index modification to construct 3D optical microcomponents including optical waveguides inside transparent materials. Subtractive processing can realize the direct fabrication of 3D microfluidics, micromechanics, and photonic microcomponents inside glass. Additive processing represented by two-photon polymerization (TPP) enables the fabrication of 3D micro- and nanostructures made of not only polymer but also protein for photonic, microfluidic, and biological applications. Furthermore hybrid approach of different schemes can create much more complex 3D structures and thereby promises to enhance functionality of micro- and nano-devices.

For example, a successive procedure of subtractive 3D glass micromachining and the undeformative optical waveguide writing realizes optofluidics for detection, manipulation, and sorting of bio samples.[1] Meanwhile, combination of subtractive 3D glass micromachining and additive TPP is not only an instrument that can tailor 3D structures but also a tool to fabricate biomimetic in vivo environment inside glass microfluidic chips.[2] Specifically, the subtractive 3D glass micromachining can flexibly fabricate 3D microfluidic structures embedded in glass microchips without a complicated procedure of stacking and bonding of glass substrates. Successive TPP can then integrate complex shapes of polymer structures with a submicrometer feature size due to its high fabrication resolution to create biomimetic structures inside the glass microfluidics. Thus, such advanced biochips can be utilized to study the mechanism of cancer cell invasion and metastasis.[3] Furthermore, the subtractive 3D glass micromachining followed by femtosecond laser direct write ablation and successive electroless metal platig enables selective metalization of 3D glass microfluidic chips for electrical control of livng cell movement in 3D.[4] This selective mtallization technique is also applied to fabricate 3D microfludic surface-enhanced Raman spectroscopy (SERS) sensers with an extremely high enhancement factor by formation of pereodic nanodot structures on the plated metal thin fills by using the fa laser.[5]

This talk presents our recent achievements on fabrication of functional 3D micro- and nano-systems including microfluidics, optofluidics, microsensors, and 3D proteinaceous microstructures by femtosecond laser 3D processing.

Keywords: femtosecond laser, 3D processing, biochip, SERS sensor, LIPSS.

References:

1. K. Sugioka, et al., Laser Photon. Rev. 3, 386-400 (2010).
2. D. Wu, et al., Light Sci. Appl. 4, e228 (2015).
3. F. Sima, et al., ACS Appl. Bio Mater. 1, 1667-1676 (2018).
4. J. Xu, et al., Microsystems Nanoengin. 3, 16078 (2017).
5. S. Bai, et al., Adv. Func. Mater. 28, 1706262 (2018).

Fabrication and proformance analysis of protective coating deposited on nickel alloy used in nuclear reactor

Yanhong.Liu,[1*] Mingmin.Zheng [1], Xiaojing.Wang[1], Huailin.Li[1], Yanghui.Lu[1],Haihong.Xia[1]

[1] State Power Investment Corporation Science and Technology Research Institute, Beijing, China

Abstract:
Surface modification and coating technology has extensive used in industry fields. It is an economic and short times period method. Structure materials of nuclear power plant faced serious corrosion wear and oxidation problems. Surface modification or coating method is an effective technique to solve these problems. In this research, we use protective coating to alleviate corrosion problem of nuclear structural materials. Electro-deposition method is applied to obtain pure nickel layer on nickel alloy substrate, the interface between coating and substrate is analysis by EBSD and the microstructure and component of coating was observed by SEM and EDS. The application performance of materials on molten salt reactor (MSR) was tested used an experimental apparatus in molten FLiNaK salts at 700 ℃.Results show that nickel layer on the inside of nickel alloy tube has excellent corrosion resistance. The main depleted element of sample in molten salts is Ni. Ni contents in molten salts that after corrosion higher than before. It does indicate that pure nickel coating was responsible for the better corrosion resistance.

Keywords:coating, corrosion resistance,electrodeposition, nickel alloy, nuclear.

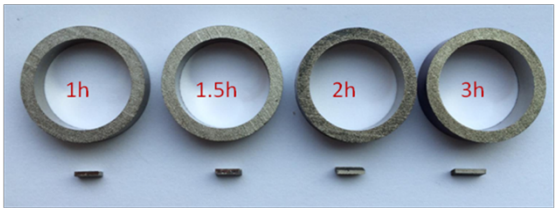

Figure 1: The samples were obtained at the different durations respectively: 1h,1.5h,2h and 3h from left to right.

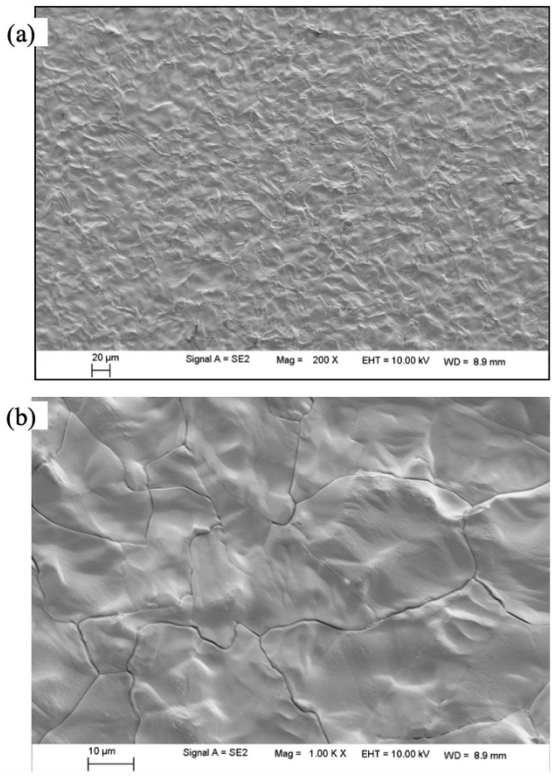

Figure.2: The SEM micrography of protective coating on alloy substrate after molten corrosion test at 700℃ for 400 hours.(a) 200x magnified image;(b) 1000x magnified image; SEM images show the excellent corrosion resistance of the coatings. The surface is uniform and density after molten corrosion.

References:

1. Zheng M G, Ye C, Han X. Nuclear power development in new energy sources [J]. Nucl. Tech., 2010, 33(2): 81-86
2. David L. Too good to leave on the shelf [J]. Mech. Eng., 20l0(5): 29-33

Product Orientated Optimization of Coating Processes by Acoustic Levitation

D. L. Wong,[1] A. Reinbeck,[1] S. C. Müller,[1] H.-U. Moritz,[1] W. Pauer[1*]

[1]University of Hamburg, Institut for Technical and Macromolecualr Chemistry, Hamburg, Germany

Abstract:
In a fluidized bed reactor the pellets swirl randomly around, causing difficulties to track the coating process of a single particle. Moreover, the coating process can be influenced by many constraints, such as the coating material, the temperature and the spraying method. Therefore, a direct optimization of a coating process in the fluidized bed reactor is inefficient, especially regarding the resources.
To solve this issue, the acoustic levitation was applied as a model system to optimize a coating process in the fluidized bed reactor, since non-spherical and light particles can be levitated.[3] As pellets are small, light and not completely spherical, an aerodynamic levitator cannot be used.[1, 2] In an acousitc levitation a single particle can be placed in a contactless position while being coated by an ultrasonic nozzle. Here, the single pellet was coated with nanomaterial, either polyvinylpyrrolidone (PVP, adhesive) or EUDRAGIT® polymers, in order to have coatings of different polarity. For each coating a design of experiments has been performed in the acoustic levitator in order to analyze the effects of the coating material, the temperature, the spraying time and compressed air on the mass of coating thickness. The coating process of a pellet was tracked in the acoustic levitator by means of a high speed camera and a light source. In addition, the pellets were coated in a fluidized bed reactor in order to compare the morphology of the obtained thin film by means od scanning electron microscopy and to deviate scale up rules. This noval and innovative transfer [3] from the acoustic levitator into the fluidized bed reactor will contribute to future coating processes. Commonly various coating processes of small particles can be analyzed in the acoustic levitator.

Keywords: coating process, model system, pellets, acoustic levitation, fluidized bed reactor, polymer, nanomaterial, adhesive, process tracking, thin film

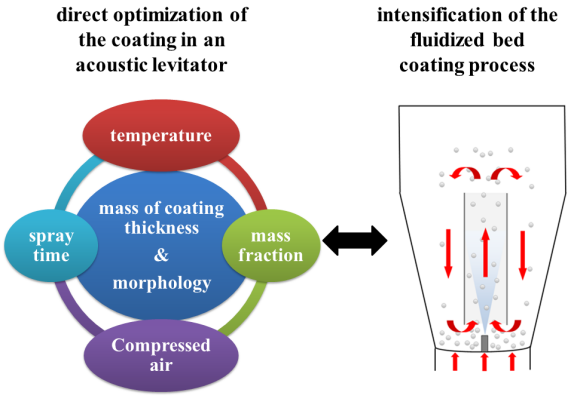

Figure 1: A noval and innovative optimization of a coating process has been illustrated, where a direct optimization has been performed in an acoustic levitator and where those results have been transferred from the acoustic levitator into the fluidized bed reactor.

References:

1. KARLSSON, S., A. RASMUSON, I.N. BJÖRN und S. SCHANTZ. Characterization and mathematical modelling of single fluidised particle coating [online]. *Powder Technology,* 2011, **207**(1-3), 245-256. ISSN 00325910. Verfügbar unter: doi:10.1016/j.powtec.2010.11.006
2. GANDHI, A.S., A. SARAVANAN und V. JAYARAM. Containerless processing of ceramics by aerodynamic levitation [online]. *Materials Science and Engineering: A,* 1996, **221**(1-2), 68-75. ISSN 09215093. Verfügbar unter: doi:10.1016/S0921-5093(96)10449-4
3. UNIVERSITY OF HAMBURG. VERFAHREN UND VORRICHTUNG ZUR BESCHICHTUNG EINES EINZELNENPARTIKELS. Erfinder: D. L. WONG, S.C. MÜLLER, A.-L.S. WIRSCHING, W. PAUER UND H.-U. MORITZ. Anmeldung: 13. Dezember 2017. Germany. amt. Aktenzeichen 10 2017 129 763.4.

Influence of processing conditions on deposit layer formation by barrel nitriding treatment on aluminum alloy

K. Nambu,[1,*] K. Sayo,[1,] M. Okumiya[1]

[1] Toyota technological Institute, Aichi, Japan

Abstract:
In recent years, demand for aluminum alloys has increased in transportation equipment such as automobiles. However, since the strength is lower than that of steel, high strength by surface treatment is required. Nitriding is one of surface treatments. The nitriding treatment can improve hardness and frictional wear characteristics by forming aluminum nitride on the surface. For the formation of AlN, a reduction nitriding method, an ion nitriding method, or the like can be mentioned.Since the former is a process above the melting point, it can not be processed, and the latter has a problem that the processing time is long.
In this study, the barrel nitriding method was focused at a temperature lower than the melting point of Al and short process time. However, in the barrel nitriding process, there is a problem that a deposition layer is formed as AlN is formed and the surface shape is deteriorated. In this study it has been investigated the effects of processing conditions on the formation of the deposited layer
In the barrel nitriding method, an abrasive and an activator are charged into a furnace, and a rotary motion is applied to perform treatment while polishing and removing a surface oxide film of Al which hinders nitriding.Fig. 1 shows a schematic view of a barrel nitriding apparatus. Experiments were conducted under the three conditions shown in Table 1 in consideration of nitriding time, gas flow rate and furnace rotation speed. The cross-sectional structure after treatment is shown in Fig.2. The nitrided layer and the deposited layer were confirmed under all the conditions. In Condition 1, it was confirmed that the deposition layer was most suppressed. However, the nitride layer thickness also decreases accordingly. From this result, it is considered that the nitrided layer is formed by supply of nitrogen from the deposited layer to the aluminum alloy.

Keywords: Surface modification, Barrel nitriding, Aluminum Nitrid.

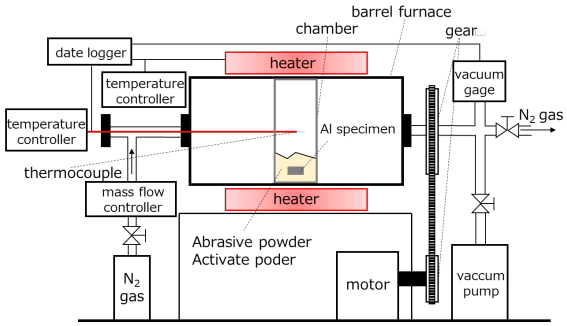

Figure 1: Experimental apparatus of barrel nitriding treatment.

Table 1:Treatment conditions

Treatment condition	1	2	3
Nitriding time	3 hour		
Nitrogen gas flow	10 l/min.		1 l/min.
Rotating velocity	72 r.p.m	36 r.p.m	9 r.p.m

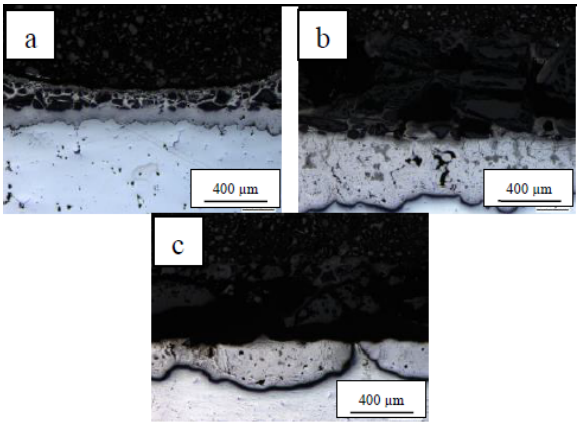

Figure 2: Cross-sectional micrographs of deposit layer and nitriding layer.(a: condition 1, b: condition 2, c: condition 3)

SurfCoat Korea 2019
Session II A: Functional / Multi-functional, composite / hybrid, graded and multilayers coatings

Siloxane Based Flexible Hard Coating for Foldable Smartphone Cover Window Film

Byeong-Soo Bae[1,2*], Gwang-Moon Choi[1,2], Jihoon Ko[2]

[1] Wearable Platform Materials Technology Center, Department of Materials Science and Engineering, KAIST, Daejeon, Republic of Korea
[2]Solip Tech. Co., Ltd., Dajeon, Republic of Korea

Abstract:
Recently, major smartphone companies have unveiled prototypes of the foldable smartphone and publicized it would be commercialized maybe in this year. The biggest technical challenge in implementing a foldable smartphone is replacing the glass used on the cover with a plastic film. Cover plastic film that replace chemically reinforced (Gorilla®) glass must be mechanically durable enough to withstand a smaller folding radius when folded hundreds of thousands of times. In addition, additional hard coating on the surface are required to protect against scratches. In terms of the reliability of the smartphone, it must have excellent mechanical properties to withstand the various stresses and strains that occur when the device is folded. A flexible hard coating for foldable displays is realized by the highly cross-linked polymer siloxane hybrid using structure-property relationships in organic-inorganic hybridization. Nanoindentation and micro-bending tests of siloxane hybrid material were made to confirm high strength but low modulus with excellent elastic recovery. Thus, glass-like wear resistance, plastic-like flexibility and highly elastic resilience are demonstrated together with outstanding optical transparency. It provides a framework for the application of epsiloxane hybrids in protective hard coatings with high scratch resistance and flexibility for flexible displays. This is currently being commercialized as a brand name of Flex9H® for application to foldable smartphone.

Keywords: flexible hard coating, foldable smart phone, cover window film, siloxane hybrid, sol-gel process

References:

1. Choi, G.-M., Jin, J., Shin, D., Kim, Y.H., Ko, J.-H., Im, H.-G., Jang, J., Jang D., Bae, B.-S. (2017) Flexible Hard Coating: Glass-like Wear Resistant, yet Plastic-like Compliant, Transparent Protective Coating for Foldable Displays *Advanced Materials*, 29, 1700205.

Silver nanowire/graphene-based Thin Film for Transparent Electrode and Thermal Heater Applications

Ji Won Shin,* Eunhye Jeong, Yong-Ho Choa

Hanyang University, Department of Material Science and Chemical Engineering, Ansan, Korea

Abstract:
A transparent electrode (TE) has attracted great attention as a transparent thin film heater in various industrial applications, including outdoor display, smart window in automobile or residence, and flexible optoelectronic device. TE materials, such as carbon nanotube, graphene, and metallic nanowires have emerged for an alternative of indium tin oxide due to its low cost-efficiency and brittleness. Among them, silver nanowire (AgNW) is the most promising material for a next-generation flexible TE with a high transparency, electrical conductivity and mechanical flexibility. There have been many studies on the fabrication of AgNW-based TE by employing a scalable solution process.
Herein, a solution process coating has been developed *via* a formation of uniform AgNW networks assisted by a cellulose as a dispersant and binder to enhance an adhesion on polyethylene terephthalate (PET) substrate. The effective formation of AgNW networks on PET substrate reduced the sheet resistance and improved the transmittance of TE. By controlling the composition of solution; solvent-binder-AgNW ratio, the AgNW-based TE was constructed with an outstanding Figure of Merit (> 250). In addition, graphene was coated on the AgNW to enhance a heating performance. Graphene plays a role toward transfer heat in a lateral direction as well as diffuse the local heat distribution uniformly. The morphology of graphene-coated AgNW was confirmed by field emission scanning electron microscope (FE-SEM).
The AgNW-based thermal heater exhibited a high operating temperature and heat distribution by Joule heating, which resulted in a saturated temperature of ~93°C at a low input voltage below a bias of 10 V. The thermal heater also has excellent optical and electrical properties with a transmittance (> 90%) at wavelength of 550 nm and low sheet resistance (< 50 Ω/□). By coating a few layers of graphene, the thin film heater has an optical transparency of 88%T and sheet resistance of 20 Ω/□. Uunder applying voltage of 5 V, AgNW/graphene-based heater showed a high average temperature (60°C). (Figure 1) In contrast, an AgNW-based heater exhibited a heating characteristic of 50°C at the same condition.
We expect that AgNW/graphene-based heater will be attributed to a large area transparent thin film heater through a uniform temperature distribution.

Keywords: transparent electrode, thermal heater, silver nanowire, graphene, thin film, solution process.

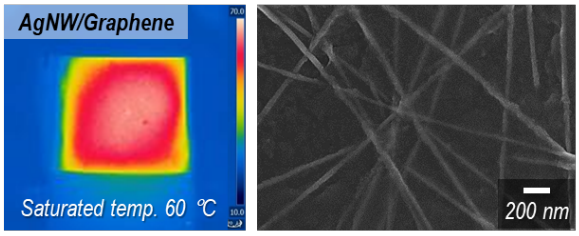

Figure 1: (left) infrared image of the AgNW/graphene-based thin film composite; (right) FE-SEM micrograph of the morphology of graphene-coated AgNW network.

References:

1. S. Ye, A. R. Rathmell, Z. Chen, I. E. Stewart, B. J. Wiley, Metal nanowire networks: the next generation of transparent conductors. *Advanced Materials* **26**, 6670-6687 (2014).
2. L. Hu, H. S. Kim, J.-Y. Lee, P. Peumans, Y. Cui, Scalable coating and properties of transparent, flexible, silver nanowire electrodes. *ACS nano* **4**, 2955-2963 (2010).

Corona discharge mitigation of HV transmission lines by surface modification

N. K. Tnyshtykbayev[1], N. Zhakiyev[1], J. Norem[2], Z. Insepov,[1,3,4*]

[1] Nazarbayev University, Astana, Republic of Kazakhstan
[2] Nanocynergy Corp., Downers Grove, IL USA
[3] National Nuclear Research University (MEPhI), Moscow, Russian Federation
[4] Purdue University, West-Lafayette, IN USA

Abstract:
On HVAC transmission lines the second type of electric power losses (up to 30% of total losses) after Joule heating is corona discharge (CD). A peak of losses happens under adverse (wet) weather conditions, such as rain and snow. New aluminum surface coatings were developed based on high-temperature alumina α-Al2O3, reinforced with graphene oxide and carbon nanotubes.
Surface modification based on high-temperature alumina α-Al2O3 microarc oxidation for changing droplet formation conditions (or parameters) on transmission lines were carried out. As a result, a significant decrease of the power loss due to corona of 30-50% has been measured. At the same time, the voltage of the corona initiation increases in the conditions of rain to 40% and dry climate to 15%. High anti-corona resistance of wire samples is achieved by coatings based on the alloys of high-temperature alumina α-Al2O3, silicon oxide SiO2, and silicon carbide SiC, modified with graphene oxides and carbon nanotubes[1].
Finite element method (FEM) showed a significant dependence of a local electric field enhancement factor for surface wettability. The simulation results on COMSOL Multiphysics obtained using Plasma Physics and Electrostatics interfaces. Surface modification changes (decreases) contact angle of water droplet on an alumina surface and reduced surface roughness.
The results of high-voltage testing showed that the samples with proposed coatings were more resistant to corona discharge development. Indeed, the onset of CD generationon these samples was observed at higher voltages as compared to those for the uncoated wire-A4.

Keywords: alumina α-Al2O3, graphene oxide, carbon nanotubes coatings. Electric field mitigation.

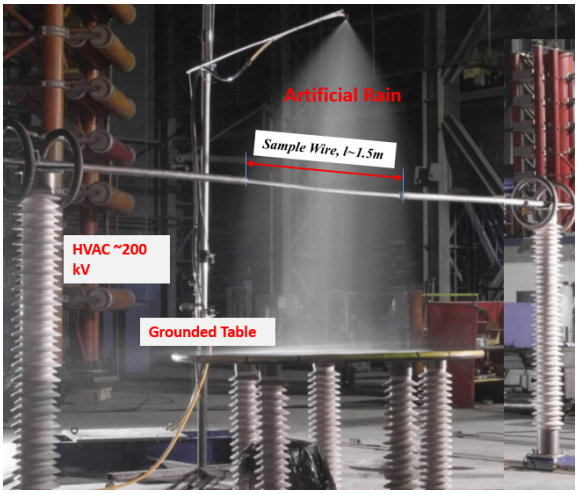

Figure 1: HVAC~200 kV real conditions tests were carried out on the wire–plane electrode system under rainfall and dry climate conditions [1].

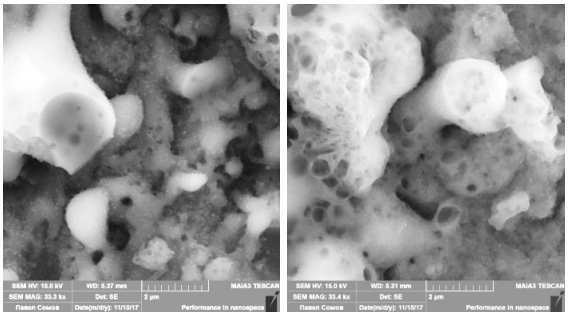

Figure 2: Electron-microscopic images of the surface of wire samples showed high anticorona resistance due to their hydrophilic properties related to the surface porosity.

References:

1. Tynyshtykbaev, K. B., Imanbaev, G. Z., Ainabaev, A. M., & Insepov, Z. A. (2018). Reducing Power Losses in Corona Discharge under Rainfall Conditions. *Technical Physics Letters,* 44(6), 545-547.

SurfCoat Korea 2019
Session II B: Surfaces and coatings characterization and properties

Roughness influence on self-adaptation and self-healing of DLC-MoS_2 wear protective, low-friction coatings on 3D printed polymers

J.M. Lackner[1,*], W. Waldhauser[1], L. Major[2], M. Kot[3], Paul Angerer[4]

[1] JOANNEUM RESEARCH Forschungsges.m.b.H., Institute for Surface Technologies and Photonics, Niklasdorf (Austria)
[2] Polish Academy of Sciences, Institute for Metallurgy and Materials Sciences, Krakow (Poland)
[3] AGH University of Science and Technology, Faculty of Mechanical Engineering and Robotics, Krakow (Poland)
[4] MCL Materials Center Leoben Forschung GmbH, Leoben (Austria)

Abstract:
The 3D printing of polymers is becoming increasingly important as an industrial manufacturing process for small and medium series in automotive and aerospace production. However, the post-processing to fulfil the necessary mechanical-tribological properties for high-performance applications, e.g. for sliding bearings, are currently unsolved for common 3D printing thermoplast polymer materials. In particular, the high roughness of e.g. selective laser sintered (SLS) components from polyamide (PA 12) poses a major challenge for any surface treatment.
This work solves this bottleneck by means of physical vapour deposition (PVD), applying coatings of solid lubricants (diamond-like carbon (DLC, a-C: H) and MoS_2) by high-power pulsed magnetron sputtering (HIPIMS) with a thickness of 4-5 µm, whereby the coating temperature is kept low (<60°C) to prevent polymer degradation or distortion. However, this thickness, chosen due to economic feasibility for future transfer to production, is significantly less than the substrate roughness of the PA 12 surfaces after SLS layer-by-layer manufacturing and standard ball-blasting post-processing. Consequently, additional standard post-processing based on dip and spray coating with paints of different viscosity was performed in order to check the influence of reduced surface roughness on dry, unlubricated sliding under conditions of high Hertzian pressures.
Results show, that even extreme overloading conditions (Hertzian contact pressures of ~130 MPa) lead to only minimal wear at very low coefficients of friction (<0.15) in the performed reciprocal linear-tribological tests. Further, the rougher, non-organically and only PVD coated samples show completely different initial wear mechanisms compared to the dip- and spray-coated PA12 substrates with 50-70% lower roughness due to partial melting of the thermoplastic polymer (especially at the roughness tip sites) under the friction heat, while the cross-linked thermoset coatings have higher thermal stability. For the non-organical coated PA12, especially a-C:H coatings with low MoS_2 content reveal a transfer of sheared coatings and polymer particles from roughness peaks in valleys (self-adaptation to the counterpart surface), whereby the formed transfer layer is rather free of cracks. After this run-in phase and the adaptation to the Al_2O_3 counterbody geometry, the friction mechanisms and level of friction cefficients are rather similar to the PVD coatings on the smoother thermoset layers: In both cases, any developing cracks were found to be filled with transferred abraded low friction coating material as a self-healing mechanism. In conclusion, this keeps friction and, reasonably, shear forces and the wear rate low.

Keywords: Selective laser sintering, magnetron sputtering, polyamide, molybdenum disulfide, diamond-like carbon

Wear Resistance of Electrodeposited Ni-P and Ni-B-TiO_2 Sol-enhanced Nano-composite Coatings

S. Sheikholeslami,[1*] W. Gao,[1] Y. Wang,[1]

[1] The University of Auckland, Department of Chemical and Materials Engineering, Auckland, New Zealand

Abstract:
Applying coatings is one of the most efficient methods to combat wear. Among different coating methods, electrochemical deposition is the most common and appreciated method due to its simple processing and low cost. For the coating material selection, there are many available options that are compatible with electrodeposition methods. Nickel is one of the major preferences since it has both good corrosion resistance and mechanical properties. To improve the coating properties, many developments have been introduced. This paper is focused on the Ni-P, Ni-B and doping enforcing particles in the coating to create a composite. NI-P coatings are known to have both good corrosion and wear resistant coatings to be used in many different industries. Compared with conventional coatings, however, composite coatings have exquisite properties. If the size of doping particles decreases and their dispersion through the coating improves, the overall properties of the coating are enhanced. Thus, instead of simple composite coatings, micro and nano-composite coatings have been developed. Ni-B was believed to be the best coating regarding tribological behavior. Our work indicated that the sol-enhanced nano-composite Ni-B-TiO_2 coating is the best coating to protect the surface against wear. Heat treatment of the electrodeposited Ni coatings also results in excellent effect on the tribological behavior according to the studies in this research group.

Keywords: electrodeposition, nano-composite, sol-gel enhancement, Ni-B coating, Ni-P coating, duplex coating, wear resistance

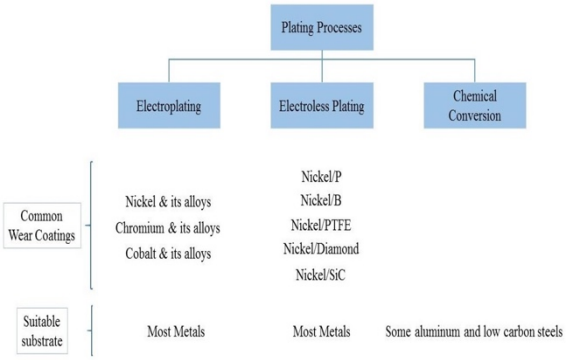

Figure 1: Iillustration of the significance of Ni based wear-resistant coating applications in industries. Ni is typically used to provide steels with a harder surface. It is believed that approximately 90% of plated wear resistant coatings consist of the mentioned coatings in this figure.

References:

1. Wang, Y., Shua, X., Wei, S., Liu, C., Gao, W., Shakoor, R.A., Kahraman, R. Duplex Ni–P– ZrO2/Ni–P electroless coating on stainless steel. *Journal of Alloys and Compounds*, 2015, 630, 189-194.
2. Chen, W., He, Y., Gao, W. Electrodeposition of sol-enhanced nanostructured Ni-TiO2 composite coatings. *Surface & Coatings Technology*, 2010, 204, 2487–2492.

Synergistic Effect Of Different Nanocontainers For Self-healing Corrosion Protection Coatings On AA2024-T4

S. Manasa,[1,2 *] K. V. Gobi,[2] R. Subasri,[1]

[1] International Advanced Research Centre for Powder Metallurgy and New Materials (ARCI), Centre for Sol-Gel Coatings, Balapur, Hyderabad - 500005, Telangana State, India.
[2] National Institute of Technology, Department of Chemistry, Warangal-506004, Telangana State, India.
* Presenting Author, Email: manasasamavedam2@gmail.com

Abstract:
Aluminum alloy 2024-T4 is extensively used in aerospace industry due to the advantage of its high strength-to-weight ratio. However, during the service period, these surfaces will be exposed to extreme atmospheric conditions and get corroded, which is an inherent shortcoming. Due to strict regulations on usage of commercially used carcinogenic hexavalent chrome based conversion coatings, there is an urgent need to develop chrome-free coatings. Sol-gel based coatings are found to be a good replacement. Encapsulation of active corrosion inhibitors inside the nanocontainers to develop self-healing coatings is a recent strategy, that prevents the leakage of inhibitors and releasing them only on the onset of damage to the substrate. Moreover, use of combination of nanocontainers will be of more interest. Hence in this investigation, we have studied effect of combination of different nanocontainers such as halloysite nanotubes (HNT) and layered clays like montmorillonite clay (MMT). These nanocontainers were loaded with cationic corrosion inhibitors such as Ce^{3+}/Zr^{4+}, subsequently dispersed into organic-inorganic hybrid sol-gel matrix and were coated on to AA2024-T4 substrates by dip coating method. Coated substrates were cured at 130° C for 1 h. Corrosion behaviour of these developed coatings were studied by electrochemical impedance spectroscopy and Potentiodynamic polarization studies at different durations of exposure to 3.5 wt % NaCl solution. Corrosion currents of HNT based coatings and MMT based coatings as individual layers on AA2024-T4 is given in Figure 1. HNT based coatings exhibited least corrosion currents than MMT based coatings.

Keywords: Halloysite nanotubes, Montmorillonite clay, Cationic inhibitors, Sol-gel coatings, Self-healing, Corrosion protection, AA2024-T4.

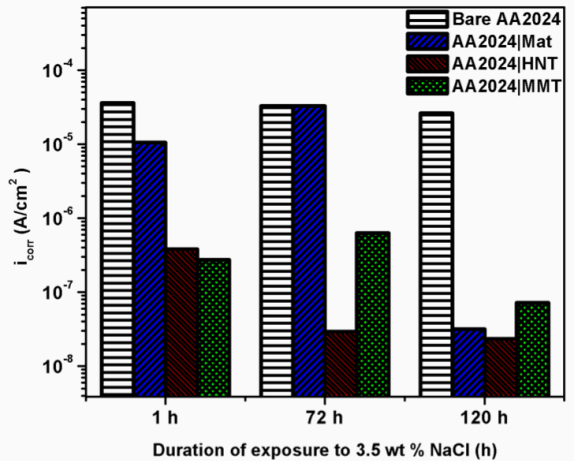

Figure 1: Comparison of corrosion currents of bare AA2024, matrix coated (AA2024|Mat); HNT based coating (AA2024|HNT) and MMT based coating (AA2024|MMT) at different durations of exposure to 3.5 wt % NaCl .

References:

1. Wang D., Bierwagen GP. (2009), Sol-gel coatings on metals for corrosion protection. *Prog. Org. Coat.,* 64, 327–338.
2. Montemor MF. (2014), Functional and smart coatings for corrosion protection : A review of recent advances. *Surf. Coat. Technol*., 258, 17–37.

Barrier Coatings in Food Packaging Applications

M. Bendig,[1] H.-U. Moritz,[1] W. Pauer [1*]

[1] University of Hamburg, Institute for Technical and Macromolecular Chemistry, Hamburg, Germany

Abstract:
Paper is widely used in packaging applications, as it is environmentally friendly and flexible.[1] Thus, there are many activities documented to extend the application fields of paper. Here, barrier coatings are applied to overcome the weakness of paper like wettability or permeability. Regarding food packaging applications, barrier coatings protect the product from external influences like oxygen, water, oil or grease.[2] Moreover, the coating needs to be resistant to components of the food itself. The emphasis of this work is to combine the conflicting properties of water and the grease resistance in a coating. In order to improve the understanding of barrier coatings, the factors which affect the barrier properties qualitatively and quantitatively were examined. As coating solutions polymer dispersions are widely used. To expand the field of applications for polymer dispersions as barrier coatings, the influence of different parameters of the polymerization process were analyzed, e.g. the emulsifier and the variation of monomers, and the surface of the obtained coating was characterized. Styrene-butyl acrylate copolymers were produced by emulsion polymerization. In this system the glass transition temperature can be adjusted in a wide range. Copolymers with a high glass transition temperature form brittle films, while copolymers with a low glass transition temperature form sticky films. The minimum film formation temperature (MFFT) depends strongly on the glass transition temperature. The glass transition temperature and the MFFT are influenced by the monomer ratio. Here, butyl acrylate should provide hydrophobicity and styrene should enhance the thermal stability. The tribological characteristics of the coating can also be affected by the monomer ratio. Furthermore, the emulsifier plays a key role in the effectiveness of water resistance, so a dispersion containing hardly any emulsifier would be the best option. In this case the stability of the dispersion is insufficient. In order to find a balance between a stable dispersion and an efficient barrier against water, the emulsifier concentration was decreased to five times the critical micelle concentration while applying a high monomer content of 40 wt%. Contact angle measurements of the coating with water showed that a reduced emulsifier concentration induces higher contact angles of around 100 °, which indicates an increased water resistance of the surface. The influence of glycidyl methacrylate as a third comonomer on the film formation, the surface properties and the stability of the dispersion were analyzed to develop barrier coatings with a water and grease resistance at the same time. The grease resistance increases and the water absorptiveness decreases with rising glycidyl methacrylate content. In general, these insights into the manufacturing process enable the opportunity to improve the perfomance of barrier coatings. On top of that, there is a barrier coating with a grease and water resistance at the same time.

Keywords: barrier coating, surface treatment, surface characterization, tribology, food packaging, recycling paper, emulsion polymerization.

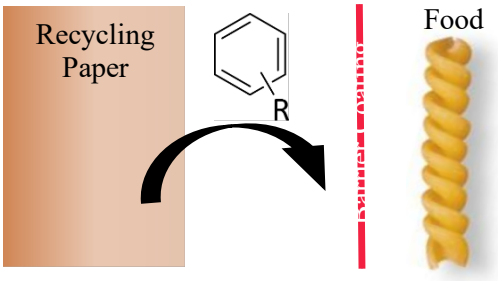

Figure 1: A key problem when using recycling paper as packaging material is the remaining ink in the paper. It contains low-molecular substances like aromatic compounds. Barrier coatings are appplied to protect the product while also being resistant to components of the food.

References:

1. Khwaldia, K., Arab-Tehrany, E. & Desobry, S. Biopolymer Coatings on Paper Packaging Materials. *Compr. Rev. Food Sci. Food Saf.* **9,** 82–91 (2010).
2. Mehtiö, T., Anghelescu-Hakala, A., Hartman, J., Kunnari, V. & Harlin, A. Crosslinkable poly(lactic acid)-based materials: Biomass-derived solution for barrier coatings. *J. Appl. Polym. Sci.* **44326,** 1–8 (2016).

Scanning Droplet Adhesion Microscopy

Maja Vuckovac[2*], Ville Liimatainen[1*], Ville Jokinen[3], Veikko Sariola[1,4], Matti J. Hokkanen[1,2], Quan Zhou[1] and Robin H. A. Ras[2,5]

[1]Aalto University School of Electrical Engineering, Maarintie 8, 02150 Espoo, Finland
[2]Aalto University School of Science, Puumiehenkuja 2, 02150 Espoo, Finland
[3]Aalto University School of Chemical Technology, Tietotie 3, 02150 Espoo, Finland
[4]Tampere University of Technology, Korkeakoulunkatu 3, 33720 Tampere, Finland
[5]Aalto University School of Chemical Engineering, Kemistintie 1, 02150, Espoo, Finland University

Abstract:
Superhydrophobic surfaces have unique wetting properties, causing water to bead up and move with low friction, enabling remarkable functions in biology and technology. While superhydrophobicity is often observed on the macroscale, it arises from the micro- and nanoscale morphological structure and chemical composition of the surface and is thus affected by spatial heterogeneity at those length scales. Irregularities in morphological structure and chemical composition lead to a spot-to-spot variation of wetting properties, which may affect or even govern droplet mobility, icing, and condensation. Thus, to advance the development of superhydrophobic surfaces and move them towards real-life applications it is critical to understand how water-repellency emerges from the micro- and nanoscale features. An effective way to quantify and map microscopic variations of wettability is still missing, because existing characterization techniques lack sensitivity and spatial resolution. Here we present a cutting-edge technique, scanning droplet adhesion microscopy, able to measure small adhesion forces between water drop and superhydrophobic surface with extraordinary nanonewton sensitivity and outstanding micrometer spatial resolution allowing to quantify precisely wetting variations on the surface in the form of wetting maps (Figure1). The microscope allows detailed wetting characterization of challenging non-flat surfaces, e.g., butterfly wings, previously difficult to characterize by contact angle method as their typically uneven or curvy surface obstructs a direct view of the drop shape. Furthermore, the technique reveals wetting heterogeneity of micropillared model surfaces previously assumed to be uniform and allows for the first time quantification of pinning and depinning forces on such surfaces when the drop is advancing or receding from pillar-to-pillar. Our results show that droplet adhesion correlates with water-repellency and is a sensitive measure for demanding superhydrophobic surface characterization.

Keywords: superhydrophobicity, wetting characterisation, adhesion forces, wetting maps.

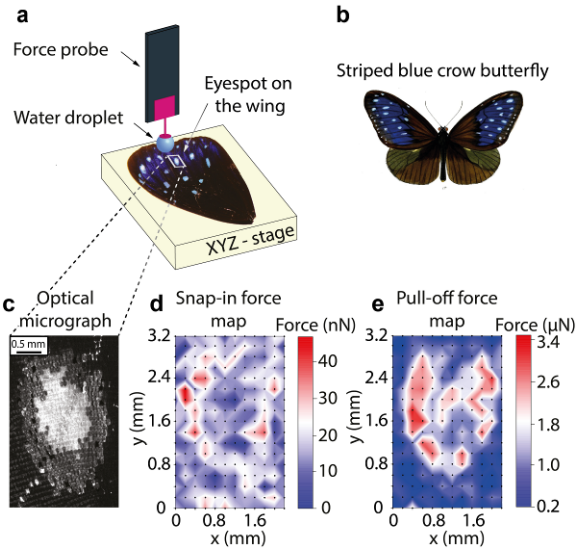

Figure 1: Concept of scanning droplet adhesion microscopy to construct wetting maps showing (**a**) schematic diagram of the microscope (not to scale) with eyespot on the wing of (**b**) striped blue crow butterfly (image by Frederic Moore, PD-1923), (**c**) optical micrograph of scanned eyespot area on the wing of with corresponding (**d**) snap-in and (**e**) pull-off force maps.

References:

1. Liimatainen, V., Vuckovac, M., Jokinen, V., Sariola, V., Hokkanen, M. J., Zhou, Q., Ras, R. H. A. (2018) Mapping microscale wetting variations on biological and synthetic water-repellent surfaces, *Nat. Commun.*, 8, 1798

SurfCoat Korea 2019
Session II C: Surface engineering / coatings in sustainable energy, conversion, optical, electric, photovoltaic and magnetic applications

Advanced Aluminium Nitride Thin Films for Piezoelectric MEMS

U. Schmid,[1,*] M. Schneider[1]
[1] Institute of Sensor and Actuator Systems, TU Wien, Gusshausstrasse 27-29, 1040 Vienna, Austria

Abstract:
Electromechanical transducers based on the piezoelectric effect are continuously finding their way into micro-electromechanical systems (MEMS), typically in the form of thin films. Piezoelectric transducers feature a linear voltage response, no snap-in behaviour and can provide both attractive and repulsive forces. This removes inherent physical limitations present in the commonly used electrostatic transducer approach while maintaining beneficial properties such as low-power operation. Furthermore, piezoelectric materials can serve for both actuation and sensing purposes, thus enabling pure electrical excitation and read-out of the transducer element in combination with a compact design. Based on these outstanding features, piezoelectric transducers are operated most beneficially in a large variety of different application scenarios, ranging from resonators in liquid environment, advanced acoustic devices to sensors in harsh environments. In order to exploit the full potential of piezoelectric MEMS in the future, interdisciplinary research efforts are needed ranging from investigations of advanced piezoelectric materials over the design of novel piezoelectric MEMS sensor and actuator devices, to the integration of PiezoMEMS devices into full low-power systems.
In this talk, we will highlight latest results on the electrical, mechanical and piezoelectrical characterization of sputter-deposited aluminium nitride (AlN) including the impact of sputter parameters, film thickness and substrate pre-conditioning [1,2]. We will present the impact of doping of AlN with scandium, which leads to an increase of the moderate piezoelectric coefficient of AlN up to a factor of four.
In a next step, these films are implemented into fabrication processes of cantilever-type MEMS devices. In combination with a tailored electrode design, resonators are realized featuring in liquids Q-factors up to about 300 in the frequency range of 1-2 MHz. This enables the precise determination of the viscosity and density of fluids up to dynamic viscosity values of almost 300 mPas [3]. Besides this application, such high Q factors are useful when targeting mass-sensitive sensors, thus paving the way to e.g. particle detection even in highly viscous media.
Given the low increase in permittivity of ScAlN compared to AlN, another field of application for this functional material class are vibrational energy harvesters, where the benefit of ScAlN compared to pure AlN is demonstrated [4].
Finally, we will present some selected results of ScAlN thin films within SAW devices ranging from high temperature applications to droplet manipulation in microfluidics [5].

Keywords: Piezoelectric MEMS, aluminium nitride, scandium aluminium nitride, viscosity/density sensor, MEMS vibrational energy harvester, high temperature SAW devices.

References:

1. M. Schneider, A. Bittner, F. Patocka, M. Stöger-Pollach, E. Halwax and U. Schmid, Impact of the surface-near silicon substrate properties on the microstructure of sputter-deposited AlN thin films, Applied Physics Letters **101** (2012) 221602.
2. M. Schneider, A. Bittner and U. Schmid, Improved piezoelectric constants of sputtered aluminium nitride thin films by preconditioning of the silicon surface, Journal of Physics D: Applied Physics **48** (2015) 405301.
3. G. Pfusterschmied, M. Kucera, E. Wistrela, T. Manzaneque, V. Ruiz-Díez, J. L. Sánchez-Rojas, A. Bittner and U. Schmid, Temperature dependent performance of piezoelectric MEMS resonators for viscosity and density determination of liquids, Journal of Micromechanics and Microengineering **25** (2015).
4. P. M. Mayrhofer, C. Rehlendt, M. Fischeneder, M. Kucera, E. Wistrela, A. Bittner and U. Schmid, ScAlN MEMS Cantilevers for Vibrational Energy Harvesting Purposes, Journal of Microelectromechanical Systems **26** (2017) 102-112.
5. W. Wang, P. M. Mayrhofer, X. He, M. Gillinger, Z. Ye, X. Wang, A. Bittner, U. Schmid and J. K. Luo, High performance AlScN thin film based surface acoustic wave devices with large electromechanical coupling coefficient, Applied Physics Letters **105** (2014).

Challenges on Adhesion in the Aqueous Processing of Cathodes for Lithium Ion Batteries

W. Bauer,* U. Kaufmann, M. Müller, L. Pfaffmann

Karlsruhe Institut of Technology, Institut for Applied Materials, Karlsruhe, Germany

Abstract:
The replacement of the previous organic solvent-based electrode manufacturing with a water-based process implies a significant reduction of the manufacturing costs.[1] However, the highly polar water also generates massive challenges for electrode manufacturing and cell properties. One problem is the poor dispersibilty of carbonaceous additives in water, which demands application of high mixing intensity. Another challenge is the reaction of cathode materials with water, which consumes lithium and effects an increase of the pH of the slurry so that corrosive attack of the aluminum foil takes place (Figure 1). In literature, typically the addition of a dispersant or of an acid is described as a measure to handle these problems.[2,3] Besides some positive effects, these additives nearly always show a massively negative impact on the adhesion of the electrode on the current collector foil. As good adhesion is an essential requirement for an reliable cell production, a better understanding and prevenion of adhesion problems is necessary in order to establish new additives in industrial processes.
The effects of dispersant and acid addition on the adhesion of aqueous processed cathodes will be presented together with other influences on slurry rheology or cell performance. It is demonstrated that surface charge, molecule size and volatility of the additives play crucial roles for the loss of adhesion.

Keywords: lithium ion battery, electrode manufacturing, aqueous dispersion, adhesion, additives.

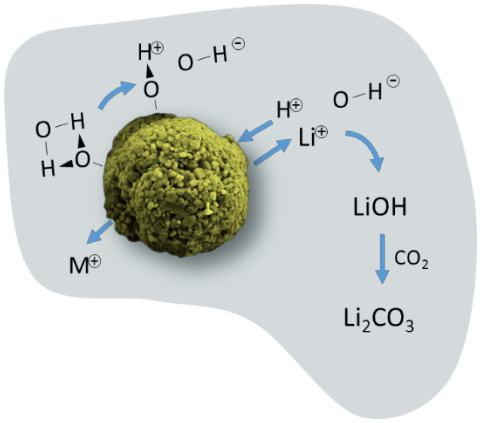

Figure 1: Interaction of active cathode materials for lithium ion batteries with water. Li/H^+-exchange initiates pH increase and carbonate formation (from ref. 4)

References:

1. Wood, D.L., Li, J., Daniel, C. (2015), Prospects for reducing the processing cost of lithium ion batteries, *J. Power Sources*, 275, 234-242.
2. Porcher, W., Lestriez, B., Jouanneau, S., Guyomard, D. (2010), Optimizing the surfactant for the aqueous processing of LiFePO4 composite electrodes, *J. Power Sources*, 195, 2835-2843.
3. Kuenzel, M., Bresser, D., Diemant, T., Carvalho, D.V., Kim, G.-T., Behm, R.J., Passerini, S. (2018), Complementary Strategies Toward the Aqueous Processing of High-Voltage LiNi0.5Mn1.5O4 Lithium-Ion Cathodes, *ChemSusChem*, 11, 562-573.
4. Bauer, W., Kaufmann, U., Müller, M., Çetinel, F. (2019), Effects of pH control by acid addition at the aqueous processing of cathodes for lithium ion batteries, submitted to *J. Power Sources*.

Oxide Surfaces, Interfaces and Thin Films: Electrochemical Studies Relevant to Perovskite Photovoltaics

L. Kavan

J. Heyrovsky Institute of Physical Chemistry, v.v.i., Academy of Sciences of the Czech Republic, Dolejškova 3, CZ-18223 Prague 8, Czech Republic, E-mail: kavan@jh-inst.cas.cz

Abstract:
The perovskite solar cell (PSC) demonstrated remarkable solar conversion efficiency jumping from 3.8% to near 23% during 2009-2018. Figure 1 depicts the traditional n-i-p architecture of PSC. The hole-collecting terminal (e.g. Au) is interfaced to hole-transporting medium (HTM), e.g. *spiro*-OMeTAD or CuSCN. The core of negative electrode is a nm-thin electron-selective layer (ESL) usually made from TiO_2 or SnO_2 [1]. It is a subject of thorough materials-screening and structural optimizations, in which electrochemistry plays an important role [2]. ESL selectively transports electrons from the perovskite to the back contact, but at the same time prevent recombination of these electrons with perovskite or hole conductor. Amorphous ALD-made SnO_2 or TiO_2 films are pinhole-free for thicknesses down to several nm, but amorphous and crystalline ALD SnO_2 films substantially differ in their conduction band positions. The mesoporous scaffold (if present) is composed of oxide semiconductors (TiO_2 or SnO_2) or insulators (Al_2O_3, SiO_2, ZrO_2). The vectorial charge-transfer over several interfaces in PSCs requires right alignment of conduction band minimum (CBM) and valence band maximum (VBM) of the relevant materials. The alignment of CBMs of perovskite/ESL is requested in addition to compact (pinhole-free) morphology. Both properties can be characterized electrochemically. The energy of CBM is usually measured by optical spectra (giving the band gap) and photoelectron spectra (XPS, UPS) providing VBM. Electrochemical alternative is the measurement of the flatband potential, which yields CBM, too. However, there is a considerable controversy between the electrochemical and vacuum (XPS, UPS) techniques about the position of CBM in TiO_2 (anatase, rutile, including the crystals with distinguished facets) [2]. To address this controversy, a refined electrochemical analysis of single crystal TiO_2 electrodes (anatase, rutile, brookite) together with vacuum and near-ambient pressure XPS studies was carried out. This, together with theoretical (DFT) modelling points at the effect of interface influencing the CBM positions. Even the adsorption of monolayer of water causes the relevant shifts, and allows thus rationalization of the mentioned literature conflicts.

Keywords: titanium dioxide, tin dioxide, perovskite solar cell, electrochemistry

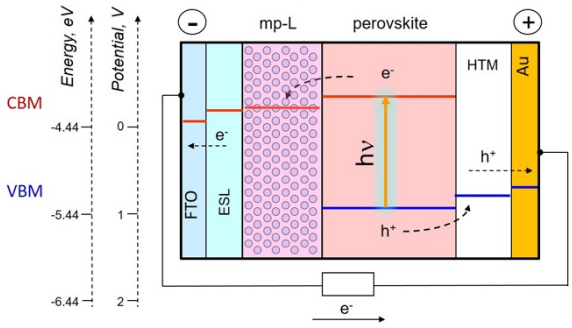

Figure 1: Scheme of the of perovskite solar cell (mesoscopic n-i-p type). ESL = electron selective layer, mp-L = mesoporous layer infiltrated by perovskite, HTM = hole-transporting medium.

References:

1. Kavan, L., Steier, L.. Grätzel, M., (2017) Ultrathin Buffer Layers of SnO2 by Atomic Layer Deposition: Perfect Blocking Function and Thermal Stability, *J. Phys. Chem. C* 121, 342-350.
2. Kavan, L., (2018) Electrochemistry and Perovskite Photovoltaics, *Curr. Opinion Electrochem.* DOI: 10.1016/ j.coelec.2018.10.003.

SurfCoat Korea 2019
Session II D: Bio-interfaces / Biomedical / Bioactive surfaces and coatings

Surface and material science of biopolymers and their potential application in biomedicine

T. Mohan,[1] M. Bračič,[1] R. Kargl,[1,2] T. Heinze,[3] K. Stana Kleinschek,[1,*]

[1] University of Maribor, Faculty of Mechanical Engineering Laboratory for Characterization and Processing of Polymers (LCPP), Maribor, Slovenia
[2] Graz University of Technology, Institute of Paper, Pulp and Fibre Technology (IPZ), Graz, Austria
[3] Friedrich Schiller University of Jena, Center of Excellence for Polysaccharide Research, Institute for Organic Chemistry and Macromolecular Chemistry, Jena, Germany

Abstract:
Understanding interactions of solid biomaterials with living systems or their constituents (proteins, nucleic acids, oligo- and polysaccharide, lipids) is prerequisite for applications in regenerative medicine, as vascular grafts, as biosensors or as low protein fouling layers. In that respect polymeric thin films and coatings are useful for basic investigations of interactions due to their defined character, reproducible preparation and accessibility to modern surface analytical techniques. Among these techniques are atomic force microscopy (AFM), X-ray photoelectron spectroscopy (XPS), quartz crystal microbalance (QCM-D), surface plasmon resonance (SPR) and fluorescence microscopy. Studying the surface properties of these materials allows for a correlation of the physicochemical composition, morphology and wetting, with polysaccharide, protein or living cells' adhesion or growth on these materials. Polymeric biomaterials can further be coated on specific substrates or shaped into 3D printed, nano-fibrous or particulate objects useful for mentioned biomedical applications. Those materials can optionally be based on synthetic biodegradable polyesters (e.g. polycaprolactone, PCL), semi-synthetic polysaccharide derivatives bearing charges or hydrophobic moieties, or other naturally occurring polymers. This lecture will give examples on what kind of chemical reactions and surface modifications can be performed with biodegradable or bio-based polymers and how these materials can be processed into various shapes ranging from thin films to 3D printed objects. Besides processing, examples on detailed surface interaction studies will be given that elucidate large differences in the physicochemical characteristics of the materials. These differences are correlated with the response of living cells exposed to and grown on materials modified and processed with the knowledge obtained from basic surface and polymer analytical studies.

Keywords: polysaccharides, biopolymers, thin films, adsorption, surface functionalization, 3D printing, cell adhesion, anti-fouling coating, biomaterial

References:

1. Mohan, T., Niegelhell, K., Nagaraj, C., Reishofer, D., Spirk, S., Olschewski, A., Stana-Kleinschek, K., Kargl, R. (2017) Interaction of tissue engineering substrates with serum proteins and its influence on human primary endothelial cells. Biomacromolecules, 18, 413-421.
2. Stana, J., Stergar, J., Gradišnik, L., Flis, V., Kargl, R., Froehlich, E., Stana-Kleinschek, K., Mohan, T., Maver, U. (2017) Multilayered polysaccharide nanofilms for controlled delivery of pentoxifylline and possible treatment of chronic venous ulceration. *Biomacromolecules*, 18, 2732-2746.

A Multiphysics Modelling of Magnetic-Sensitive Hydrogels

Hua Li

School of Mechanical & Aerospace Engineering
Nanyang Technological University, Singapore 639798

Abstract:
A multiphysics model is presented for simulation of the responsive behaviour of the magnetic-sensitive hydrogel, with the effects of magneto-chemo-mechanical-coupled fields. In this work, the magnetic susceptibility for magnetization of the general magnetic hydrogel is defined as a function of finite deformation, instead of a constant for an ideal magnetic hydrogel. The present constitutive equations, formulated by the second law of thermodynamics, account for the effects of the chemical potential, the externally applied magnetic field, and the finite deformation. In particular, a novel free energy density is proposed with consideration of the magnetic effect associated with finite deformation, instead of volume fraction. After examination with published experimental data, it is confirmed that the present model can capture well the responsive behaviour of the magnetic hydrogel, including the deformation and its instability and hysteresis under a uniform or nonuniform magnetic field. The parameter studies are then presented for influences of the magnetic and geometric properties, including the magnetic intensity, shear modulus, and volume fraction of the magnetic particles, on the behaviour of the magnetic hydrogel, for a deeper insight into the fundamental mechanism of the magnetic hydrogels.

Keywords: multiphysics modelling, magnetic-sensitive hydrogels, instability, hysteresis, biomedical applications.

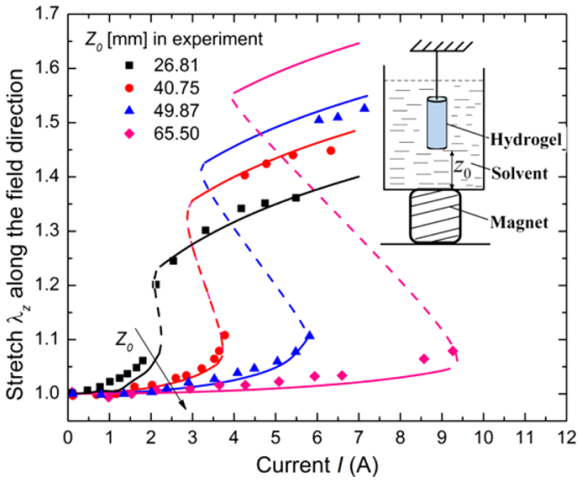

Figure: Comparison of the present theoretical simulation and published experiment for the PVA magnetic hydrogel subject to a nonuniform magnetic field,[1] where the dots denote the experimental data and the solid and dashed lines the simulation results at stable and unstable states, respectively.

References:

1. Zrínyi, M., Barsi, L., Szabo, D., Kilian, H. G. (1997) Direct Observation of Abrupt Shape Transition in Ferrogels Induced by Nonuniform Magnetic Field, *J. Chem. Phys*., 106, 5685−5692.

Bioinspired Melanin Coatings in Bioelectronics: the case of Eumelanin/PEDOT(PSS) blend for ITO-free electrodes

Alessadnro Pezzella,[1,2,*]

[1]Institute for Polymers Composites and Biomaterials (IPCB) CNR, Via Campi Flegrei 34, IT-80078 Pozzuoli (Na), Italy
[2] University of Napolel Federico II - Via Cintia n.4, Napoli, Italy

Abstract:
Organic Bioelectronics applications are largely dictated by the chemical nature of the materials that transduce signals across the biotic/abiotic interfaces[1]. Among the available materials for functional biocompatible interfaces, the human pigment eumelanin is currently gaining increasing interest. This black insoluble pigment of human skin, hair, eyes and nigral neurons (neuromelanin),[2] featuring unique assortment of chemical physical properties,[3] arises biogenetically from the aminoacid tyrosine via the oxidative polymerization of 5,6-dihydroxyindole (DHI) and/or 5,6-dihydroxyindole-2-carboxylic acid (DHICA).[2,3] To date, two main obstacles hampered a full exploitation of eumelanin based devices: (i) the actual eumelanin insolubility in any solvents, preventing easy processability of the pigment as well as the devices fabrication; (ii) its low conductivity, limiting both the range of possible working potential and functional applications. To improve the electrical performances of the eumelanin thin films, a clear-cut approach lies in the hybridization/integration with a suitable conductive counterpart. In this view, π-conjugated molecules featuring conductive pathways appear a key choice in the production of new organic materials for electronic (nano)devices.
Within this scenario, here we focus on the first (at the best of our knowledge) preparation of an eumelanin-PEDOT blend, featuring valuable functional and processing properties, like easy films preparation, high adhesion, good electrical conductivity and biocompatibility. The effect of eumelanin on conductivity was thus related to structural features in Wide Angle X-ray Scattering (WAXS) and diffraction (XRD) patterns of films with different eumelanin content and fixed PEDOT:PSS ratio. The biocompatibility and toxicity was investigated in view of its potential exploitation as bio-interface material. As a proof of concepts an OLED featuring an eumelanin-PEDOT anode was fabricated and characterized.

Keywords: bioinspired materials, conductive polymer, eumelanin, GIWAXS, PEDOT:PSS, OLED.

Figure 1: Figure illustrating a pictorial relationship between a natural source of eumelanin (eye iris) and the pigment applications as anode in ITO free OLED.

References:

1. Berggren M., and Richter-Dahlfors A. (2007). Adv Mater, Vol.19, p.3201-3213.
2. d'Ischia M., Wakamatsu K., Napolitano A., Briganti S., Garcia-Borron J. C.et al. (2013). Pigment cell & melanoma research, Vol.26, p.616-633.
3. d'Ischia M., Napolitano A., Pezzella A., Meredith P. and Sarna T. (2009).AngewChemIntEdit,Vol.48, p.3914-3921.

Derivatization of biopolymers for functional coatings

A. Bratuša,[1] L. Jurko,[1] K. Stana Kleinschek,[1] R. Kargl,[1,2,*]

[1] University of Maribor, Faculty of Mechanical Engineering Laboratory for Characterization and Processing of Polymers (LCPP), Maribor, Slovenia
[2] Graz University of Technology, Institute of Paper, Pulp and Fibre Technology (IPZ), Graz, Austria

Abstract:
Homogeneous polymer analogous derivatization reactions are useful for increasing the property range and applicability of polysaccharides and synthetic polymers. Chirality, regioselectivity, solubility and chemical stability govern the reactivity and final properties of both polymer classes. For polysaccharides, derivatization with amino acids can be an interesting option to obtain products useful for coating of substrates that are intented to be used as biomaterials. In this work derivatization of mentioned polymers with amino-acids or peptides was used to produce bioactive materials of interest. Aminoacids, peptides and other functional molecules were bound to the polymers via homogeneous esterification or amide bond reactions in organic solvents or water, employing proper activating reagents, catalysts and reaction conditions. The necessity of protecting groups was evaluated and protocols for their removal were established. Detailed analysis of the degree of substitution (DS) was performed by charge titration, NMR and IR-spectroscopy. Selected obtained materials were evaluated with respect to their bioactivity using cell viability tests. Common material forming techniques for polymers (nano-precipitation, thin film preparation, layer-by-layer coating) were employed to obtain various shapes suitable to be used as biomaterials for theranostics or regenerative medicine. These materials are intended to mimic nature's proteoglycans, glycoproteins and glycosylated enzymes in form and function and are expected to carry unprecedented properties. Development of derivatization strategies for the conjugation of polysaccharides with amino acids are the crucial step for obtaining these materials and were elaborated in detail.
Studying interactions of living cells with the described biomaterials gives insights into the mechanisms and applicability of this relatively unexplored group of semi-synthetic bioconjugates.

Keywords: polysaccharide derivatives, adsorption, esterification, amide bond formation, biomaterial coating

References:

1. Elschner, T., Bračič, M., Mohan, T., Kargl, R., Stana-Kleinschek, K. (2018) Modification of cellulose thin films with lysine moieties: a promising approach to achieve antifouling performance. *Cellulose*, 25, 537-547.
2. Mohan, T., Rathner, R., Reishofer, D., Koller, M., Elschner, T., Spirk, S., Heinze, T., Stana-Kleinschek, K., Kargl, R. (2015) Designing hydrophobically modified polysaccharide derivatives for highly efficient enzyme immobilization. *Biomacromolecules*, 16, 2403-2411.

Biopolymer-based coatings on the plasmochemical activated surface of NiTi alloy

P. Jabłoński[1] W. Niemiec[1], Ł. Kaczmarek[2], M. Hebda[3], H. Krawiec[4], K. Kyzioł[1]
[1]AGH University of Science and Technology, Faculty of Materials Science and Ceramics, Krakow, Poland
[2] Institute of Materials Science and Engineering, Łódź University of Technology, Poland
[3] Cracow University of Technology, Institute of Materials Engineering, Krakow, Poland
[4]AGH University of Science and Technology, Faculty of Foundry Engineering, Krakow, Poland

Abstract:
Metal alloys are commonly used materials in field of orthopedic implants because of relatively low elastic modulus, biocompatibility with bone tissue, and durability. NiTi alloy is an excellent example of mentioned properties, moreover, it represents special mechanical properties such as shape memory effect (SME) and pseudoelasticy. In the case of alloys based on titanium their surface is covered by titanium oxide. While, in the case of NiTi alloy due to about 50% content of nickel this superficial oxide layer is not sufficiently mechanical durable to provide efficient corrosion resistance and metalosis protection. Moreover, high corrosion of NiTi alloy causes the release of high concentration of Ni^+ ions, which have allergenic and irritant character for tissues. This, in turn, can lead to rejection of implant.
One of perspective solutions for common applications of metal alloys in medicine is modification of the implant surface with biopolymers. The latter are widely used in biomaterial engineering thanks to their biocompatibility, biodegradability, availability, and cheapness. Chitosan, an example of biopolymers, is obtained by deacetylation of chitin sourced from the exoskeleton of crustaceans. Antimicrobial activity, susceptibility to chemical modifications, and high mechanical strength distinguish chitosan from other biopolymers. This makes chitosan often used in surface modification of polymeric and metallic medical implants, devices, and other biomaterials.
In this work, the functional coatings based on biopolymers (chitosan) were studied as prospective and attractive approach in surface functionalization of shape memory alloy. Alloy substrates were pre-modified in two steps: (1) piranha solution treatment, and (2) plasmochemical etching (Ar^+) and activation in RF CVD reactor in argon-ammonia atmosphere. Then, the activated substrates were immersed in biopolymer solution(s) resulting in formation of biopolymer layer(s). The microstructure and chemical composition of the modified surfaces were characterized using scanning electron microscopy (SEM-EDS). The topography was revealed using atomic force microscopy (AFM). Furthermore, the atomic structure of coatings was characterized by IR and Raman spectroscopy. Surface wettability and surface energy were also determined. Moreover, biological properties was evaluated *in vitro* towards the selected cell lines. In addition, the corrosion properties of alloys after and before surface modification were also investigated in the Hank solution. In order to determine the corrosion resistance of NiTi in the physiological saline, the potentiodynamic polarization curves were plotted. Presented data allow to propose the investigated surface modification of NiTi alloy for medical applications. It was shown, *inter alia*, that the obtained coatings, incl. prefunctionalization in RF reactor and polymer-based layers, inhibit corrosion of NiTi alloy. The obtained chitosan coatings on modified surface after plasma treatment in Ar/NH_3 mixture are homogeneous, possess good adhesive properties and improved mechanical properties as well as are characterized by non-cytotoxicity. Furthermore, the modified alloy limits its transfer of the metals (Ni, Ti) to Hank's solution.

Keywords: NiTi alloy, plasma modification, corrosion resistance, biocompatibility

References:

1. Kong M., *et. al.* (2010) Antimicrobial properties of chitosan and mode of action: A state of the art review, *Int. J. Food Microbiol..,*144, 51-63.
2. Ahmed R. A., *et. al.* (2014) Improvement of corrosion resistance and antibacterial effect of NiTi orthopedic materials by chitosan and gold nanoparticles, *Appl. Surf. Sci., 292, 390-399*

Acknowledgement. This work has been supported by the European Union and Ministry of Science and Higher Education, project "Najlepsi z najlepszych! 3.0" POWER cofounded by European Social Fund titled "Bioactive chitosan layers on the plasmochemical activated surface of NiTi alloy".

TiO_2 / CaP as a bioactive coating produced by using plasma electrolytic oxidation technique

A. Zakaria,[1,*] M. Hamdi,[2] and M. Todoh,[1]

[1] Hokkaido University, Graduate School of Engineering, Hokkaido, Japan
[2] University of Malaya, Centre of Advanced Manufacturing and Material Processing, Kuala Lumpur, Malaysia

Abstract:
While there is more benefit of Ti6Al4V compared to others metal such as good for strength to its weight ratio, it is still a bioinert metal which does not bond with the adjacent bone and always lead to stress shielding or implant loosening. As the need to improve implant durability after the insertion into the patient, many researchers are attempting to solve this issue through advanced manufacturing and surface engineering technique. There is a few of coating techniques that have been studied and plasma electrolytic oxidation (PEO) technique is one of them. The advantages of this technique are the coating that is formed on the surface is microporous and compose of calcium and phosphate which contribute to cell attachment, propagation and bone growth [1]. The aim of this study is to develop microporous structure and incorporate Ca and P element on the Ti6Al4V metal surfaces to improve bone ingrowth rate on the implant by using plasma electrolytic oxidation technique. Here we demonstrate the change of voltage with respect to time and current during the process, the atomic concentration % of working area and its edge (Table 1 and Figure 1), the surface morphology produced by the technique as shown in Figure 2, the thickness and the adhesive strength of the coating.

Keywords: hydroxyapatite, plasma electrolytic oxidation, Ti6Al4V alloy, microporous structure, bioactive coating, biomedical applications.

Table 1: Atomic concentration % of working area and its edge.

Atomic element	Oxygen	Titanium	Calcium	Phosphate
Working area	76.29	19.74	1.11	0.62
Edge of working area	32.70	11.91	28.31	0.55

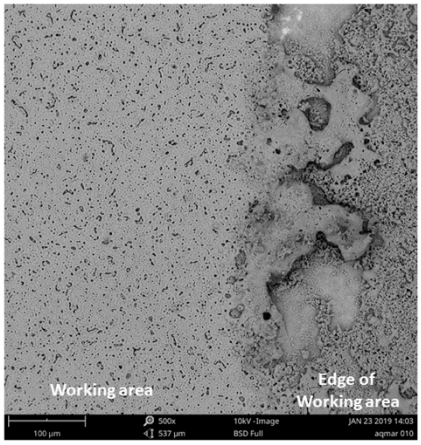

Figure 1: SEM image surface morphology of working area and its edge

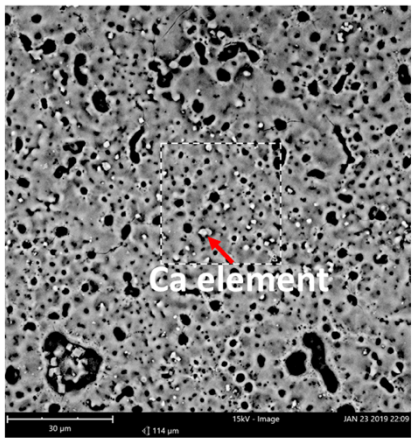

Figure 2: Microporous structure and Ca element that seals the pore

References:

1. In-Jo Hwang, Han-Cheol Choe, (2017) Hydroxyapatite coatings containing Zn and Si on Ti-6Al-4V alloy by plasma electrolytic oxidation, *Applied surface Science,* 432, 337-346.

Enhancement of Adhesion of γ-Al_2O_3 with Stainless Steel Catalytic Supports

Muzafar Abbas [1, 2,*], Myoung-Woon Moon [1, 3], Ji Young Byun [1, 2], Sang Hoon Kim [1, 2,]

[1] Division of Nano & Information Technology in KIST School, University of Science and Technology, Daejeon, 34113, Republic of Korea
[2] Materials Architecting Research Center, Korea Institute of Science and Technology, Seoul, 02792, Republic of Korea
[3] Computational Science Research Center, Korea Institute of Science and Technology, Seoul, 02792, Republic of Korea

Abstract

γ-Al_2O_3 slurry deposited on metal substrate (SUS-304) shows a weak adhesion to metal substrates and it can lead to a cracking, depletion and peeling of coating in hard conditions. Rough samples were fabricated by chemical etching, micro-milling and sintering to enhance the adhesion of γ-Al_2O_3 slurry on SUS-304 substrate. Samples were designed with square microarrays pillars of depths (h), spacing (b) and width (w) in order to create roughness on SUS-304 substrates. Experimental results showed that the adhesion of γ-Al_2O_3 slurry on SUS-304 substrate could be enhanced by making the surfaces rough with square micropillar arrays and micro roughness which is a result of concave pits, cracks and convexities during machining and etching. It was observed that samples fabricated by sintering process showed good adhesion and wettability than acid etching and micro-milling for catalytic reactions. In addition, the effect of heat treatment and viscosity of γ-Al_2O_3 slurry was also investigated.

Keywords: Microstructured rough surfaces, wettability, adhesion, metallic catalytic support

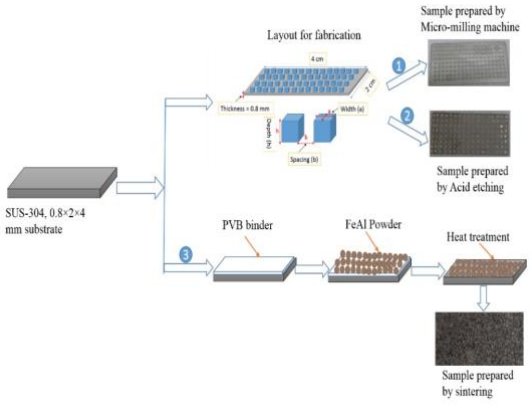

Figure 1: Schematic diagram of fabrication of SUS-304 microstructured rough surface samples by Micro-milling, acid etching and sintering.

References:

1. Visakh Vaikuntanathan and D. Sivakumar, "Maximum Spreading of Liquid Drop Impacting on Groove-Textured Surfaces: Effect of Surface Texture", Langmuir, 2016, 32, 2399−2409
2. Jose´ Bico, Uwe Thiele, David Que´re, "Wetting of textured surfaces", Colloids and Surfaces A: Physicochem. Eng. Aspects, 2002, 206, 41–46.

SurfCoat Korea 2019
Session III: Coatings for energy and environmental applications

Active Corrosion Protection of Metals by Ce-containing Conversion Coatings

R. Ramanauskas, O. Girciene, L. Gudaviciute, S. Butkute, A. Kirdiekiene, I. Morkvenaite-Vilkonciene, J. Juodkazyte, A. Selskis

Center for Physical Sciences and Technology, Department of Electrochemical Materials Science, Vilnius, Lithunia

Abstract: Active corrosion protection of metals implies not only mechanical covering of the protected surface with a dense barrier coating, but also self-healing properties, which ensure durable protection even after partial damage of the coating.

The aim of the present study was to evaluate the protective and self-healing capacities of Ce-doped phosphate, phosphate/permanganate and phosphate/molybdate conversion coatings on a carbon steel surface and to study the process of a new passive film formation on the artificially damaged areas of these coatings.

The SEM, TEM, XRD and XPS techniques were applied for the structural, phase and composition characterization, while voltammetric and EIS measurements yielded information on the self-healing and protective properties of different protective systems.

Phosphate coating on the steel surface was chosen as the base for the active corrosion protection film. An appropriate addition of permanganate or molybdate ions to the phosphate treatment solution resulted in the enhancement of the protective properties of the conversion film, while additional treatment with Ce ions containing solution provided the self-healing ability. Both, the highest protective and self-healing abilities were exhibited by Ce-modified molybdenum/phosphate (Fe-P/Mo-Ce) coatings, which were deposited in $Ce(NO_3)_3$ solution containing sulphate ions. The recovery of the conversion film in the zone of artificial defect was observed after the exposure of the latter sample in NaCl solution and subsequent examination with TEM technique (Figure 1). The newly formed film consisted of Ce oxide phase, princilpally. The active corrosion protection ability of the Fe-P/Mo-Ce conversion coating was secured by a larger amount of Ce^{4+} in the top layer of the film and lower amount of the structural defects in the boundary between the substrate and conversion layer compared to other investigated coatings.

Keywords: active corrosion protection, steel, Ce conversion coatings, self healing.

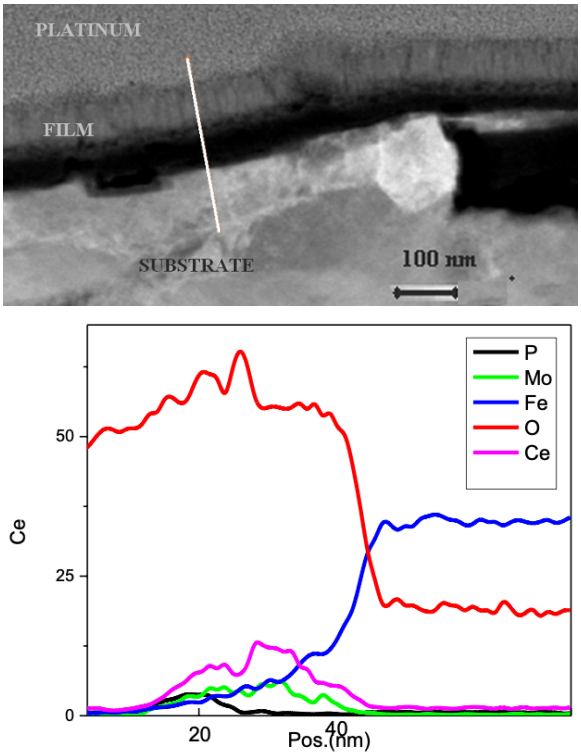

Figure 1: TEM image and the top layer element distribution of Fe-P/Mo-Ce sample in the region of defect after the coating exposure in 0.5 M NaCl solution for 1 h.

Insight into the structure-property relationship of the protective coatings at the atomic level

Zaoli Zhang

Erich Schmid Institute of Materials Science, Austrian Academy of Sciences, Leoben, Austria

Abstract:
Transition metal nitrides have found widespread applications in the cutting- and machining-tool industry due to their extreme hardness, thermal stability and resistance to corrosion. The increasing demand of these nitrides requires an in-depth understanding of their structures at the atomic level. This has led to numerous experimental and theoretical studies.

In this paper, I will firstly present some recent results on the atomic and electronic structures of the interface between various metal nitride mono-layer films (CrN, VN and TiN) on MgO and Al_2O_3 substrate by using spherical aberration-corrected high resolution transmission electron microscopy (HRTEM), scanning TEM, electron energy loss spectroscopy (EELS), quantitative atomic displacement measuremen, complmented by theoretical calculations. Interface induced phenomena between nitride films and substrates are revealed [1-2]. The emphasis is also placed on the nitrogen vacancy effect at the interface.

The second example will be on CrN/AlN nanolayers, which exhibit a peak in hardness of ~40 GPa under a certain bilayer period (Λ). The improvement in mechanical properties in comparison with their monolithic counterparts have a close relationship with the existence of a metastable face-centered cubic (*fcc*) AlN phase which can be epitaxially stabilized in the films. Here, oscillations of interplanar spacing in cubic CrN/AlN multilayers were experimentally observed by using HRTEM, and clearly corroborated by first principles calculations. Electron spectroscopy and microscopy were employed to analyze the strain distribution in the multilayers and obtain generalized relationships between the electronic structure on the one hand, and (non-) stoichiometry or strains in the multilayers on the other hand. The current study provides atomic-scale insights on the mechanisms of extraordinary strength pertaining to the CrN/AlN multilayers [3].

The third example will be regarding the biased-TiN thin films. The atomic-resolution investigations exhibit that the low-angle boundaries are dominant, and the twins are surprisingly fomed under a certain bias voltage[3]. The conductivity of the films is remarkably improved with increasing bias voltage due to the structural evolution. Both in hardness and Young's modulus show, first increase respectively to ~30 GPa and ~340 GPa, and then decrease with further increase of the bias voltage.

Keywords: hard coatings, HRTEM, EELS, density functional theory

References:

1. Zhang, Z., Li, H., Daniel, R., Mitterer, C., Dehm, G., (2013) Insights into the atomic and electronic structure triggered by ordered nitrogen vacancies in CrN. *Physical Review B* 87, 014104-9.
2. Zhang,Z., Gu, X., Holec, D., Bartosik, M., Mayrhofer, P.H. , Duan, H. P., (2017) Superlattice-induced oscillations of interplanar distances and strain effects in the CrN/AlN system. *Physical Review B* 95, 155305.
3. Xu, Z., Zhang, Z., Bartosik, M., Zhang, Y., Mayrhofer,P.H., He, Y., (2018) Insight into the structural evolution of TiN films via atomic resolution TEM, *Journal of Alloys and compounds* 754, 257-267.
4. The author would like to thank David Holec, Rostislav Daniel and Christian Mitterer (Montanuniversität Leoben), Matthias Bartosik and Paul H.Mayrhofer (TU Wien) for helpful discussions and preparing the film materials.

Hybrid Organic-Inorganic Coatings of Double Layered Hydroxide on Aluminum Alloy for Enhanced Alkaline Resistance

Shang-Tien Tsai[1], WenChyuan ChangJean[1], Pei-Hsiun Chao[1], Tseng-Chang Tsai[2*]

[1] Hawing GemS Technology Corporation, Taichung, Taiwan
[2] National University of Kaohsiung, Kaohsiung, Taiwan

Abstract:
Aluminum alloy suffers from corrosion upon exposure in some environments such as acid, alkaline, or chloride anion (Cl^-) containing solution. Many researches have been pursuing on the development of non-chrome coating for anti-corrosion against Cl^-. Layered double hydroxide (LDH) is an anion-exchangeable material consisting of stacks of positively charged divalent - trivalent metal oxide layers, such as Zn(II)-Al(III) oxide. Tedim et al. reported that LDH could be used as a nano-container for encapsulation of inhibitor for control release application. Upon the attack of Cl^- from corrosive environment, the gallery incorporated anion could be exchangeable with the invading Cl^-, therefore LDH having additional Cl^- capacity provides strong protection capability in against chloride corrosion. Furthermore, Zhang et al. reported that sodium dodecyl sulfate (SDS) intercalated LDH has superhydrophilicity and strong anti-corrosion capability. Recently, Yan et al. reported that LDH film could self-heal defects in NaCl solution by dissolution/recrystallization mechanism [5].
Growth of oriented Zn-Al LDH film on AA6061 substrate was achieved through hydrothermal crystallization by which partial dissolved alloy substrate during the hydrothermal synthesis was used as the in-situ Al source with addition of external Zn precursor as Zn source. With increasing hydrothermal temperature and time, the LDH film grown on AA6061 became increasing oriented and intergrowth, resulting in increasing dense film structure. Depending on LDH crystallinity, film density and hydrophobicity, LDH film could significantly enhance the corrosion resistance of AA6061 in 0.1 M NaOH solution (pH of 13) by reduction of corrosion current (i_{corr}) by four orders of magnitude. When Poly(methyl methacrylate) (PMMA) or sodium dodecyl sulfate was intercalated into the LDH film, the functionalized LDH film exhibited even more reduced icorr and also more positive corrosion potential (E_{corr}), as an indication of reduction of the corrosion activity of AA6061. The improved corrosion resistance of intercalated LDH film could be attributed to the dense film structure of polymer – LDH composite. In contrast, when PMMA and some other polymers were coated on the LDH film, polymer acted as a physical protection layer enabling only for reduction in corrosion rate without metal passivation.sion protection property for AA6061 in NaCl solution.

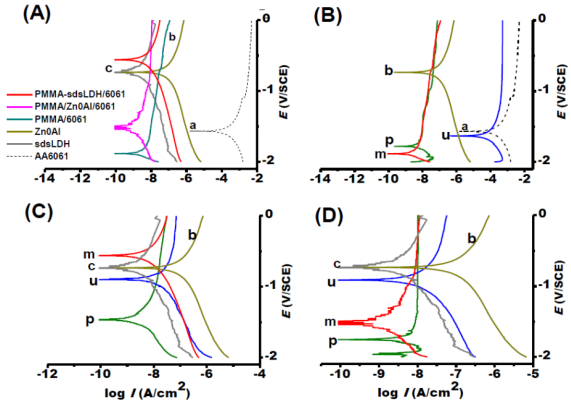

Fig. 1 Electrochemical polarization spectroscopy of (A) PMMA functionalized AA6061; (B) polymer coated AA6061; (C) polymer intercalated sdsLDH film coated AA6061; and (D) AA6061 coated with polymer and Zn0Al140C48h films. Measurement was done while immersing in 0.1 M NaOH solution (pH = 13).

Keywords: LDH film; Oriented film; Alkaline corrosion resistance; Al alloy; Polymer functionalization.

References:

1. Hernandez, M., Covelo, A., Menchaca, C., Uruchurtu, J., Genesca J. (2012) Characterization of the Protective Properties of Hydrotalcite on Hybrid Organic-Inorganic Sol-Gel Coatings, *Corrosion,* 70, 828-840.

Graphene Korea 2019
Session I A: Graphene and 2D Materials, Growth, synthesis, modification and functionalization and Characterization

Graphene Oxide Liquid Crystal

Sang Ouk Kim

National Creative Research Initiative Center for Multi-Dimensional Directed Nanoscale Assembly, Department of Materials Science & Engineering, Daejeon 34141, Republic of Korea

Abstract:
Graphene Oxide Liquid Crystal (GOLC) is a newly emerging chemically modified graphene based two-dimensional material, which exhibits nematic type colloidal discotic liquid crystallinity with the orientational ordering of graphene oxide flakes in good solvents, including water. Since our first discovery of GOLC in aqueous dispersion in the year of 2009 [1], this interesting mesophase has been utilized over world-wide for many different application fields, such as liquid crystalline graphene fiber spinning, highly ordered graphene membrane/film production, prototype liquid crystal display and so on [2,3]. Interestingly, GOLC also allow us a valuable opportunity for the highly ordered molecular scale assembly of functional nanoscale structures. This presentation will introduce our current research status of GOLC research particularly focusing on the nanoscale assembly of functional nanostructures, including fibers, films and three-dimensionl nanoporous materials. Besides, relevant research works associated to the nanoscale assembly and chemical modification of various nanoscale graphene based materials will be presented [4,5].

Keywords: graphene, graphene oxide, liquid crystal, assembly, fiber, dispersion, colloid, nematic, lyotropic, suspension,

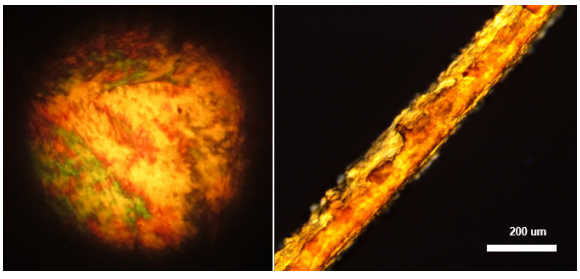

Figure 1: GOLC in aqueous dispersion can be ordered into multi-dimensional structures such as fiber structure by molecular scale assembly. Optical microscopy images of GOLC dispersion and highly aligned GOLC fiber between crossed polar-izers.

References:

1. J. E. Kim, T.H. Han, S.H. Lee, J.Y. Kim, C.W. Ahn, J.M. Yun, S.O. Kim, *Angewandte Chemie International Edition* **50**, 3043 (2011).
2. R. Narayan, J.E. Kim, J.Y. Kim, K.E. Lee, S.O. Kim, *Advanced Materials* **28**, 3045 (2016).
3. J.Y. Kim, S.O. Kim, *Nature Materials* **13**, 325 (2014).
4. U. N. Maiti, W. J. Lee, J. M. Lee, Y. T. Oh, J. Y. Kim, J. E. Kim, J. W. Shim, T. H. Han, S. O. Kim, *Advanced Materials* **26**, 40 (2014).
5. S. H. Lee, D. H. Lee, W. J. Lee, S. O. Kim, *Advanced Functional Materials* **21**, 1338 (2011).

Strategies for the Synthesis of Wafer Scale Graphene Single Crystal

Feng Ding[1,2]

1Department of Material Science and Engineering, Ulsan National Institute of Science and Technology, 50, UNIST-gil, Ulsan 44919, Republic of Korea
2Center for Multidimensional Carbon Materials, Institute for Basic Science, Advanced Material Building (101), UNIST, 50, UNIST-gil, Ulsan 44919, Republic of Korea

Abstract:
Wafer scale graphene single crystal the ideal for maximizing the performances of graphene based devices and various applciations, such as corrosion protection. Here we demonstrate a few routes and their experimental realizations towards the synthesis of wafter scale graphene crystal.
(i) Consideing the weak van der Waals interaction between graphene bulk and the surfaces of various transition metals, we showed that a single crystal graphene island may across a grain boundary (GB) of the substrate without changing its single-crystallinity. Based on this theoretical prediction, we propose that wafer scale graphene single crystal might be synthesized on a polycrystal metal surface via nulceation suppression.[1] Such a strategy was realized by the method of feedstock local feeding during graphene CVD growth on Cu-Ni surface.[2]
(ii) The preferencial alignment of nucleated graphene island on a transition metal surface allows us to grow single crystal graphene on a symmetry matching catalyst surface and, therefore, wafer scale graphene single crystal growth might be achieved on a wafer scale single crystalline metal surface.[1,3,4] Experiemtnally, large area single crystal Cu (111) foils was synthesized and the realization of wafter scale graphene single crystal CVD growth was demonstrated.[5,6]
(iii) Besides the (111) surface of fcc crystal and the (0001) surface of the hcp crystal, our theoretical analysis predicts that unidirectional growth of graphene on a high index metal foil is also possible.
(iv) The free rotation of graphene islands on a liquid metal surface may leads to the seamless stiching of graphene islands and, therefore, the growth of wafter scale graphene single crystal might be achieved on a liquid metal surface is possible.

Keywords: graphene, single crystal, chemical vapor deposition

References:

1. X Zhang, Z Xu, L Hui, J Xin, F Ding, (2012), How the orientation of graphene is determined during chemical vapor deposition growth. *The Journal of Physical Chemistry Letters* 3, 2822-2827
2. T Wu, X Zhang, Q Yuan, J Xue, G Lu, Z Liu, H Wang, H Wang, F Ding, Q Yu, X Xie, M Jiang, (2016) Fast growth of inch-sized single-crystalline graphene from a controlled single nucleus on Cu–Ni alloys, *Nature materials* 15, 43
3. J Gao, J Yip, J Zhao, BI Yakobson, F Ding, (2011) Graphene nucleation on transition metal surface: structure transformation and role of the metal step edge, *Journal of the American Chemical Society* 133, 5009-5015
4. Q Yuan, BI Yakobson, F Ding (2014) Edge-catalyst wetting and orientation control of graphene growth by chemical vapor deposition growth, *The journal of physical chemistry letters*, 5, 3093-3099
5. S Jin, M Huang, Y Kwon, L Zhang, B Li, S Oh, J Dong, D Luo, M Biswal, B V Cunning, (2018) Colossal grain growth yields single-crystal metal foils by contact-free annealing, *Science* 362, 1021-1025
6. X Xu, Z Zhang, J Dong, D Yi, J Niu, M Wu, L Lin, R Yin, M Li, J Zhou, S Wang, J Sun, X Duan, P Gao, Y Jiang, X Wu, H Peng, R S Ruoff, Z Liu, D Yu, E Wang, F Ding, K Liu, (2017), Ultrafast epitaxial growth of metre-sized single-crystal graphene on industrial Cu foil, *Science Bulletin* 62, 1074-1080

Transfer-Free Large-Scale High-Quality Monolayer Graphene Synthesized at Lower Temperatures than Boiling Point of Water

Byeong-Ju Park,[1] Yire Han,[1] Jin-Seok Choi,[1,2] Hyunwoo Ha,[1] Hyun You Kim,[1] Cheolho Jeon,[3] Ji-Ho Eom,[1] Gangho Park,[4] Hee-Tae Jung,[4] Yun-Ho Kim,[5] and Soon-Gil Yoon,[1,*]

[1]Department of Materials Science and Engineering, Chungnam National University, Daeduk Science Town, 34134, Daejeon, Rep. of Korea
[2]Analysis Center for Research Advancement (KARA), Korea Advanced Institute of Science and Technology, 291 Daehak-ro, Yuseong-gu, 34141, Daejeon, Rep. of Korea
[3]Advanced Nano-Surface Group, Korea Basic Science Institute (KBSI) 169-148 Gwahangno, Yuseong-gu, Daejeon 34133, Rep. of Korea
[4]Department of Chemical and Biomolecular Engineering, Korea Advanced Institute of Science and Technology, Daejeon 34141, Rep. of Korea
[5]Advanced Polymer Materials, Korea Research Institute of Chemical Technology, Daejeon, 34114, Rep. of Korea

Abstract

Direct and large-scale graphene synthesis on flexible substrates is challenging approach to manufacturing flexible electronic devices, as it avoids the drawbacks of transferred graphene.[1,2] To fabricate flexible devices on plastic substrates, the graphene synthesis temperature must be below ~150 °C to prevent substrate deformation.[3,4] In this letter, high-quality graphene was directly synthesized on 10 nm-thick Ti-buffered polyethylene terephthalate (PET) substrates. Herein, we demonstrate theoretical and experimental evidence for 4-inch-scale, high-quality graphene grown at low temperatures below 150 °C *via* plasma-assisted thermal chemical vapor deposition (PATCVD) that reduces a CH_4 into carbon at room temperature. The monolayer graphene synthesized directly with no transfer revealed the surprising results such as predominant electromechanical properties, a low sheet resistance of 81 ± 4.0 Ω $\square^{-1}$, a giant average grain size of ~ 130 μm, a high field-effect-transistor (FET) mobility of (8.4 ± 0.03) × 10^3 cm^2 $V^{-1}s^{-1}$, a Dirac point of around ~ 0 V, and room temperature on/off current ratio of ~ 10^3 in monolayer graphene-FET. We further use layer-by-layer direct stacking to fabricate three-layers for lower sheet resistance, which showed values as low as ~ 10 Ω $\square^{-1}$ at ~ 93% transparency. Graphene films of three layers stacked directly revealed a predominant flexibility by 10^4 bending cycles under tensile strain of 5%. These findings could pave the way for a practical exploitation of flexible electronic devices *via* large-scale, high-quality monolayer graphene synthesized directly with no need for transfer processes.

Graphene anode for organic and perovskite light-emitting diodes

Tae-Woo Lee,[1,*]

[1] *Department of Materials Science and Engineering, Seoul National University, 1 Gwanak-ro, Gwanak-gu, Seoul 08826, Republic of Korea*

Abstract:
Although graphene has exceptional electrical and mechanical properties, lower work function (~4.4 eV) and higher sheet resistance (>300 ohm/sq) of pristine graphene than those of conventional indium-tin-oxide (ITO) has been a critical drawbacks to be used for flexible organic optoelectronics. Here, we strategically modify and employ the unique natures of graphene on various optoelectronic devices (organic light-emitting diodes (OLEDs) and perovskite light-emitting diodes (PeLEDs).
First, we improve the electrical properties (conductivity, work function) of graphene with outstanding stability for anode application in (OLEDs). We demonstrate an extremely environmentally-stable graphene electrode doped with macromolecular acid (perfluorinated polymeric sulfonic acid: PFSA) as a chemical p-type dopant. The PFSA doping on graphene provided not only ultra-high ambient stability for a very long time (> 64 d) but also high chemical and thermal stability even after exposure to various solvents and high temperature (300 °C), which have been almost impossible by doping with conventional small-molecule acids. Furthermore, PFSA doping induced a substantial increase of the surface potential (~0.8 eV) of graphene, reduced its Rs by ~56%, and achieved a smooth surface without negligible loss of optical transmittance at the same time. A hole-only device using the PFSA-doped graphene demonstrates improved hole injection capability by reducing the energy barrier. High-efficiency green phosphorescent OLEDs were fabricated with the PFSA-doped graphene anode (~98.5 cd/A, ~95.6 lm/W without out-coupling structures)[1].
Second, we use graphene anode of high work function and conductivity in PeLEDs using chemical doping and PEDOT:PSS based hole-injection layers. As ITO is vulnerable to acidic condition, PEDOT:PSS can chemically etch the ITO and In+, Sn+ ions are generated and diffused into overlying emitting layers, which cause quenching effect and degrade the luminous properties. Since perovskite layer has long exciton diffusion length that organic emitter did, quenching issue is more critical in PeLEDs. In contrast to the ITO, graphene is chemically stable and does not generate metallic ions, which cause quenching. By employing chemical doping with PEDOT:PSS based polymeric hole injection layer, PeLEDs with graphene anode exhibited higher luminous properties (18.0 cd/A, EQE: 3.8%) than that with ITO anode did. Furthermore, PeLEDs with graphene anode exhibited outstanding flexibility due to mechanical robustness of graphene anode. These works lay a solid platform for various optoelectronic applications of graphene anodes[2]. **Keywords**: protein folding, nanoporous sol-gel glasses, silica-based biomaterials, circular dichroism spectroscopy, surface hydration, crowding effects, micropatterning, biomedical applications.

References:

1. S.-J. Kwon, T.-H. Han, T. Y. Ko, N. Li, Y. Kim, D. J. Kim, S.-H. Bae, Y. Yang, B. H. Hong, K. S. Kim, S. Ryu, T.-W. Lee (2018) Extremely stable graphene electrodes doped with macromolecular acid, *Nat. Commun.* 9, 2037 (2018).
2. H.-K. Seo, H. Kim, J. Lee, M.-H. Park, S.-H. Jeong, Y.-H. Kim, S.-J. Kwon, T.-H. Han, S. Yoo, T.-W. Lee (2017) Efficient Flexible Organic/Inorganic Hybrid Perovskite Light-Emitting Diodes Based on Graphene Anode, *Adv. Mater.* 29, 1605587.

POINT-LIKE DEFECTS IN TRANSITION METAL DICHALCOGENIDES CHARACTERIZED BY SPM SIMULATIONS

Blanca Biel[1,*], Aurelio Gallardo[2], Pablo Pou[3]

[1]Dep. of Atomic, Molecular and Nuclear Physics, Faculty of Science, Campus de Fuente Nueva, University of Granada, 18071 Granada, Spain
[2]Institute of Physics of the Czech Academy of Sciences, v.v.i., Cukrovarnická 10, 162 00 Prague, Czech Republic
[3]Dpto. Física Teórica de la Materia Condensada, Facultad de Ciencias, Campus de Cantoblanco, Universidad Autónoma de Madrid, E-28049 Madrid, Spain

Abstract:

Defects are frequently present in 2D materials, and as such have been extensively studied on suspended samples. However, the presence of the metallic substrates commonly employed during the growth and the characterization processes might substantially alter the electronic structure of the 2D material. In order to describe realistically the electronic properties and the SPM characterization of such samples, simulations need to take the impact of the substrate into account.

The interaction between metallic substrates and pristine transition metal dichalcogenides (TMDs) can greatly vary depending on the metal [1]. In this work, we have studied the interaction of several point-like defects in TMDs monolayers with underneath Ir(111) and Au(111) substrates by means of DFT calculations and SPM simulations, revealing a notably different behavior depending on the metallic substrate considered. The hybridization of the S states with those of the Ir(111) substrate induces a shift of ~1 eV of the MoS_2 states towards the valence band and a large broadening of the defect states [2]. The interaction with a gold substrate leads to a similar shift but is much weaker, as confirmed by experimental data [3], leading to sharper defect states (Fig.1), much more similar to those found for freestanding MoS_2.

Keywords: transition metal dichalcogenides (TMDs), Density Functional Theory (DFT), SPM, defects, metallic substrates

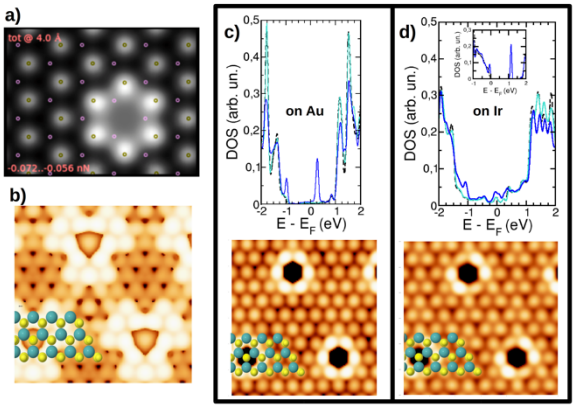

Figure 1: Fig 1. Left panel: AFM (a) and STM at -0.1 V (b) images of a S vacancy at the top layer for freestanding MoS_2. Right panel: LDOS of top S atoms close (blue) and far (cyan) of the defect site and STM images at V = -0.1 V for a top S vacancy in epitaxial MoS_2/Au(111) (c) and MoS_2/Ir(111) (d) . Inset in d): LDOS of a top S vacancy in freestanding MoS_2.

References:

1. Chen, W. *et al*. (2013) Tuning the Electronic and Chemical Properties of Monolayer MoS_2 Adsorbed on Transition Metal Substrates, *Nano Letters* 13, 509; Gong, C. *et al*. (2014) The Unusual Mechanism of Partial Fermi Level Pinning at Metal–MoS_2 Interfaces, *Nano Letters*, 14, 1714.
2. Delac Marion, I., Capeta, D., Pielic, B., Faraguna, F., Gallardo A., Pou P., Biel B., Vujicic N. and Kralj M. (2018), *Nanotechnology*, 29 (30), 305703.
3. Krane, N., Lotze, Ch., Pou, P., Biel, B. and Franke, K. (in preparation)

The structure of graphene folds in single crystal graphene film grown on a Cu(111) foil

Da Luo,[1] Myeonggi Choi,[2] Meihui Wang,[3] Youngwoo Kwon,[1] Zonghoon Lee,[1,2] Rodney S. Ruoff[1,2,3,4*]

[1] Center for Multidimensional Carbon Materials (CMCM), Institute for Basic Science (IBS), Ulsan, Rep. of Korea
[2] School of Materials Science and Engineering, Ulsan National Institute of Science and Technology (UNIST), Ulsan, Rep. of Korea
[3] Department of Chemistry, Ulsan National Institute of Science and Technology (UNIST), Ulsan, Rep. of Korea
[4] School of Energy and Chemical Engineering, Ulsan National Institute of Science and Technology (UNIST), Ulsan, Rep. of Korea

Abstract:
We have discovered a 3-layer thick ribbon-like structure in monolayer graphene grown by chemical vapor deposition (CVD) on Cu(111) foils and we refer to this as a "graphene fold". These folds are essentially parallel to each other, have widths of 80-100 nm, lengths of up to a centimeter or so, and are separated from each other by about ~20-50 μm. (We evaluated many papers published in the literature and found from images shown in figures in those papers that what *we* now know is a 'graphene fold' had been "mis-assigned" as "graphene wrinkle", "graphene grain boundary", or an "overlapped grain boundary".)
The parallel graphene folds are very likely tall wrinkles that built up due to deadhesion in particular regions after compressive stress built up during cooling of the Cu(111) foil/single crystal graphene film; it is reasonable to conjecture that these wrinkles "fell over" and adhered to the surface. We have discovered that these folds are not continuous straight ribbon-like structures (as they appear to be under low magnification optical microscopy or low magnification SEM) but have an "alternating" pattern (per high-resolution AFM, SEM and TEM). We thought that the fold was likely "cracked" at the region between alternating fold sections along the "fold line", and atomic resolution TEM performed on such "joints" proves this to be true.

Keywords: monolayer graphene, chemical vapor deposition, Cu(111) foil, single crystal, compressive strain, folds, wrinkles.

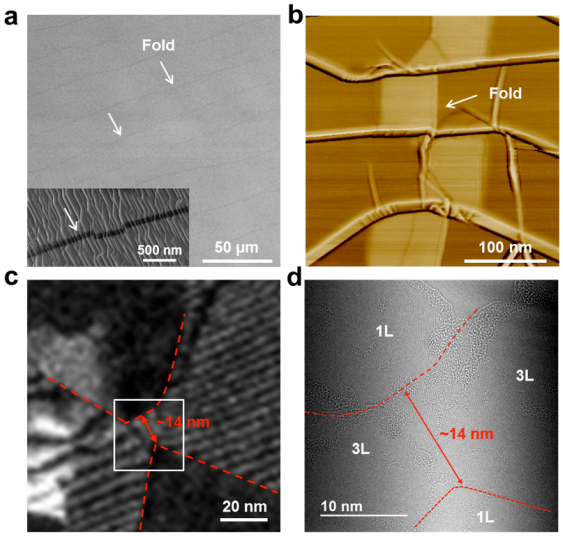

Figure 1: (a) SEM image, (b) AFM phase image, (c) Dark field TEM image, and (d) atomic resolution TEM image of graphene fold(s) in single crystal graphene film grown on Cu(111) foil.

References:

1. Jin, S., Huang, M., Kwon, Y., Zhang, L., Li B., Oh, S., Dong, J., Luo, D., Biswal, M., Cunning, B., Bakharev, P., Moon, I., Yoo, W., Camacho-Mojica, D., Kim, Y., Lee, S., Wang, B., Seong, W., Saxena, M., Ding F., Shin, H., Ruoff, R. (2018), Colossal grain growth yields single-crystal metal foils by contact-free annealing. *Science*, 362 (6418), 1021-1025.
2. Li, B., Luo, D., Zhu, L., Zhang, X., Jin, S., Huang, M., Ding, F., Ruoff, R. (2018), Orientation-Dependent Strain Relaxation and Chemical Functionalization of Graphene on a Cu(111) Foil. *Adv. Mater.*, 30, 1706504.

Acknowledgement
This work was supported by IBS-R019-D1

Many-body quantum Monte Carlo study of 2D materials: Cohesion, band gap, and strain effect in phosphorene

T. Frank,[1] R. Derian,[2] K. Toár,[2] L. Mitas,[3] J. Fabian,[1] and I. Štich[2],

[1] University Regensburg, Institute for Theoretical Physics, 93040 Regensburg, Germany
[2] Institute of Physics, Slovak Academy of Sciences, 84511 Bratislava, Slovakia
[3]Department of Physics, North Carolina State University, Raleigh, NC 27695-8202, U.S.A

Abstract:
Quantum Monte Carlo (QMC) is applied to obtain the fundamental electronic band gap, Δ_f, of a semiconducting two-dimensional (2D) phosphorene [1]. Similarly to other 2D materials, the electronic structure of phosphorene is strongly influenced by reduced screening, making it challenging to obtain reliable predictions by single-particle density functional methods. Advanced GW techniques, which include many-body effects as perturbative corrections, are hardly consistent with each other, predicting the band gap of phosphorene with a spread of almost 1 eV, from 1.6 to 2.4 eV. Our QMC results, from infinite periodic superlattices as well as from finite clusters, predict Δ_f to be about 2.4 eV, indicating that available GW results are systematically underestimating the gap. Using the recently uncovered universal scaling between the exciton binding energy and Δ_f [2], we predict the optical gap of 1.75 eV that can be directly related to measurements even on encapsulated samples due to its robustness against dielectric environment. The QMC gaps are indeed consistent with recent experiments based on optical absorption and photoluminescence excitation spectroscopy. We also predict the cohesion of phosphorene to be only slightly smaller than that of the bulk crystal. The same technology is also used to study the effect of strain. Our investigations not only benchmark GW methods and experiments, but also open the field of 2D electronic structure to computationally intensive but highly predictive QMC methods which include many-body effects such as electronic correlations and van der Waals interactions explicitly.

Keywords: 2D materials, phosphorene, band gap, cohesion, strain effects, QMC.

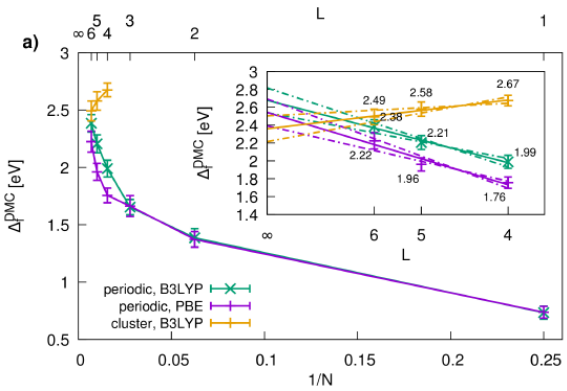

Figure 1: Finite-size scaling of the computed fundamental gap, Δ_f, with the number of atoms, N, in the periodic supercell (green line, B3LYP/DMC; purple line, PBE/DMC) and in the cluster approach (yellow line, B3LYP/DMC) along the series of $L \times L$ supercell approximants, L = 1 to 6, for the periodicsetup and L = 4, 5, and 6 in the cluster approach. The inset shows the zoom-in of the scaling for large N with the dashed lines showing the linear extrapolation to the infinite size limit.

References:

1. T. Frank, R. Derian, K. Tokár, L. Mitas, J. Fabian, and I. Stich, Many-body quantum Monte Carlo study of 2D materials: cohesion and band gap in single-layer phosphorene, submitted (2018); https://arxiv.org/abs/1805.10823.
2. Z. Jiang, Z. Liu, Y. Li, and W. Duan, Scaling Universality between Band Gap and Exciton Binding Energy of Two-Dimensional Semiconductors, Phys. Rev. Lett. **118**, 266401 (2017).

A novel approach to grow the bulk TMDC with two-dimensional material properties

Shi Wun Tong*, Henry Medina and Dongzhi Chi*
Institute of Materials Research and Engineering, Agency for Science Technology and Research,
2 Fusionopolis Way, #08-03 Innovis, Singapore 138634
Email: tongsw@imre.a-star.edu.sg and dz-chi@imre.a-star.edu.sg

Abstract:
The two-dimensional (2D) transition metal dichalcogenides (TMDCs), such as MoS_2, with strong in-plane covalent bonds and weak out-of-plane van der Waals interactions have demonstrated many interesting anisotropic charge transport and optical properties. For example, a strong photoluminescence can be detected via thinning down the bulk MoS_2 counterparts into a monolayer thick owing to the indirect-to-direct band gap transition. The optically active MoS_2 can be effectively achieved by isolating the individual atomic layers from bulk MoS_2 and being further applied into some novel optical applications. Numerous effective approaches in isolating monolayer from bulk have been reported based on mechanical cleavage with scotch tape, electrochemical intercalation with alkali metal, organo-alkali metal compound and Lewis base molecular intercalates. Though mechanical cleavage is the simplest process among these approaches, it is on a small scale and has limits in commercial high-end applications. The electrochemical intercalation involves the complicated top-down set-ups which also limits the production scale-up of the monolayer TMDCs.
Herein, we report a facile process to grow multi-layered MoS_2 thin film with 2D material-like optical property. Based on the CVD growth process, the scalable continuous multi-layered MoS_2 film with sodium intercalation can be effectively attained. Contrary to the conventional intercalated 2D nano-sheets prepared from liquid-phase exfoliation, our approach provides a new pathway for the large-area growth of intercalated TMCs with 2D material properties. The growth of intercalated MoS_2 film includes the pre-deposition of the unique solution-processible molybdenum precursor and subsequent sulfurization in the well optimized manner. As shown in the schematic drawing, the theoretical interlayer spacing of the MoS_2 (Figure 1a-1b) will be expanded from ~0.61 to ~0.74 nm owing to the Na intercalation. Successful Na intercalation into multi-layered MoS_2 has been demonstrated from the cross-sectional HRTEM images (Figure 1c) where MoS_2 thickness with the interlayer spacing of 0.73 nm can be indexed to Na_xMoS_2. The detailed electrical and optical properties of this novel intercalated MoS_2 will be discussed in the presentation.

Keywords: 2D material, photoluminescence, electron mobility, intercalation, sulfurization.

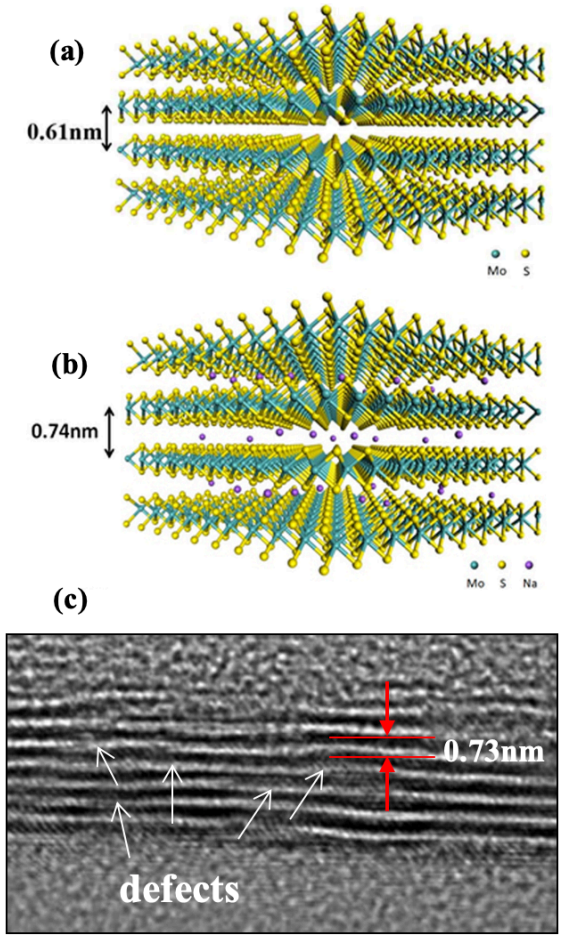

Figure 1: The schematic crystal structure of the (a) MoS_2 and (b) Na-intercalated films. (c) The cross-sectional HRTEM image of the our as-grown intercalated MoS_2 film. The yellow, green and purple balls are S, Mo and Na atoms, respectively.

Influence of Nano-confined Water on the Frictional Properties of Single-layer Graphene Coated Rough Silica Surface

Hsiang-Chih Chiu[1]* and En-De Chu[1]

[1] Department of Physics, National Taiwan Normal University, Taipei City, Taiwan

Abstract:
Graphene has been a promising candidate for protective coatings in micro- or nano-electro-mechanical systems (MEMS or NEMS) due to its extreme thinness, flexbiity, mechanical rigidity, and chemical inertness. Here, by using atomic force microscopy based (AFM) techniques, we have investigated how nanoscale water layers confined between the single-layer graphene (SLG) and rough silica surface will influence the friction characteristics of the supported SLG in ambient conditions. Through the AFM friction and surface potential measurements, we occasionally found polygonal features in both the AFM friction and surface potential images of SLG-covered silica surface that show simultaneously higher friction and surface potential as compared to their adjacent areas due to water layers confined under SLG. Nano-confined water layers underneath SLG can induce the hole-doping effect, leading to a more positively-charged and hydrophilic SLG surface that favors the adsorption of ambient water molecules. When performing AFM friction measurements within the polygonal features on the SLG surface, the enhanced surface hydrophilicity on the SLG will promote the formation of nanoscale water bridges at the interstices between the AFM probe and SLG surface due to the nanoscale capillary effect, leading to a negative dependence of friction on the logarithm of sliding velocity. However, outside these polygonal regions, the measured friction shows a positive dependence on the logarithm of velocity due to relatively higher surface hydrophobicity of SLG. Our results indicate that it is possible to manipulate the frictional properties of SLG coated surface by controlling the amount of water confined under SLG.

Keywords: nanotribology, single-layer graphene, atomic force microscopy, capillary effect, nano-confined water.

References:

1. En-De Chu, Po-Hsiang Wang, Yi-Zhe Hong, Wei-Yen Woon and Hsiang-Chih Chiu (2019) Frictional characteristics of nano-confined water mediated hole-doped single-layer graphene on silica surface, *Nanotech*. 30, 045706.

Similarities and differences of fractional end charges in graphene zigzag ribbon and polyacetylene

S.-R Eric Yang
Physics Department, Korea University, Seoul, Korea

Abstract:
In polyacetylene and graphene nanoribbons a solition with a fractional charge exists as a domain wall connecting two different phases. In polyacetylene a fermion mass potential in the Dirac equation produces an excitation gap, and a twist in this scalar potential produces a zero energy soliton. Similarly, in gapful graphene nanoribbons a distortion in the chiral gauge field can produce a solitonic domain wall between two neighboring zigzag edges with different chiralities [1]. The existence of a soliton in polyacetylene can lead to formation fractional charges on the opposite ends of polyacetylene. However, the situation is different in graphene nanoribbons since antiferromagnetic coupling between the opposite zigzag edges gives rise to integer boundary charges [2].
We show that presence of disorder in graphene nanoribbons partly mitigates the effect of antiferromagnetic coupling between the opposite zigzag edges. As a consequence of this, midgap states can have fractional charges on the opposite zigzag edges in the weak disorder regime [3]. The probability density of such a state is shown in Fig.1. The measurement of the differential conductance in atomically precise graphene zigzag nanoribbons [4] using a scanning tunneling microscopy may provide rich information on the distribution of edge charges.

Keywords: fractional charge, toological insulator, soliton

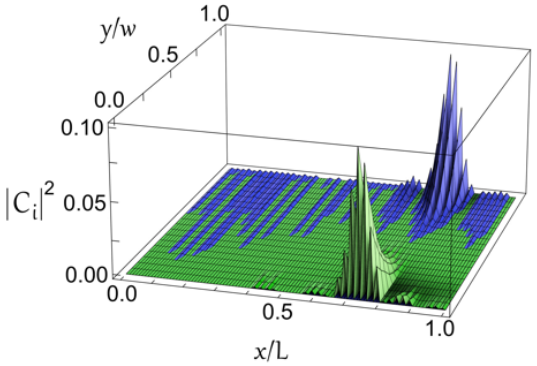

Figure 1 A midgap state with fractional charges of 1/2 residing on the opposite zigzag edges. Plot displays the probability density of the midgap state as a function of coordinate (x,y).

References:

1. Y. H. Jeong, S.C. Kim and S.-R. Eric Yang, Topological gap states of semiconducting armchair graphene ribbons, *Phys. Rev. B* **91**, 205441 (2015).
2. Y. H. Jeong and S.-R. Eric Yang, Topological end and Zak phase states of rectangular armchair ribbon, *Annals of Physics* **385**, 688 (2017).
3. Y. H. Jeong, S.-R. Eric Yang, and M. C. Cha, Fractional edge charges of interacting disordered graphene zigzag nanoribbon (submitted).
4. J. Cai , P. Ruffieux, R. Jaafar , M. Bieri , T.Braun , S. Blankenburg , M. Muoth , A. P. Seitsonen, M. Saleh, X. Feng , K. Mullen and R. Fasel, *Nature* **466**, 470 (2010); P. Ruffieux, S. Wang , B. Yang , C. Sanchez-Sanchez , J. Liu, T. Dienel, L. Talirz , P. Shinde, C. A. Pignedoli, D. Passerone, T. Dumslaff , X. Feng, K. Mullen and G. Fasel R, *Nature* **531**, 489 (2016).

Single layer h-BN grown on curved Ni(111) crystal: oxidation and oxygen intercalation

A. A. Makarova,[1,*] L. Fernandez,[1] D. Yu. Usachov,[2] A. Fedorov,[2,3] K. A. Bokai,[2] D. A. Smirnov,[1] C. Laubschat,[1] D. V. Vyalikh,[4,5] F. Schiller,[6] and J. E. Ortega[4,6,7]

[1] Technische Universität Dresden, Institut für Festkörper- Materialphysik, Dresden, Germany
[2] St. Petersburg State University, St. Petersburg, Russia
[3] IFW Dresden, Dresden, Germany
[4] Donostia International Physics Centre, San Sebastian, Spain
[5] IKERBASQUE, Basque Foundation for Science, Bilbao, Spain
[6] Centro de Física de Materiales CSIC/UPV-EHU-Materials Physics Center, San Sebastian, Spain
[7] Universidad del Pas Vasco, Departamento Física Aplicada I, San Sebastian, Spain

Abstract:
Curving crystals to expose surfaces of variable orientation is a straightforward approach to explore appropriate templates and tunable substrates for two-dimensional materials. It allows the systematic search and rational determination of an optimal growth substrate. A cylindrical crystal with a high-symmetry axis is the simplest curved geometry, but sufficient to span a full set of vicinal planes with close-packed steps. As demonstrated repeatedly, the cylindrical geometry is easy to handle and process in standard vacuum setups.[1,2] Moreover, it is particularly convenient for electron spectroscopies that make use of micron-sized photon beams in synchrotrons, such as Near-Edge X-ray Absorption and X-ray photoemission, since these can be scanned on the curved surface to smoothly probe different vicinal planes.
Recently, we investigated the growth of h-BN on a Ni surface curved around the (111) direction [c-Ni(111)].[1] We observed the formation of a well-defined, homogeneous h-BN monolayer all across the curved crystal, exhibiting an increasing presence of h-BN-covered microfacets, as the surface plane tilted away from the (111) plane.
In the present study we systematically investigate the effect of thermal oxygen exposure of the h-BN monolayer interfacing a full variety of vicinal orientations around the Ni(111) high-symmetry direction.[2] Using Scanning Tunneling Microscopy, X-ray Absorption and Photoemission Spectroscopies we demonstrate the occurrence of two processes upon oxygen exposure: oxygen intercalation underneath the h-BN layer, which leads to decoupling of the h-BN from the substrate, and oxidation of h-BN itself, which proceeds via substitution of nitrogen atoms.

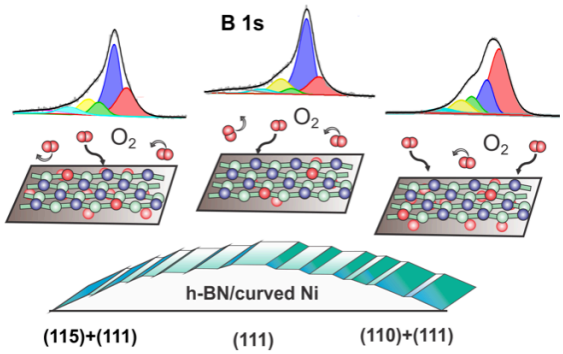

Figure 1. Schematic representation of the thermal oxygen exposure of h-BN/c-Ni(111) and corresponding B 1s photoemission spectra.

Keywords: curved crystals, Ni, 2D materials, hexagonal BN, oxygen exposure, oxidation, intercalation, Photoelectron Spectroscopy, X-ray absorbption spectrocopy.

References:

1. Fernandez, L., et al. (2019) Boron nitride monolayer growth on vicinal Ni(111) surfaces systematically studied with a curved crystal, *In Press*.
2. Makarova, A., et al. (2019) Oxygen Intercalation and Oxidation of Atomically Thin h-BN Grown on a Curved Ni Crystal, *J. Phys. Chem. C*, 123, 593–602.

Development of Roll to Roll CVD system for mass production of high quality and large area Graphene

Youn-Su Kim.,[1*] Jinwoo Sung,[1] Jin San Moon,[1] Won Bae Park,[1] Jonghyun Rho,[1] Myung Hee Jung[1]

[1] LG electronics, Materials and Production Engineering Research Institute, Seoul, Korea

Abstract:
A roll-to-roll chemical vapor deposition (CVD) system has been developed for mass production of high-quality graphene on copper foil. In vertically loaded Cu film in CVD chamber, tension was deliberately manipulated for balancing in lateral direction, allowing high throughput (25 m^2 /hr) roll-to-roll process without deformation of Cu film, and high quality of single-layered graphene was synthesized on Cu (111) surface, which is favored due to minimum lattice mismatch, rendered by the homogeneous tension [1, 2]. The large area graphene of 400 mm in width having a uniform quality of mono-layer coverage in the manner of suppressed multi-dots and controlled grain size (5 ~ 200 um^2) demonstrated a sheet resistance of 240 Ω/ □ (without intentional doping) on plastic films. Moreover, the CVD grown graphene consisted of large grain (200 um^2) and minimized number of multi-dots (10 - 30 / 100 X 100 um^2) exhibited as high as 2500 cm^2 V/ s in mobility by Hall measurement under ambient condition [3].

Keywords: Thermal Chemical Vapor Deposition, Carbon, Graphene, Roll-to-Roll process, Hall measurement, Mobility, Sheet resistance, Raman Spectrum, Mass production, Quality control, Large area graphene.

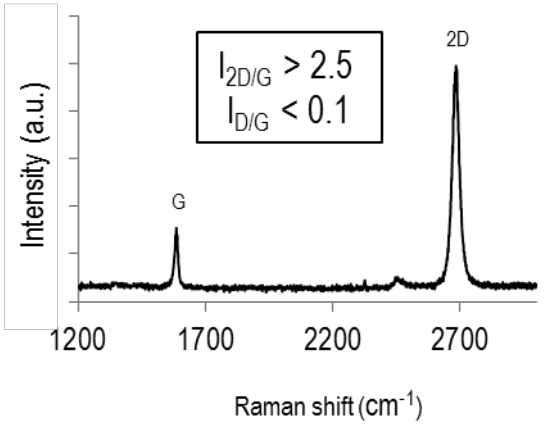

Figure 1: Raman Spectrum of graphene on SiO_2 substrate measured at an excitation wave length of 532 nm.

References:

1. Deng, B., Liu, Z., Peng, H. (2018), Toward mass production of CVD graphene films, *Adv. Mater.,* 30, 1800996.
2. Jo, I. et al. (2018), Tension-controlled single-crystallization of copper foils for roll-to-roll synthesis of high-quality graphene films, *2D materials,* 5, 024002.
3. Chen, J.-H., Jang, C., Xiao, S., Ishigami, M., & Fuhrer, M. S. (2008), Intrinsic and extrinsic performance limits of graphene devices on SiO2, *Nat. Nanotech*., 3, 206-209.

Graphene Korea 2019
Session II A: Graphene for Electronic, Photovoltaic and Magnetic Applications

Moiré superlattices and minibands for Dirac electrons in graphene heterostructures

Vladimir Falko

National Graphene Institute, the University of Manchester, M13 9PL, Manchester, UK

Abstract:
When graphene lattice is aligned with the hBN lattice, a long-wavelength periodic moiré pattern forms due to a weak incommensurability of the two lattice structures, leading to a long-range superlattice affecting properties of electrons in graphene, including formation of miniband spectra for Dirac electrons [1-3] and reappearance of magnetic minibands [4,5] at the rational values of magnetic field flux through the supercell area (in units of $\phi 0=h/e$), also known as Hofstadter butterfly [6].
Here, we show that the quantum effect of the minibands formation in long-period moiré superlattices (mSL) in graphene/hBN heterostructures affect their transport measurements up to the room temperature. In relation to the low-magnetic-field regime, we find signatures of miniband formation in capacitance spectroscopy, resistivity and Hall effect, and also in magnetic focusing of electrons in ballistic structures. We also find that the overall temperature dependence of resistivity displays the opening in a new scattering process: the umklapp electron-electron scattering in which two electrons coherently transfer the mSL Bragg momentum to the crystal [7].
The formation magnetic minbands and their manifestation in magneto-oscillation of the diagonal conductivity tensor persist up to the room temperature [8], too, with full hierarchy of features that are attributed to the rational flux values $\phi=(p/q)\phi 0$, with p=1, 2 and up to 3 (and $7<q<1$), now, observed [9] at the intermediate range of $50K<T<200K$.

References:

1. J. Wallbank, et al. PRB 87, 245408 (2013).
2. L. Ponomarenko, et al. Nature 487, 594 (2013).
3. J. Wallbank, et al. Annalen der Physik, 527, 259 (2015).
4. E. Brown, PR 133, A1038 (1964); a. J. Zak, PR 134, A1602/A1607 (1964).
5. X. Chen, et al. PRB 89, 075401 (2014); X. Chen, et al. PRB 94, 045442 (2016); a. G.. Yu, et al. Nature Physics 10, 525 (2014).
6. D. R. Hofstadter, PRB 14, 2239 (1976).
7. J Wallbank et al, to appear in Nature Physics (2018).
8. R. Krishna Kumar, et al, Science 357, 181 (2017).
9. R. Krishna Kumar, et al, PNAS 115, 5135 (2018).

Programmable van der Waals materials

A. Mishchenko [1,*]

[1] The University of Manchester, School of Physics and Astronomy, Manchester, UK
*email: artem.mishchenko@gmail.com

Abstract:
The advent of van der Waals technology[1,2] enabled the development of many materials, which never existed before, and led to the observation of numerous exciting physical phenomena[2]. Novel materials created using van der Waals technology, made possible the discoveries of a diverse range of exciting new physics within these heterostructures, owing to unique electronic, optical and mechanical properties of 2D atomic crystals. These discoveries enabled many new functional devices, including tunnel transistors[3-5], light-emitting diodes[6] and photovoltaic sensors[7]. Recently, more elaborate mechanisms to deterministically control the properties of van der Waals materials were introduced: twist-angle[5,8-10], pressure[11], high magnetic field[3], and many other techniques[12]. In this talk, I will overview this recent progress towards electronic properties programmed on demand in the fast-growing field of van der Waals materials.

Keywords: graphene, 2D materials, van der Waals heterostructures.

References:

1. Geim, A. K. & Grigorieva, I. V. Van der Waals heterostructures. *Nature* **499**, 419-425, doi:10.1038/nature12385 (2013).
2. Novoselov, K. S., Mishchenko, A., Carvalho, A. & Castro Neto, A. H. 2D materials and van der Waals heterostructures. *Science* **353**, aac9439, doi:10.1126/science.aac9439 (2016).
3. Wallbank, J. R. *et al.* Tuning the valley and chiral quantum state of Dirac electrons in van der Waals heterostructures. *Science* **353**, 575-579, doi:10.1126/science.aaf4621 (2016).
4. Georgiou, T. *et al.* Vertical field-effect transistor based on graphene-WS2 heterostructures for flexible and transparent electronics. *Nat Nanotechnol* **8**, 100-103, doi:10.1038/nnano.2012.224 (2013).
5. Mishchenko, A. *et al.* Twist-controlled resonant tunnelling in graphene/boron nitride/graphene heterostructures. *Nat Nanotechnol* **9**, 808-813, doi:10.1038/nnano.2014.187 (2014).
6. Withers, F. *et al.* Light-emitting diodes by band-structure engineering in van der Waals heterostructures. *Nat Mater* **14**, 301-306, doi:10.1038/nmat4205 (2015).
7. Britnell, L. *et al.* Strong light-matter interactions in heterostructures of atomically thin films. *Science* **340**, 1311-1314, doi:10.1126/science.1235547 (2013).
8. Cao, Y. *et al.* Unconventional superconductivity in magic-angle graphene superlattices. *Nature* **556**, 43-50, doi:10.1038/nature26160 (2018).
9. Cao, Y. *et al.* Correlated insulator behaviour at half-filling in magic-angle graphene superlattices. *Nature* **556**, 80-84, doi:10.1038/nature26154 (2018).
10. Ribeiro-Palau, R. *et al.* Twistable electronics with dynamically rotatable heterostructures. *Science* **361**, 690-693, doi:10.1126/science.aat6981 (2018).
11. Yankowitz, M. *et al.* Dynamic band-structure tuning of graphene moire superlattices with pressure. *Nature* **557**, 404-408, doi:10.1038/s41586-018-0107-1 (2018).
12. Basov, D. N., Averitt, R. D. & Hsieh, D. Towards properties on demand in quantum materials. *Nat Mater* **16**, 1077-1088, doi:10.1038/nmat5017 (2017).

Emergence of Black Phosphorus as Anisotropic 2D Material for Electronics and Optoelectronics

Kah-Wee ANG

Department of Electrical and Computer Engineering, National University of Singapore,
4 Engineering Drive 3, Singapore 117583 , Email: eleakw@nus.edu.sg

Abstract:
The rediscovery of graphene in the recent past has propelled the rapid development of exfoliation and other thin layer processing techniques, leading to a renewed interest in black phosphorus (BP). Since 2014, BP has been extensively studied due to its superior electronic, photonic, and mechanical properties. In addition, the unique intrinsic anisotropic characteristics resulting from its puckered structure can be utilized for designing new functional devices. In retrospect, significant efforts have been directed toward the synthesis, basic understanding, and applications of BP in the fields of nanoelectronics, nanophotonics, and optoelectronics.
In this talk, the recent development of black phosphorus-based devices such as nanoribbon field-effect transistors[1], complementary logic circuits[2], photodetectors[3], and the progress made in meeting the challenges associated with contact resistance, advanced gate stack, doping and in-plane anisotropy will be presented. Moreover, the prospects of 2D materials in meeting the International Technology Roadmap for Semiconductor (ITRS) requirements for 'More-Moore' and 'More-than-Moore' will also be discussed.

Keywords: black phosphorus, field-effect transistors, complementary logic circuits, photodetectors.

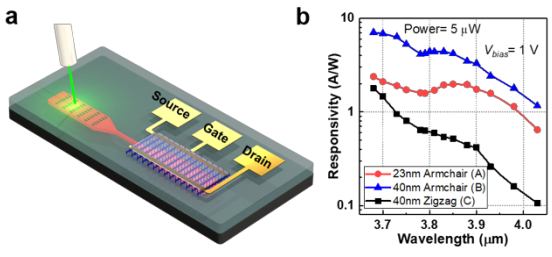

Figure 2: (a) Waveguide-integrated on-chip system with BP photodetector. (b) Spectral responsivity covering 3.69–4.03 μm.

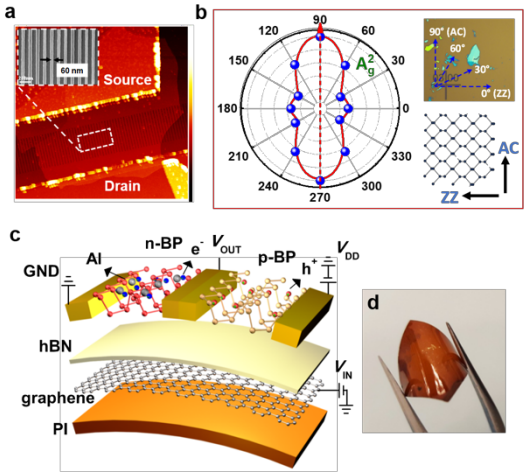

Figure 1: (a) Optical image of armchair-oriented BP nanoribbons field-effect transistor (BPNR-FET). (b) Angular dependence of Raman A^2_g intensity. (c) Schematic of flexible BP complementary inverter circuit. Graphene and h-BN were used as the back gate and gate dielectric layer, respectively. (d) Inverter circuit prototype realized on flexible polyimide substrate.

References:

1. Feng, X., Huang, X., Chen, L., Tan, W. C., Wang, L., Ang, K.-W. (2018), High mobility anisotropic black phosphorus nanoribbons field-effect transistor, *Advanced Functional Materials* 28, 1801524.
2. Liu, Y., Ang, K.-W. (2017), Monolithically integrated flexible black phosphorus complementary inverter circuits, *ACS Nano* 11, 7416-7423.
3. Huang, L., Dong, B., Guo, X., Chang, Y., Chen, N., Huang, X., Liao, W., Zhu, C., Wang, H., Lee, C., Ang, K.-W. (2019), Waveguide-integrated black phosphorus photodetector for mid-infrared applications, *ACS Nano* 13.

Acknowledgement: This research is supported by A*STAR Science and Engineering Research Council Grant (No. 152-70-00013), and by the National Research Foundation Competitive Research Program (NRF-CRP15-2015-01 and NRF-CRP15-2015-02).

Growth of Single-Crystalline Nanobelts Composed of Transition Metal Ditellurides for Future Electronic & Energy Applications

Soon-Yong Kwon[1]

[1] Ulsan National Institute of Science and Technology (UNIST), School of Materials Science and Engneering, Ulsan 44919, Korea

Abstract:
Following the celebrated discovery of graphene, considerable attention has been directed towards the rich spectrum of properties offered by van der Waals crystals. However, studies have been largely limited to their two-dimensional (2D) properties, due to lack of 1D structures. Here, I report the growth of high-yield, single-crystalline 1D nanobelts composed of transition metal ditellurides at low temperatures (T ≤500 °C) and in short reaction times (t ≤10 min) *via* the use of tellurium-rich eutectic metal alloys [1]. The synthesized semimetallic 1D products are highly pure, stoichiometric, structurally uniform, and free of defects, resulting in high electrical performances. Furthermore, complete compositional tuning of the ternary ditelluride nanobelts is achieved with suppressed phase separation, applicable to the creation of unprecedented low-D materials/devices. This approach may inspire new growth/fabrication strategies of 1D layered nanostructures, which may offer unique properties that are not available in other materials.
We also investigated single-crystalline WTe_2 nanobelts grown from a eutectic metal alloy, which can be a prominent interconnect candidate because of their superior electrical performance and robustness [2]. High-field electrical measurements and self-heating modeling demonstrate that the WTe_2 nanobelts have a breakdown current density approaching ≈100 MA·cm^{-2}, remarkably higher than those of conventional metals and other transitionmetal chalcogenides, and sustain the highest electrical power per channel length (≈16.4 W·cm^{-1}) among the interconnect candidates. The results suggest superior robustness of WTe_2 against high-bias sweep and its possible applicability in future nanoelectronics.The successful choice of new interconnect materials from the current 2D library will drive improvements to existing process technologies and will exploit the potential of the assembly of 2D atomic crystals into atomic crystal-based systems and circuits.
I will also present on-going research at UNIST, especially on the future electronic and energy applications of the 1D ditellurides.

Keywords single-crystalline nanobelts, transition metal ditellurides, eutectic metal alloy, nanoscale interconnect, electronic and energy applications.

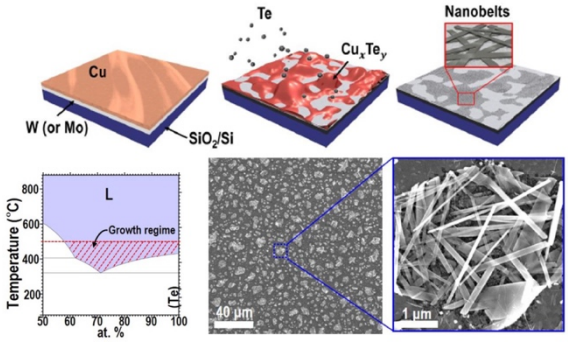

Figure 1: Figure illustrating the fundamental growth method and mechanism for the growth of the single-crystalline 1D nanobelts composed of $(W_xMo_{1-x})Te_2$ ($0 \le x \le 1$)), which can be prepared on any arbitrary substrates at low temperatures and in short reaction times via the use of Te-rich eutectic metal alloys [1].

References:

1. Kwak, J., Kwon, S.-Y.* *et al*., (2018) Single-crystalline nanobelts composed of transition metal ditellurides, *Adv. Mater.,* 30, 1707260.
2. Song, S., Kwon, S.-Y.* *et al*., (2019), Electrically robust single-crystalline WTe_2 nanobelts for nanoscale electrical interconnects, *Adv. Sci*., 6, 1801370.

Towards the integration of 200 mm graphene into microlelectronics

Lukosius[1*], M. Lisker[1], G. Dziallas[1], J. Dabrowski[1], G. Lippert[1], C. Alvarado[1], A. Mai[1,2], Ch. Wenger[1,3]

[1]IHP– Leibniz-Institut für innovative Mikroelektronik, Im Technologiepark 25, 15236 Frankfurt (Oder), Germany
[2]Technical University of Applied Science Wildau, Hochschulring 1, 15745, Wildau, Germany
[3]Brandenburg Medical School Theodor Fontane, 16816 Neuruppin, Germany
* lukosius@ihp-microelectronics.com

Abstract:
Graphene based devices are considered to have a potential to extend the functionalities of Si CMOS technology [1,2]. However, the success-ful integration of graphene into the novel mi-croelectronic devices is strongly dependent on several key challenges: 1) the availability of wafer scale high quality graphene on CMOS compatible materials (dielectrics or semicon-ductors) 2) the depositions of the reliable pas-sivation layer on top of the graphene and 3) the complete processing of the wafers with gra-phene in the standard Si CMOS pilot line.
In this paper, we present the attempts to integrate graphene into the CMOS line, where several graphene concepts have been realized (Fig. 1) in 200mm silicon technology platform. We investigated different process module develop-ments such as graphene synthesis on silicon compatible materials like germanium, a non-destructive deposition of dielectric materials on the graphene sheet as well as the combinations of these processes for various concepts of con-tacting on a full 200 mm wafers.

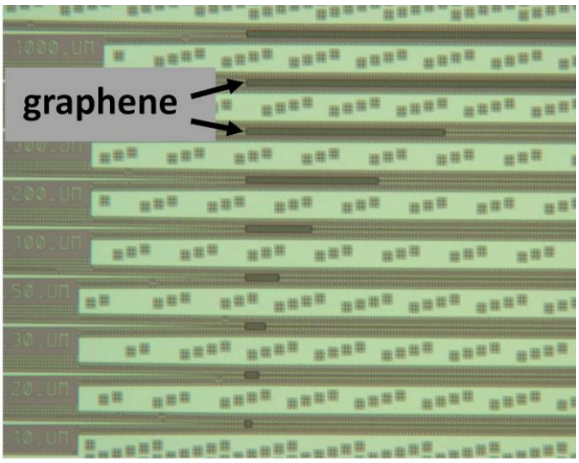

Figure 1: Modulator structures with developed Graphene stripes on Si_3N_4 waveguides.

Keywords: Graphene, Integration, 200 mm, CMOS, Photonics, Chemical Vapor Deposition.

References:

1. Novoselov K., Falko V., Colombo L., Gellert P., Schwab M., and Kim K. (2012), A Roadmap for graphene, *Nature* 490, 192.
2. Kim K., Choi J.-Y., Kim T., Cho S.-H., and H.-J. Chung H.-J. (2011), A role for graphene in sili-con-based semiconductor devices, *Nature* 479

Keywords: Graphene, Integration, 200 mm, CMOS, Photonics, Chemical Vapor Deposition.

Finding Chiral Valleys in 2D Semiconductors

K. E. Johnson GOH[1,2,*]

[1] Institute of Materials Research & Engineering, Agency for Science, Technology and Research (A*STAR) 2 Fusionopolis Way, #08-03, Innovis, Singapore 138634
[2] Department of Physics, National University of Singapore, 2 Science Drive 3, Singapore 117551

Abstract:
The valley pseudospin is a promising information carrier with potential device realizations in spintronics and quantum information processing [1]. Conveniently, a class of 2D semiconductors known as transition metal dichalcogenides (TMDCs) possesses intrinsic valley pseudospins (Figure 1) in their monolayer form due to inversion asymmetry. Towards a scalable processing of 2D TMDCs, various growth methods have been explored (e.g. chemical synthesis, chemical/physical vapor deposition, molecular beam epitaxy, etc.). Often, these processes might include growth promoters, and post growth transfer/processing which could contaminate the 2D semiconductors or alter their intrinsic valley properties. It is therefore important to ascertain the presence of the valley pseudospins in such materials post growth/processing. In this talk, I will share the recent developments in our group towards a comprehensive tool suite for performing such assessments that can be hosted in typical laboratories in adjacent to the growth or processing facility [2, 3]. The advantages and limitations of such lab-scale facilities will be discussed in the context of our recent studies of 2D TMDCs produced by scalable processes.

Keywords: 2D semiconductors, valley pseudospin, transitional metal dichalcogenides, characterization.

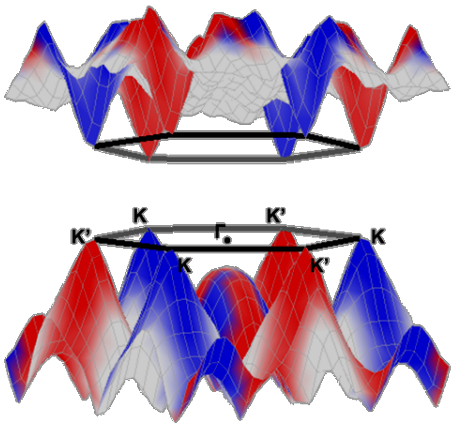

Figure 1: Band edges for a prototypical TMDC monolayer in the hexagonal Brillouin zone showing K or K′ points at the vertices, and the Γ point at the centre. Blue and red shadings represent the degree of up and down spin polarizations respectively, imparting opposite spin characters to the K and K′ valley – valley pseudospin.

References:

1. Schaibley, J. R., Yu, H., Clark, G., Rivera, P., Ross, J. S., Seyler, K. L., Yao, W., and Xu, X. (2016), Valleytronics in 2D materials, *Nature Reviews Materials*, 1, 16055.
2. Bussolotti, F., Zhang, Z., Kawai, H., and Goh, K. E. J. (2017), A Lab-scale Spin and Angular Resolved Photoemission Spectroscopy Capability for 2D Valleytronics, *MRS Advances*, 2, 1527-1532.
3. Fabio Bussolotti, Hiroyo Kawai, Zi En Ooi, Vijila Chellappan, Dickson Thian, Ai Lin Christina Pang and Kuan Eng Johnson Goh (2018), Roadmap on finding chiral valleys: screening 2D materials for valleytronics, *Nano Futures*, 2, 032001.

Charge density wave and superconducting order in TiSe2 driven by excitonic condensation and its fluctuations

Vitor M. Pereira[1,2]

[1] Department of Physics, National University of Singapore, Singapore 117542.

[2] Centre for Advanced 2D Materials and Graphene Research Centre.
National University of Singapore, Singapore 117546

Abstract:
The interplay of charge-density wave (CDW) order and superconductivity (SC) is of perennial interest in condensed matter physics since the underlying physics might unlock the promise of high-temperature SC. Experimental research on these correlated phases has been explosively revived recently in different realizations of two-dimensional crystals, which have highly tunable carrier density by field effect. Their nature in the semimetal TiSe2 presents a notable case since it had been conjectured, from as early as 1976, as a candidate excitonic insulator. Despite long-standing theoretical proposals for their existence, unequivocal identification of an excitonic insulator material has remained elusive. Recent experiments have changed that, and reinforce the view that the CDW phase in TiSe2 is a direct manifestation of its intrinsic excitonic character.

I will present an encompassing theoretical framework that describes how the excitonic instability and excitonic fluctuations likely underpin the entirety of the experimental phase diagram in this compound. First, I will show how the excitonic mechanism captures the experimental suppression of the CDW phase upon doping with very good quantitative agreement. In particular, fixing the only parameter in the theory to the undoped state, the predicted reduction of critical temperature with doping follows the experimental curve without further adjustment [1,2]. Subsequently, a model of coupled CDW and SC order parameters will be shown to naturally harbour a dome-shaped SC phase at finite doping that tallies with experiments. A novel and unusual SC phase is predicted, characterized by spatial non-uniformity and multiple dimensional crossovers that have well defined experimental implications [3]. Finally, excitonic fluctuations are shown to mediate SC pairing among electronic quasiparticles with the appropriate energy scales to explain the SC transition temperatures, which further reinforces the view that SC is boosted by loss of CDW commensurability, as seen experimentally [4]. By tackling different microscopic aspects of both the CDW and SC phases, in particular their interplay, this work is able to, for the first time, reproduce the experimental phase diagram with extremely good quantitative agreement. It thus represents an important theoretical counterpart of recent experiments in establishing TiSe2 as an example of a correlated excitonic material.

Keywords: excitonic instabilities, superconductivity, charge density waves, transition-metal dichalcogenides, fluctuation-induced pairing, interaction-driven instabilities, correlated phases in two dimensions.

References:

1. B. Singh, C. H. Hsu, W. F. Tsai, V. M. Pereira, H. Lin (2017), Stable charge density wave phase in a 1T-TiSe2 monolayer. *Phys. Rev. B* 95, 245136.
2. C. Chen, B. Singh, H. Lin, V. M. Pereira (2018), Reproduction of the Charge Density Wave Phase Diagram in 1T-TiSe2 Exposes its Excitonic Character. *Phys. Rev. Lett.* 121, 226602.
3. C. Chen, L. Su, A. H. Castro Neto, V. M. Pereira (2018), Discommensuration-enhanced superconductivity in the charge density wave phases of transition-metal dichalcogenides. *arXiv*:1806.08064.
4. C. Chen, V. M. Pereira (2019), Pairing induced by fluctuations of an excitonic insulator: the case of superconductivity in TiSe2 (*in preparation*).

Graphene Fibers for Energy Applications

S. Padmajan Sasikala,* S.O. Kim,

Korea Advanced Institute of Science and Technology (KAIST), Daejeon, South Korea

Abstract:
Graphene fiber (GF) is a well-aligned assembly of graphene sheets. Research on GF based micro-supercapacitors have tremendously advanced in recent years by incorporating functional materials such as CNT, activated carbon, pseudo capacitive inorganic moieties, and conducting polymers which were demonstrated to improve the capacitive energy storage performance. Yet, there is room for improvement as desirable performance for real world electronic application is still very high. We report graphene@polymer core−shell fibers (G@PFs) composed of N and Cu codoped porous graphene fiber cores uniformly coated with semiconducting polymer shell layers with superb electrochemical characteristics. Aqueous/organic interface-confined polymerization method produced robust highly crystalline uniform semiconducting polymer shells with high electrical conductivity and redox activity. When the resultant core−shell fibers are utilized for fiber supercapacitor application, high areal/volume capacitance and energy densities are attained along with long-term cycle stability. Desirable combination of mechanical flexibility, electrochemical properties, and facile process scalability makes our G@PFs particularly promising for portable and wearable electronics.

Keywords: graphene, liquid crystal, fiber, wet spinning, doping, semiconducting polymers, interfacial polymerization, supercapacitor, elelctrocatalysis, high energy density, wearble application

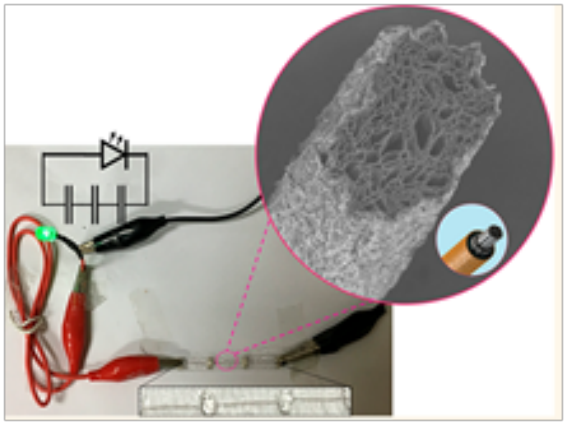

Figure 1. Photograph showing a serially connected three graphene based fiber supercapacitors that lights up a green LED. Inset shows SEM image displaying the cross section of sigle fiber and a schematic of graphene plymer coreshell fiber.

References

1. Xu, Z.; Gao, C. (2015) Graphene fiber: a new trend in carbon fibers. *Mater. Today* 18, 480−492.
2. Sasikala, S. P., Lee, K. E., Lim, J., Lee, H. J., Koo, S. H., Kim, I. H., Jung, H.J., Kim, S. O. (2017), Interface-confined high crystalline growth of semiconducting polymers at graphene fibers for high-performance wearable supercapacitors, *ACS Nano*., 11, 9424-9434.

2D Metal Chalcogenide Nanopatterning by Block Copolymer Lithography

Taeyeong Yun,[1] Gang San Lee,[1] Jin Goo Kim,[1] Sang Ouk Kim,[1*]

[1] Korea Advanced Institute of Science and Technology, Department of Materials Science and Engineering, Daejeon, Korea

Abstract:
Nanoscale structure engineering is in high demand for various applications of 2D transition metal dichalcogenides (TMDs). We demonstrate edge-exposed 2D polycrystalline MoS_2 nanomesh thin film *via* block copolymer (BCP) nanopatterning. Molybdenum nanomesh structure is formed by direct metal deposition of hexagonal cylinder BCP nanotemplate and the following lift-off process. Subsequent sulfurization of the molybdenum nanomesh creates MoS_2 nanomesh thin films without any degradative etching step. Our approach is not only applicable to other metal sulfides and oxides but also to other nanoscale structures of TMD thin films including nanodot and nanowire array by means of various BCP nanotemplate shapes. As the edge site of MoS_2 is highly active for NO_2 sensing, our edge-exposed MoS_2 nanomesh demonstrates 7-fold enhancement of sensitivity for NO_2 molecules compared to uniform thin film as well as superior reversibility even under 80 % relative humidity environment. This structure engineering method could greatly strengthen the potential application of 2D TMD materials with the optimal customized nanoscale structures.

Keywords: block copolymer, nanopattern, self-assembly, sensor, transition metal dichalcogenide

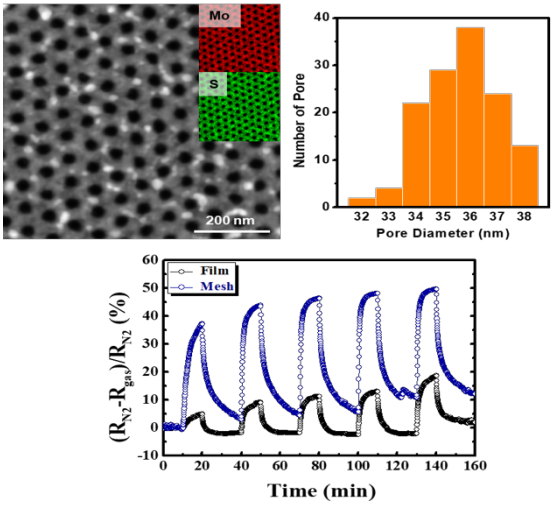

Figure 1: TEM images of TMD nanomesh, the distribution of nanopores, and NO_2 gas sensing performance of MoS_2 film and nanomesh

Graphene Korea 2019
Session III: Application of Graphene in Energy / Health and biomedical

Flexible graphene-based gas sensors of low power consumption

Ho Won Jang[1,*]

[1] Seoul National University, Department of Materials Science and Engineering, Seoul, Korea

Abstract:
The Internet of Everything (IoE) refers to billions of objects having intelligent connections with processed data. Sensors hold the key to the IoE as they detect and assess the internal and external states of objects. In particular, gas sensors contribute greatly to make people's lives better via transmitting information about gas species in ambient air. Graphene is being extensively studied for gas-sensing applications due to its high sensitivity at room temperature, transparency, flexibility, and low electrical noise level. However, graphene also has drawbacks such as low selectivity and irreversible sensing behaviors. To overcome these drawbacks, the chemoresistive sensing properties of graphene have been modified by diverse approaches such as introducing extrinsic defects, functionalization, and noble metal decoration. Here, we present unprecedented room temperature hydrogen detection by Au nanoclusters supported on self-activated graphene. Compared to pristine graphene sensors, the Au-decorated graphene sensors exhibit highly improved gas-sensing properties upon exposure to various gases. In particular, an unexpected substantial enhancement in H_2 detection is found, which has never been reported for Au decoration on any type of chemoresistive material. Density functional theory calculations reveal that Au nanoclusters on graphene contribute to the adsorption of H atoms, whereas the surfaces of Au and graphene do not bind with H atoms individually. The discovery of such a new functionality in the existing material platform holds the key to diverse research areas based on metal nanocluster/graphene heterostructures.

Keywords: graphene, gas sensor, surface decration, noble metal, self-heating, microchannel, low power consumption, IoE, transparent, flexible.

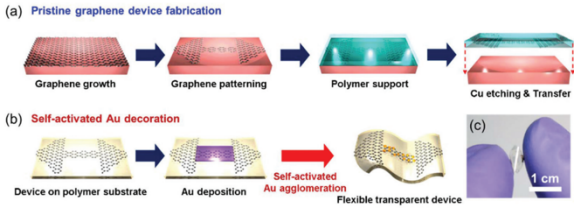

Figure 1: Fabrication procedure of (a) pristine and (b) Au-decorated sensors. After self-activation, the Au thin film becomes NCs due to the heat induced by the self-activation. (c) Photographic image of the final device.

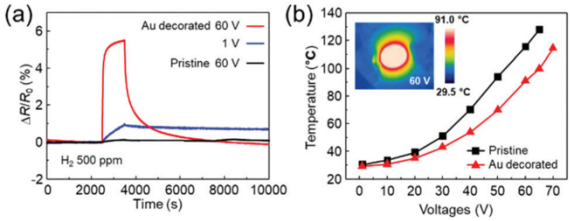

Figure 2: (a) Dynamic sensing transient of Au-decorated and pristine sensors under different bias voltages. (b) Thermographic images and thermal characteristics of Au-decorated and pristine sensors.

References:

1. Y. H. Kim et al., Self-Activated Transparent All-Graphene Gas Sensor with Endurance to Humidity and Mechanical Bending, *ACS Nano*, 2015, 9, 10453–10460.
2. Y. H. Kim et al., Au decoration of a graphene microchannel for self-activated chemoresistive flexible gas sensors with substantially enhanced response to hydrogen, *Nanoscale*, 2019,11, 2966-2973.

Photoluminescence properties of monolayer monolayer transition metal dichalcogenides in an aqueous solution

Wenjin Zhang, Kazunari Matsuda, and Yuhei Miyauchi*

Institute of Advanced Energy, Kyoto University, Uji, Kyoto 611-0011, Japan

Abstract:
Monolayer (1L) transition-metal dichalcogenides (TMDCs) MX_2, where M and X are a transition metal (typically Mo, W) and a chalcogen (typically S, Se, or Te), respectively, have recently attracted a great deal of attentions as a new class of two-dimensional (2D) direct gap semiconductors for promising future electronics and optoelectronics applications[1]. Their physical and chemical properties are expected to be strongly affected by various surface interactions because of their large specific surface area. In particular, variety of phenomena occurring at the interfaces of water and atomically thin TMDCs may be critical for their practical applications[2-4]. However, knowledge on the optical properties of these materials in water has still been limited and it is important to clarify the impacts of the surface electrochemical reactions in solutions on their optical properties.
Here we report photoluminescence (PL) properties of mechanically exfoliated monolayer (1L) MoS_2 in aqueous solutions with various pH which provide a unique platform for examining the impacts of physical chemistry phenomena at the liquid/TMDC interface on their physical properties. The sample was prepared using mechanically exfoliated methods and the optical properties were measured using a home-made optical setup.
Figure 1 shows the PL spectra after immersing 1L-MoS_2 into distilled water. After the immersion into distilled water, considerable modifications in the PL intensity and spectral line shape were observed compared to those in ambient air condition for 1L-MoS_2. The results are mainly attributed to the electrochemical reactions at the interface between the 1L-MoS_2 and the aqueous solution that cause electron extraction from or injection into the 1L-MoS_2 depending on the redox potentials in the O_2/H_2O redox system that strongly depend on the pH of the aqueous solution[4].
The stability of 1L-MoS_2 under light irradiation conditions was also studied using PL spectroscopy in air and water conditons. 1L-MoS_2 was irradiated using visible light (580 nm) under a power density of 800 Wcm^{-2} which is in linear region of the PL. The results suggest that 1L-MoS_2 has excellent stability and high potential for application in realistic enviroments with finite moisture or solutions under light irradiation conditions.

Keywords: transition metal dichalcogenides, photoluminescence, electrochemical

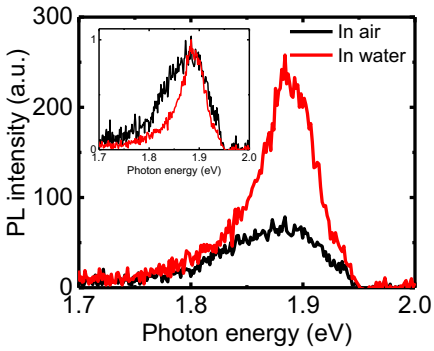

Figure 1: PL spectra of 1L-MoS_2 in air and water conditions. Inset shows normalized PL spectra in air and water.

References:

1. Q. H. Wang, et al., Nat. Nanotechnol. 7, 699 (2012).
2. Y. Miyauchi, et al. Nature Comm. 9, 2598 (2018)
3. S. Mouri, Y. Miyauchi, and K. Matsuda, Nano Lett. 3, 5944 (2013).
4. W. Zhang, K. Matsuda, and Y. Miyauchi, J. Phys. Chem. C 122, (2018)

Competing energy scale in Bilayer Graphene Quantum Point Contacts

Y. Lee,[1*] A. Knothe,[2] H. Overweg,[1] P. Rickhaus,[1] M. Eich,[1] A. Kurzmman,[1] K. Watanabe,[3] T. Taniguchi,[3] V. I. Fal'ko,[2] T. Ihn,[1] and K. Ensslin,[1]

[1]Department of Physics, ETH Zurich, Otto-Stern-Weg 1, 8093 Zurich, Switzerland
[2]National Graphene Institute, University of Manchester, Manchester, M13 9PL, UK
[3]National Institute for Material science, 1-1 Namiki, Tsukuba 305-0044, Japan

Abstract:
We present transport measurements of quantized conductance in electrostatically induced quantum point contacts in bilayer graphene at low-temperature $T = 1.8K$. A dual (Split Top/Back, schematic see Fig. 1a) gated structure in bilayer graphene can be used to form the electrostatic barrier and define one-dimensional channels.[1] In previous experiments[2,3] at zero magnetic field quantized conductances with a step size of $\Delta G = 4e^2/h$ for high mode number have been observed accounting for a fourfold (spin and valley) degeneracies. Here we focus on experiments where the displacement field can be tuned, and with it the bandstrcuture displaying a Mexican hat-like feature. For small displacement fields we observe in the small mode number regime a quantized state at $2e^2/h$ state. For increasing displacement field the first conductance plateaus can occur at $2e^2/h$ or even $8e^2/h$. For increasing magnetic fields, conductance plateaus related to four-fold degeneracies reemerge. The degeneracies are fully lifted again for high magnetic fields in the quantum Hall regime. Depending on the displacement field and confinement potential of the constriction, the Landau levels of the broken symmetry states reveal features related to the nature of spin, valley and orbital states.

Keywords: Bilayer graphene, Quantum point contacts, Berry curvature

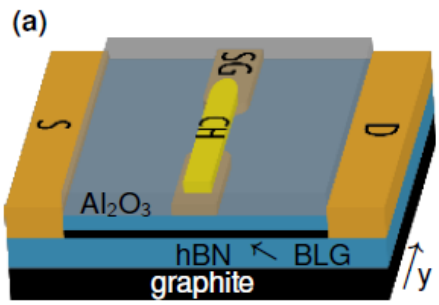

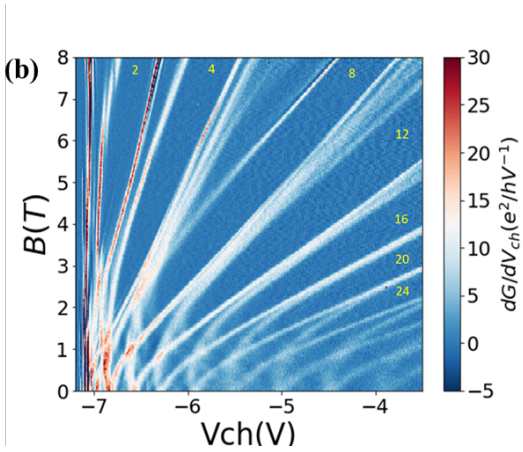

Figure 1: (a) Schematic of the device of bilayer graphene encapsulated in hBN on top of a graphite back gate. Split gates were evaporated on top of the device. A layer of Al_2O_3 serves to separate the split gates from the channel gate. (b) Differential conductance as a function of $B(T)$ and V_{ch}(V) at V_{bg}= 4.5V and V_{sg}= -2.87V. Numbers in yellow point out the conductance values in the units of e^2/h in the quantum Hall regime.

References:

1. H. Overweg et al., Nano Lett 18, 553-559 (2018)
2. H. Overweg *et al.,* PRL 121 257702 (2018)
3. R. Kraft et al., PRL 121, 257703 (2018)

Tuning the performance of graphene-field-effect-transistors using Self-Assembled Monolayers

Sami Ramadan, Yuanzhou Zhang, Deana Kwong Hong Tsang, Olena Shaforost, Clare Watts, Iain E. Dunlop, Peter K. Petrov, Norbert Klein

Department of Materials, Imperial College London, London, SW7 2AZ, UK

Abstract:
High-performance graphene-field-effect devices are crucial to implement graphene based devices in real and reliable applications. However, the performance of graphene-field-effect-transisotrs (GFETs) are generally degraded by defects and impurities induced during the device processing. Polymer residue on surface of graphene left from photoresist processing can increase electron scattering and limit electron transport [1]. Furthermore, exposing graphene to plasma-related processing such as during metallization can increase defect density in graphene and modify the electronic properties of the devices [2]. This can result in decrease in device mobility, increase in contact resistance, unintentional device doping and shift in Diract point.
Here we show that passivating graphene surface using self-assembled monolayers (SAMs) prior to photolithography and metallization processes can significantly enhance device properties.
By investigating graphene and GFETs using surface characterization methods including Raman spectroscopy, Atomic Force Microscopy (AFM) and X-ray photoelectron spectroscopy (XPS) and electrical measurements including Current-Voltage I-V and circular transmission line measurements (CTLM), we found large reduction in defect density of graphene after sputtering, improved homogeneity and intensity of graphene 2D/G peak surface after lithography, ten-times improvement in specific contact resistivity, and obtaining transfer characteristics of GFETs near to the intrinsic properties of graphene. This approach is simple and offers a practical route for the fabrication of high-quality GFET devices without the need of additional processing steps.

Keywords: CVD graphene, Graphene-field-effect-transistors GFETs, self-assembled monolayers (SAMs), Hexamethyldisilazane (HMDS), contact resistance, sputter, and lithography

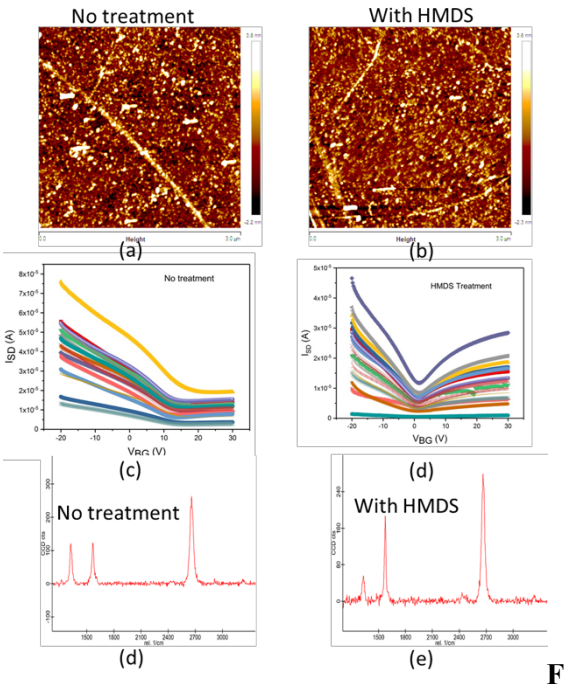

Figure 1: (a) AFM image of the graphene surface after lithography Rq=1.15 nm; (b) AFM image of the graphene surface with HMDS after lithography Rq=1.01 nm; (c) Transfer characteristics of GFETs with no surface treatment; (d) Transfer characteristics of GFETs with HMDS treatment; (e) Raman profile of graphene after 5 nm sputtering with Ti with no surface treatment; (f) Raman profile of graphene after 5 nm sputtering with Ti with HMDS surface treatment of graphene before metallization

References:

1. Masa Ishigami, J. H. Chen, W. G. Cullen, M. S. Fuhrer, and E. D. Williams, Nano Letters **7** (6), 1643 (2007).
2. Xiaohui Tang, Nicolas Reckinger, Olivier Poncelet, Pierre Louette, Ferran Ureña, Hosni Idrissi, Stuart Turner, Damien Cabosart, Jean-François Colomer, Jean-Pierre Raskin, Benoit Hackens, and Laurent A. Francis, Scientific Reports **5**, 13523 (2015).

Development and fabrication of graphene oxide membranes for water desalination

Z. Balgin [1], Z. Yelemessova [1], Z. Yermogambetov [1], K. Tynyshtykbayev[1], Z. Insepov[1,2,3*]

[1] Nazarbayev University, Astana, Republic of Kazakhstan
[2] National Nuclear Research University (MEPhI), Moscow, Russian Federation
[3] Purdue University, West-Lafayette, IN USA

Corresponding author: zinsepov@purdue.edu

Abstract:
This report presents the results of using graphene oxide GO as inclusions in standard polymer GO/PVDF and proton-exchange GO/Nafion membranes for water desalination. Composite GO/PVDF and GO/Nafion membranes with graphene oxide inclusions were created on the basis of standard polymer membranes by deposition of graphene oxide onto polymeric (PVDF, polyvinylidene difluoride, 45 micron pores), cellulose acetate (45 micron pores, Whatman), aluminum oxide AAO (Sigma Aldrich), proton-exchange membrane (pores 1 nm, Nafion) by vacuum filtration and drying. Graphene oxide prepared using the modified Hammers method showed high dispersion stability of aqueous suspensions due to electrostatic stabilization of charges resulting from the protonation of functional groups present on the fixed cavities and ionization of hydroxyl groups. The observed high dispersibility in water is due to the presence of hydroxyl groups attached to sheets of reduced graphene r-GO oxide and accessible to include non-polar molecules. The presence of functional groups on the surface of r-GO sheets makes it possible to modify the surface and additionally increase its hydrophobicity using water-repellent substances in one material dispersed in water, which is confirmed by IR spectroscopy data.

Keywords: graphene oxide, polymer GO/PVDF, proton-exchange GO/Nafion membranes. water desalination.

Prospective Study of Graphene Combined Semiconductor and its Potential Application

Won-Chun Oh
Department of Advanced Materials Science & Engineering, Hanseo University, Seosan-si, Chungnam, Korea, 356-706
College of Materials Science and Engineering, Anhui University of Science & Technology, Huainan 232001, PR China, E-mail: wc_oh@hanseo.ac.kr

Abstract:
Graphene semiconductor or metal nanoparticle composites have the potential to function as efficient, multifunctional materials for Solar Energy Conversion, Gas and Bio Sensing, CO_2 Reduction and Photo catalytic degradation. The fundamental principle of a graphene-based solar energy conversion is that graphene can change one absorbed photon of a few electrons, which increase in efficiency of solar panels. The adsorption energies and direction of charge transfer (from gas molecules to graphene or vice versa) are calculated based on the optimal adsorption configuration. The total density of states (DOS) of graphene-gas molecule adsorption system provides further insights into the effect of gas molecule adsorption on the electronic structure of graphene.During the bio recognition event, the electric charge produced changes in the conductivity of the channel between source and drain. Graphene allows for band gap tuning through surface modification and can detect gate voltage change formed from small amounts of single stranded DNA. It was found that graphene nanosheet can significantly enhance the electron–hole separation rate and specific surface area of the photocatalyst the photoinduced electrons on photocatalyst can be transferred to the graphene immediately for reduction process; thereby resulting in a high spatial separation of the photoinduced electron–hole pairs and graphene nanosheet can be also enhanced, which favors multi-electron reactions for photocatalytic CO_2 reduction.
The degradation of organic pollutants takes place mostly at the semiconductor surface. The nanostructured electrodes provide more adsorption sites for organic pollutants owing to their larger surface area. 2-D structured graphene oxide offer more effective channels for electron transport due to the reduced junctions and grain boundaries. Such fast electron transport decreases the rate of recombination and enhances PC degradation performance.

Keywords: CO_2 Reduction, Quaternary Nanocomposites, Gas and Bio Sensing.

References:

1. Dowla, B.M.R.U., Cho, J.Y., Jang, W.K. and Oh, W.C., 2017. Synthesis of BiVO4-GO-PTFE nanocomposite photocatalysts for high efficient visible-light-induced photocatalytic performance for dyes. Journal of Materials Science: Materials in Electronics, 28(20), pp.15106-15117.
2. Areerob, Y., Cho, K.Y., Jung, C.H. and Oh, W.C., 2019. Synergetic effect of La2CdSnTiO4-WSe2 perovskite structured nanoparticles on graphene oxide for high efficiency of dye sensitized solar cells. Journal of Alloys and Compounds, 775, pp.690-697.

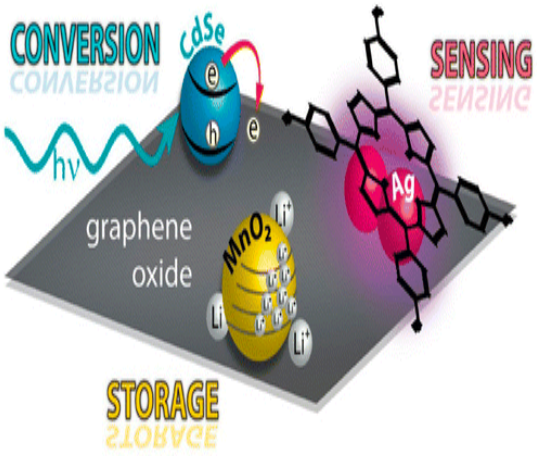

Fig. 1: Application fields of graphene nanocomposites.

Characterization of Hybrid MnO_2/RGO/PANI Supercapacitor with Green Reducing Agent

S.I. Khairul,[1*] M. N. M. Ansari,[1] S.Z. Omar,[1] P.J.Ker,[1] M.N.Saifuddin,[2] A.Q. Al-Amin,[3] H.Hasmaizan[3]

[1] Universiti Tenaga Nasional, Institute of Power Engineering, Kajang, Malaysia
[2]Universiti Tenaga Nasional, Institute of Sustainable Engineering, Kajang, Malaysia
[3]Universiti Tenaga Nasional, Institute of Energy Policy and Research, Kajang, Malaysia

Abstract:
With the ever growing demand and need for environmental friendly and high performance of energy storage device, supercapacitors have attracted many interest mainly for their short charging time and longer lifecycle [1] compared to batteries. They had been seen as a traverse between capacitors and electrochemical batteries; with their high power density property which stores power electrostatically. Increasing number of studies recently had shown that graphene is the desired material candidate for this application for its high surface area, good electronic conductivity and high electrochemical stability. In this study, we develop a graphene-based electrode for electrical double layer capacitor (EDLC) in which the graphene is reduced from its oxide using green reduction agents such as beta-carotene, ascorbic acid and red palm oil as opposed to the hazardous hydrazine. To improve the capacitance of the electrode, we synthesize the graphene with MnO_2 using self-assembly method. We then integrate this hybrid material at different percentages of Polyaniline (PANI) and Polypyrrole (PPy) in which graphene will function as a conductive channel for charge transfer which contributes to the overall increase in conductivity, while pseudocapacitance arises from the metal oxides and conductive polymer using in-situ anodic electro polymerization of aniline monomer with metal oxide functionalized graphene sheet. Mechanical testing is conducted to the composites to see the increase in Young modulus, tensile strength and hardness with scanning electron microscopy (SEM) and X-Ray Diffraction (XRD) analysis are conducted to observe how graphene impeded the propagation cracks in the composite. Electrical properties characterization of the composite electrode was conducted to evaluate the specific capacitance and characterization of the composite in polymer electrolyte at the scan rate of 10mV/s and capacitance loss after 500,1000 and 2000 cycles.

Keywords: graphene, green reduction agent, polyaniline, polypyrrole, manganese oxide, EDLC, pseudocapacitance, specific capacitance.

References:

1. J. Libich, J. Máca, J. Vondrák, O. Čech, and M. Sedlaříková, "Supercapacitors: Properties and applications," J. Energy Storage, vol. 17, no. March, pp. 224–227, 2018.
2. D. G. Papageorgiou, I. A. Kinloch, and R. J. Young, "Mechanical properties of graphene and graphene-based nanocomposites," Prog. Mater. Sci., vol. 90, pp. 75–127, 2017.
3. Mazen Yassine and Drazen Fabris, "Performance of Commercially Available Supercapacitors," Energies, vol. 10, no. 9, p. 1340, Sep. 2017.
4. S. Kannappan et al., "Thiolated-graphene-based supercapacitors with high energy density and stable cycling performance," Carbon, vol. 134, pp. 326–333, 2018.
5. N. Ma et al., "High-performance hybrid supercapacitor of mixed-valence manganese oxide/N-doped graphene aerogel nanoflower using an ionic liquid with a redox additive as the electrolyte: In situ electrochemical X-ray absorption spectroscopy," Electrochimica Acta, vol. 271, pp. 110–119, May 2018.
6. D. G. Papageorgiou, I. A. Kinloch, and R. J. Young, "Mechanical properties of graphene and graphene-based nanocomposites," Progress in Materials Science, vol. 90, pp. 75–127, 2017.
7. Q. Cheng, J. Tang, J. Ma, H. Zhang, N. Shinya, and L.-C. Qin, "Graphene and nanostructured MnO2 composite electrodes for supercapacitors," Carbon, vol. 49, no. 9, pp. 2917–2925, Aug. 2011.
8. Wu et al., "Flexible solid-state symmetric supercapacitors based on MnO2 nanofilms with high rate capability and long cyclability," AIP Advances, vol. 3, no. 8, pp. 2–7, 2013.
9. M. Kim, Y. Hwang, and J. Kim, "Graphene/MnO2-based composites reduced via different chemical agents for supercapacitors," Journal of Power Sources, vol. 239, pp. 225–233, Oct. 2013.

Dielectric properties of semiconductor armchair graphene nano-ribbon arrays

C. Vacacela Gomez,[1,2,*] A. Sindona,[2,] M. Pisarra,[1,2] T. Tene[1,] M. Guevara[4]

[1] Escuela Superior Politécnia de Chimborazo, Physics Research Group, Panamera Sur Km 1 1/2, Riobamba, Ecuador
[2] Università della Calabria, Dip. di Fisica, Via P. Bucci, Cubo 30C, I-87036 Rende (CS), Italy
[3]Universidad Autónoma de Madrid, Departamento de Quimica, C/ Fco. Tomás y Valiente 7, E-28049 Madrid, Spain
[4]Escuela Superior Politécnica de Chimborazo, Facultad de Ingeniería Mecánica, Panamera Sur Km 1 1/2, Riobamba, Ecuador

Abstract:
With the rise of low-dimensional materials, several theoretical and experimental studies have been oriented to launch, control, manipulate and detect single- and collective-particle transitions in graphene related structures, which are expected to be embedded in next-generation nanodevices that may operate from infrared to terahertz frequencies [1]. As a noteworthy example, we present a comprehensive characterization of dielectric properties in semiconductor armchair graphene nanoribbons organized in periodic planar arrays, by time-dependent density functional theory in the random phase approximation [2]. Both undoped (intrinsic) and doped (extrinsic) conditions are explored by a probe particle of energy below 20 eV. The results are analyzed, with particular reference to their induced charge-density fluctuation , i.e., plasmons resonance and corresponding dispersions.
Semiconductor armchair graphene nanoribbons arrays display two distinct intraband and interband plasmons, whose fascinating interplay is extremely responsive to either inhejectior of ejection of charge carriers or increase in electronic temperature. These oscillation share common trend with recent nanoinfrared imagin of confined edge and surface plasmons modes detected in graphene nanoribbons of 100-500 nm width [3]. Our predictions are expected to be of immediate help for measurements of plasmonic features in nanoscale architectures of nanoribbon devices.

Keywords: Dielectric properties, plasmons, raphene nanoribbons, TDDFT

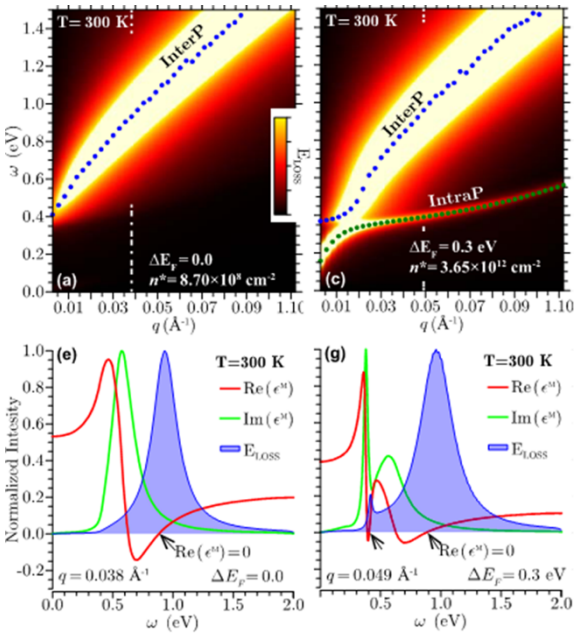

Figure 1: Dielectric response and plasmon dispersion of 5AGNR at T=300 K. The blue and green dots mark the interband and intraband plasmon dispersions, respectively.

References:

1. Egorov, D., Dennis, B. S., Blumberg, G., & Haftel, M. I. (2004). Two-dimensional control of surface plasmons and directional beaming from arrays of subwavelength apertures. Physical Review B, 70(3), 033404.
2. Vacacela Gomez, C., Pisarra, M., Gravina, M., Pitarke, J. M., & Sindona, A. (2016). Plasmon modes of graphene nanoribbons with periodic planar arrangements. Physical review letters, 117(11), 116801.
3. Fei, Z., Goldflam, M. D., Wu, J. S., Dai, S., Wagner, M., McLeod, A. S., ... & Fogler, M. M. (2015). Edge and surface plasmons in graphene nanoribbons. *Nano letters*, *15*(12), 8271-8276.

Chemically Functionalised Graphene Biosensor for the Label-free Sensing of Exosomes

D. Kwong Hong Tsang,[1,*] T. J. Lieberthal,[2] C. Watts,[1] I. E. Dunlop,[1] S. Ramadan,[1] N. Klein[1]

[1] Imperial College London, Department of Materials, London, UK
[2] Imperial College London, Department of Bioengineering, London, UK

Abstract:
Exosomes are a subpopulation of vesicles that are expelled from all cells and are speculated to have some role in the development of cancerous tissue through cell-cell communication[1]. By using graphene biosensors for the sensitive and specific detection of disease biomarkers, effective point-of-care medical devices can be fabricated that could provide information for early cancer diagnosis. A graphene field-effect transistor (gFET) biosensor, which was non-covalently functionalised with an intermediate linker and specific antibodies for the detection of exosomes as biomarkers (figure 1). The intermediate linker is a pyrene-based molecule, which π-stacks to the graphene surface without disruption, or introduction of high defect density. Conjugation with anti-CD63 antibodies allows the sensor to specifically target the CD63 transmembrane proteins present in the bilayer membrane of exosomes. The drain/source current (I_{ds}) – gate/source voltage (V_g) electrical characteristic of graphene is extremely sensitive to the presence of charged species and cause changes such as shifts in Dirac point and broadening or narrowing the curves. Using a microfluidic channel, part of a graphene film was exposed to solution. The change in electrical properties of the exposed graphene created an additional minimum alongside the original Dirac point in the I_{ds} - V_g curve. When phosphate buffered saline (PBS) was present in the channel, the additional minimum was present at a V_g lower than the original Dirac point and shifted with time when exosomes were introduced into the channel. Over time, exosomes bind to the functionalised surface and a saturation in the position of additional minimum over time indicates their presence. This saturation is attributed to an equilibrium between exosomes binding and unbinding to anti-CD63 antibodies and has been shown to be concentration dependent. The sensor has thus far been shown to be sensitive down to concentrations of 0.1 μg/mL exosomes. The design and initial optimisation of the sensor for liquid measurements has been studied as well as the principle of operation and sensing mechanism.

Keywords: exosomes, field-effect transistor, biosensor, functionalisation, biomedical applications, non-covalent modification, cancer biomarkers, label-free detection.

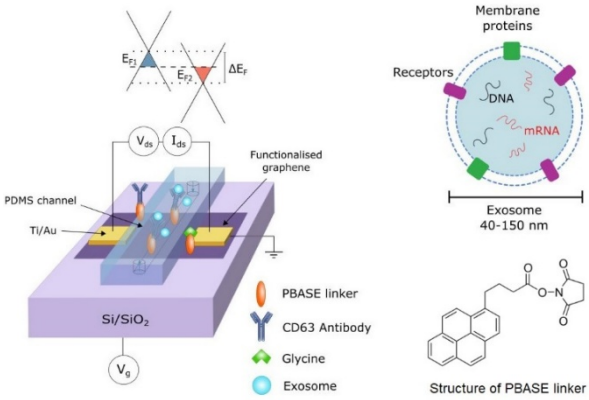

Figure 1: Schematic of the functionalised biosensor with microfluidic integration, showing the different doping levels of the covered and uncovered graphene as a result of exosome binding. Schematic of the basic structure of an exosome and molecular structure of 1-pyrenebutyric acid N-hydroxysuccinimide ester (PBASE).

References:

1. Properzi, F., Logozzi, M., & Fais, S. (2013). Exosomes: the future of biomarkers in medicine. *Biomarkers in medicine*, *7*(5), 769-778.

SurfCoat Korea 2019
Posters Session I: Surface treatments and coatings deposition processes / Characterization

In-situ thickness monitoring of dielectric layer growth using rotated silicon witness

L. Nozka,[1,*] P. Schovanek,[2] M. Pech[2], D. Mandat[2], M. Hrabovsky[1]

[1] Palacky University, Olomouc, Czech Republic
[2] Institute of Physics of Academy of Sciences of Czech Republic, Prague, Czech Republic.

Abstract:
In-situ monitoring of layer growth during a deposition process with the PVD technique is a valuable tool for a tuning of the deposition process as well as to keep production reproducibility. Usual stacionary sensors like ones based on oscillating quartz crystals are reliable assuming the shape of the evaporation lobe from the electron gun or boats is constant over the deposition process of the layer or it changes in a similar way when reproducing the deposition processes. However, this condition is not fulfilled in general notably for the deposition of materials with high melting temperature (HfO_2 for instance).
There are several solutions on market using based on transmittance or reflectance measurement of a rotating witness using an inspection-light beam[1, 2].
We decided to construct an in-situ monitor which directly calculates the geometrical thickness of a growing layer during the deposition process. The measurement is base on the measurement of the reflectivity of a rotating silicon witness. Before the measurement process starts, a background and a white spectrum are measured. These data are then used to calibrate the monitor to the calculated (theoretical) reflectivity of the silicon witness. This procedure allows for a direct thickness calculation of the deposited layer which follows the calibration. The process of the calibration and thickness measurement is easy to automatize in the appropriate software interface of the in-situ monitor.
The ligh beam is delivered by means of a proper reflectance fiber probe which is connected to a proper Xenon or Halogen source and to a fast spectrometer.

Keywords: in-situ thickness monitor, PVD deposition, spectroscopy

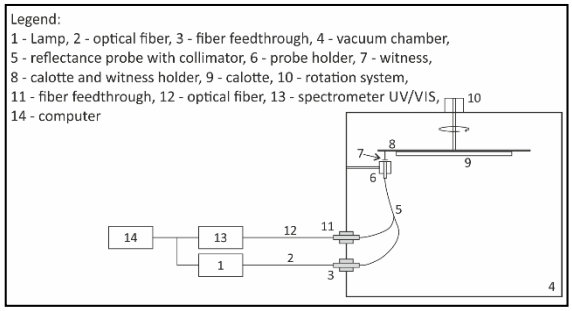

Figure 1: Scheme of the measurement setup. Witness serves both for calibration of the measurement system and for the thickness measurements.

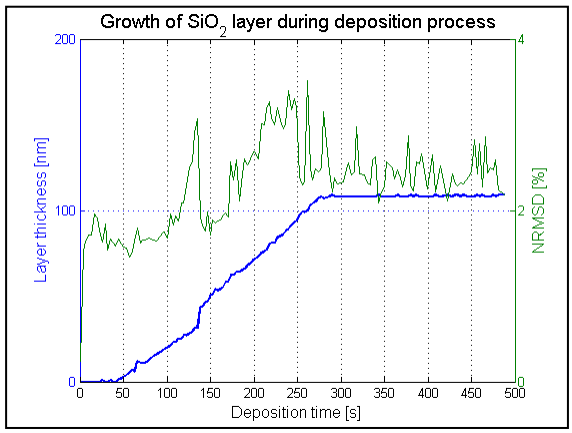

Figure 2: Example of growth of an SiO_2 layer during a deposition process (blue curve). The NRMSD (green curve) is measure of deviation of measured results with predicted ones.

References:

1. Pulker, PULKER, H.K. *Coatings on glass, 2nd edition,* Elsevier Science B.V., Amsterdam, 1999.
2. RANCOURT, J.D. *Optical thin films, User handbook*, SPIE, New York, 1996.

Characteristics of Ni/LPD-Al_2O_3/Sputtering-ZnO/Glass UV Photodetector

Che-Chun Lin[1],Jung-Jie Huang[2], Dong-Sing Wuu[1]

[1] National Chung Hsing University, Department of Materials Science and Engineering, Taichung, Taiwan

[2] Da-Yeh University, Department of Electrical Engineering, Changhua, Taiwan

Abstract:

The responsivity of photodector is one of the most important parameter and challenging problems, the surface passivation technique were very important. In this study, the passivation layer of Al_2O_3 thin films by liquid phase deposition was fabricated on ZnO film. The ZnO thin films were deposited by radio frequency magnetron sputtering. The effect of surface passivation on photoresponse and dark current for w/wo Al_2O_3 thin films of metal–semiconductor–metal photodector have been studied. The deposition solution of aluminium sulfate and sodium bicarbonate were used for Al_2O_3 thin film deposition.

Ar/O_2 ratio during sputtering ZnO film process was important, because the oxygen can control the amount of oxygen vacancy. Under optimal conditions, the Zn/O atomic ratio of ZnO film was 1:1 has lower dark current density of 2.6×10^{-10} A/cm^2, the photoresponsivity of 350 nm at 5V bias was 0.547 A/W. The photoresponsivity and dark current density of 350 nm at 5V bias was 1.1A/W and 1.7×10^{-11} A/cm^2 after the Al_2O_3 film passivated ZnO photodector.

Keywords: Al_2O_3 thin films, ZnO thin films, passivation, photodetector

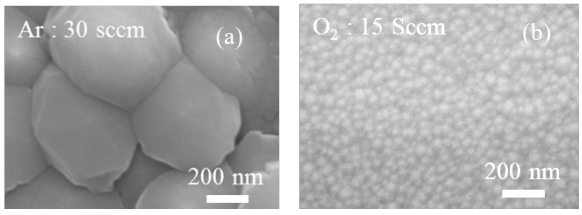

Figure 1: SEM images of ZnO film (a) Ar: 30 Sccm and (b) Ar/O_2: 30/15 Sccm.

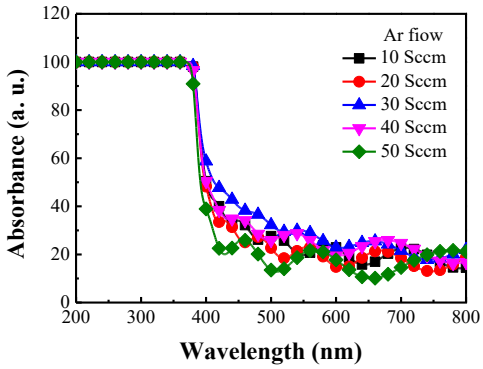

Figure 2: Absorption spectra of ZnO film as a function of Ar flow 10 to 50 Sccm.

Synthesis of N-heterocyclic complexes of Cr,Fe,Mn,Co and Ti convesion to nanoparticles and application for cyclohexane oxidation

Z. Alrufaydi,[1*] SM. Ahmad,[1] AT. Mubarak

[1] King Khalid University, Department of Chemistry, Abha, KSA

Abstract:
Cyclohexane oxidation is a challenging task for chemists both academically and industrially. The availability of raw material and the industries involved in this work needs more value-based methods to control this process. It is with this view we synthesized N-heterocyclic based metal complexes and applied them in the cyclohexane oxidation. The successful catalysts and methods suggested can be exploited and used in the petrochemical industries, particularly, and other industries in general.
The work presented describes the synthesis of Cr, Mn, Fe, Co, and Ti metal complexes using proline and phthalimide as ligands.
The synthesized complexes were fully characterized by UV, IR, NMR, TGA, XRD, and SEM – EDX analysis. The activity of the complexes as catalysts were evaluated using different methodologies for the "oxidation of cyclohexane" that is as aerial oxidation using solvent system, without solvent system and autoclaves at different pressure using oxidants. This was achieved using oxidants i.e., H_2O_2, KIO_4 and TBHP in an autoclave at fixed temperatures. Also, the stability of the complexes toward the cyclohexane oxidants were investigated, where the metal leaching was excluded since the analytical results showed no changes in the complexes structures after the oxidation performance studies. The oxidation process was monitored by a well-equipped GC technique. The evaluation of the results for the tested material has shown a promising activity towards the cyclohexane oxidation, These successfully synthesized complexes were evaluated for their catalytic activity using aerobic conditions and different oxidants in solvent system and solvent-free system. Also, these complexes were subjected to oxidation in different autoclaves using indigenously developed pressure in presence of different oxidants.
The foregone study reveals that these complexes in presence of H_2O_2 and TBHP have shown promising activities. The complexes of phthalimide with Ti and Fe with TBHP gave encouraging results. The Co- Proline complex with H_2O_2 also gave considerablly promising results.
The effect of oxidants on the stability of the complex used as catalysts, (metal leaching), after completion of the oxidation reaction was investigated. The IR result exhibited no significant structural changes.

Keywords: proline, phthalimide, cyclohexane oxidation, metal complexes.

Time / Oxidation results with respect to oxidant. The product formation	Metal Complex									
	Co-proline 1:2 (micro)					Co-phthalimide 1:2 (micro)				
Oxidant / Product	Neat	H_2O_2	TBHP			Neat	H_2O_2		TBHP	
pressure	–	2-3 bar	6-7 bar	2-3 bar	6-7 bar	–	R_1	R_2	R_1	R_2
2 hr Cy-ene	Nil	1.4%	3.2%	12%	Nil	Nil	Nil	trace	trace	1.3%
4 hr Cy-ene	No-change	1.6%	-	-	16.2%	Nil	-	-	-	-
24 hr Cy-ene	Nil	12%	Nil	trace	Nil	Nil	No-change	trace	trace	Nil

Table 1: Oxidation of cyclohexane using micro-complexes with different oxidants.

R_1, Represents the reactor (I) having 1-2 bar pressure. R_2, Represents the reactor (II) having 2-3 bar pressure.

* Co-proline 1:2 Nano 4hr 6% (Cy-ene**).**

References:

Ahmed, S. M., Mubarak, A. T., Alam, M. M., & Al-Ahmari, H. A. (2014). Cyclohexane Oxidation: Synthesis of Iron (III)-Amino Acid and Amino Acid Schiff Base Complexes and Their Catalytic Activity Evaluation. *Sci. J*, *4*(5), 600-615.

Low cost metal-free reduction catalysts of violet phosphorus synthesized by High Energy Mechanical Milling

Rak Hyun Jeong,[1,2] Dong In Kim,[1] Ji Won Lee,[1,2] Jung-Hoon Yu,[1] Antony Ananth,[1] and Jin-Hyo Boo,[1,2,*]

[1]Department of Chemistry, Sungkyunkwan University, 16419 Suwon, Republic of Korea,
[2]Institute of Basic Science, Sungkyunkwan University, 16419 Suwon, Republic of Korea

Abstract:
Violet phosphorus (VP) catalyst was synthesized by a high energy mechanical milling method using red phosphorus powder. The obtained powder was characterized using XRD, TEM, SEM, EDS, UV-Vis-NIR spectrophotometer, FT-IR and Raman spectroscopy techniques. The catalytic activity of VP was evaluated using UV-Vis absorption spectroscopy to measure the decolorization of aqueous solutions containing methylene blue. The VP catalyst exhibited a discolouring phenomenon for large amounts of light at very high speed without light. Since this decolorization phenomenon is not observed in pure red phosphorus or black phosphorus, it is unique to VP. In addition, this phenomenon occurs as a result of reduction rather than decomposition or adsorption. On the other hand, when investigating the effect of UV and visible light, photocatalytic decomposition was observed for black phosphorus. As a result, these properties suggest that other environmental catalysts, such as water splitting, hydrogen generation, and selective catalytic reduction catalysts, are possible for use in place of methylene blue. During synthesis, this material is not only crystallized into a 2D layer structure, but also has a relatively easy synthesis method, which is advantageous for mass production or use in industrial applications. Recently, Tsai et al. performed a successful study on the formation of 2D violet phosphorus on InP substrates, and the resulting violet phosphorus was observed to have a high carrier mobility and carrier concentration.

Keywords: 2D material, Violet phosphorus, Hittorf's phosphorus, Ball milling, Reduction Catalyst, Methylene blue

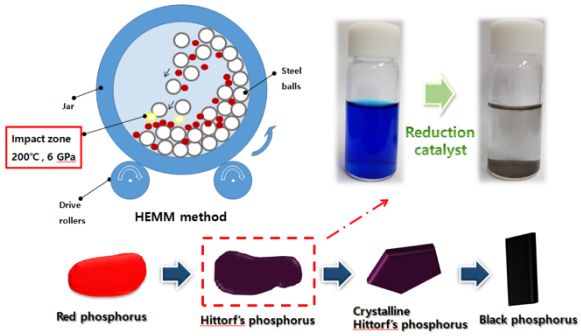

Figure 1: Synthesis experiment scheme of violet phosphorus as 2D material. It acts as a catalyst to reduce organic dye.

References:

1. Hsu-Sheng Tsai, Chih-Chung Lai, Ching-Hung Hsiao, Henry Medina, Teng-Yu Su, Hao Ouyang, Tai-Hsiang Chen, Jenq-Horng Liang, Yu-Lun Chueh ACS Appl. Mater. Interfaces (2015), 7, 13723−13727.
2. Joshua B Smith, Daniel Hagaman and Hai-Feng Ji Nanotechnology 27 (2016) 215602
3. Georg Schusteritsch,, Martin Uhrin, Chris J. Pickard Nano Lett. (2016), 16, 2975−2980

Particle Fabrication *via* Drying Droplet Method on a Super Hydrophobic Surface

Hyung-Ju Kim, Sung-Jun Kim, Chan Woo Park, Hee-Man Yang

Korea Atomic Energy Research Institute, Decommissioning Technology Research Division, Daejeon, Korea

Abstract:
Self-assembly of colloidal particles is very efficient way to fabricate functionalized materials. There are several methods developed to make array of inorganic particles. Especially, dry self-assembly method is the fabricating suprapaticles using droplet templates dispensed on solid substrate. One of the advantages of this method is that assembled particle could be easily detached and collected without other processes. Also, the shape of the dried particles is highly depending on the surface properties of substrate. Rastogi et al. developed the hydrophobic surface for particle fabrication using polyethylene (Figure 1(a)). In this study, we present the synthesis of superhydrophobic surface which has contact angle higher than 135° using silicon wafer (Figure 1(b)). Further, spherical silica particle is fabricated on this superhydrophobic surface (Figure 1(c)).
This study will also permit us to discuss a novel self-propelling particles for separation applications. Future work using nuclides separation is warranted.

Keywords: hydrophobic surface, particle synthesis, drying droplet, lotus effect, self-propelling particle, separation applications.

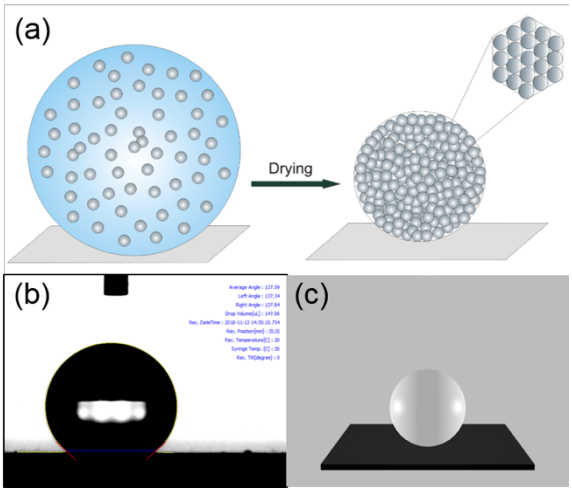

Figure 1: (a) Schematic for making spherical colloidal assemblies on superhydrophobic surface, (b) contct angle measurement for silylated silicon wafer, (c) scheme for silica particle fabrication *via* drying droplet method.

References:

1. Gao, L., McCarthy, T. (2006) A perfectly hydrophobic surface, *J. Am. Chem. Soc.,* 128, 9052-9053.
2. Rastogi V., Melle S., Calderon O., Garcia A., Marquez M., Velev O. (2008), Synthesis of Light-Diffracting Assemblies from Microspheres and Nanoparticles in Droplets on a Superhydrophobic Surface, *Adv. Mater*., 20, 4263-4268.

On the method of laser surface micromachining to increase the adhesion properties of joints

G. Witkowski,[1*] S. Tofil,[1] K. Mulczyk,[1] H. Danielewski[1]

[1] Kielce University of Technology, Faculty of Mechatronics and Mechanical Engineering, Kielce, Poland

Abstract:
The presented method of laser surface micromachining of materials was developed in order to increase their adhesive properties. The method allows to produce a spatial structure using a laser beam. In previously encountered laser applications, there is surface treatment involving the execution of simple geometric figures defined by flat geometry. Technologies such as Selective Laser Melting (SLS) or Selective Laser Sintering (SLS) are used to produce spatial geometries, but are classified as additive techniques. The method presented in the article should be included in the subtractive manufacturing techniques using the phenomenon of cold ablation. The method can be successfully used for pico and femto second lasers equipped with a galvo type scanning head. The advantage of the method is generating the trajectory and modulating the beam power based on the geometry of the spatial structure contained in the 3D data exchange file. The method uses proprietary solutions allowing for appropriate modulation of the laser beam power depending on the desired geometry. The control application for laser device and the galvo head was developed based on the LabView environment. The article also presents the results of experimental work (Figure 1, Figure 2).
The presented method was developed for the needs of the research project LIDER / 30/0170 / L-8/16 / NCBIR / 2017 financed by the National Center for Research and Development and constitutes the basis for the application in the Patent Office of the Republic of Poland.

Keywords: laser devices, surface treatment, micromachining, 3D geometry, adhesive joints, microstructure, laser ablation.

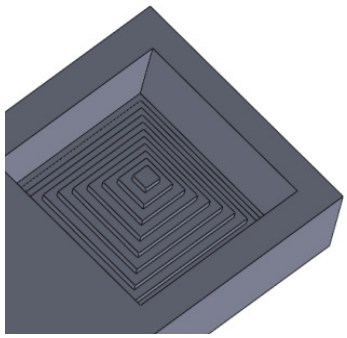

Figure 1: Desired spatial geometry.

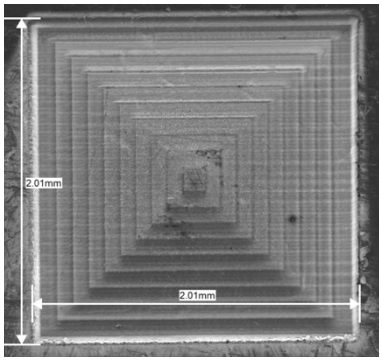

Figure 2: View of obtained microstructure

References:

1. M. Brown, C. Arnold, (2010) Laser Precision Microfabrication in Material Science vol 135, Heidelberg, Springer-Verlag.
2. G. Witkowski, S. Tofil, K. Mulczyk (2018) Control system of the ultrafast trumicro experimental laser for surface microtreatment - Part I, International Carpatian Control Conference, IEEE New York.
3. G. Witkowski, S. Tofil, K. Mulczyk (2018) Surface micro treatment of INCONEL 718 alloys with a picosecond laser to increase adhesive strength in glued joints, Laser Technology 2018: Progress and Applications of Lasers, SPIE Washington.

Surface laser micromachining to increase the strength of joints in adhesive joints

Sz. Tofil,[1*] G. Witkowski,[1] K. Mulczyk[1], H. Danielewski[1]

[1] Kielce University of Technology, Faculty of Mechatronics and Mechanical Engineering, Kielce, Poland

Abstract:
The method of increasing the shear strength of metal adhesive joints with plastics presented in the article was developed as part of the LIDER VIII project. This method uses laser microtexturing of materials to develop bonded surfaces. The TruMicro 5325c laser used in the tests allows ablation removal of material without a heat affected zone in the rest of the material. For metal and ceramic materials, the presented method significantly increases the shearing strength of the resulting joints, which was confirmed by the presented results of laboratory tests. The used parameters of the laser device did not cause cracks in the ceramic materials. An example of the micro-machining made on the ceramic surface is shown in Fig. 1 and for the metal in Fig. 2. The conducted research allows to conclude that the joints of textured elements are characterized by a several-fold increase in the strength of joints in relation to materials without micro-texture. The presented method was developed for the needs of the research project LIDER / 30/0170 / L-8/16 / NCBIR / 2017 financed by the National Center for Research and Development.

Keywords: picosecond laser devices, surface microtreatment, ceramics, plastics, adhesive joints, , laser subtractive manufacturing techniques.microstructure, laser ablation

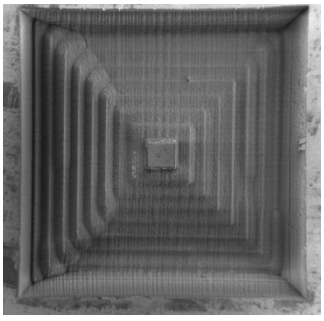

Figure 1: General view of a single microstruture on ceramics.

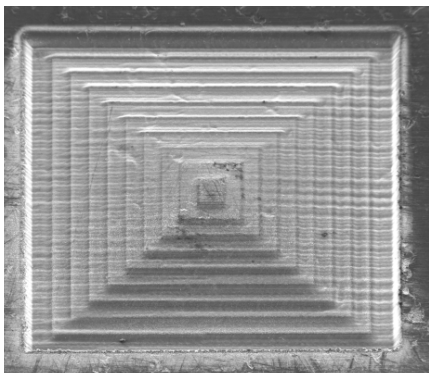

Figure 2: General view of a single microstruture on metal.

References:

1. M. Brown, C. Arnold, (2010) Laser Precision Microfabrication in Material Science vol 135, Heidelberg, Springer-Verlag.
2. G. Witkowski, S. Tofil, K. Mulczyk (2018) Surface micro treatment of INCONEL 718 alloys with a picosecond laser to increase adhesive strength in glued joints, Laser Technology 2018: Progress and Applications of Lasers, SPIE Washington.
3. S. Tofil, G. Witkowski, K. Mulczyk (2018) Surface micromachining of titanium alloys with picosecond laser to increase the adhesion force in glued joints, Laser Technology 2018: Progress and Applications of Lasers, SPIE Washington

Newly Designed TiO_2 Hollow Spheres and its Photocatalytic Properties

Chao-Nan Chen[1], Jui-Yu Wang[1], Tzu -Yuan Lin[2], Jung-Jie Huang[2,*]

[1] Department of Computer Science and Information Engineering, Asia University, Taichung, Taiwan
[2] Department of Electrical Engineering, Da-Yeh University, Changhua, Taiwan

Abstract:
In this paper, uniform titania dioxide (TiO_2) hollow spheres have been formed on polystyrene microsphere template by the liquid-phase deposition (LPD) method at a temperature below 100°C. Polystyrene microsphere deposited on glass wafers were used as substrates for the deposition of titanium dioxide hollow spheres.
This polystyrene microsphere surface has shown to be effective for promoting the growth of films from titanic aqueous solutions by the LPD method at a low temperature below 100°C. The microstructure of the as-prepared films by LPD method 30 minutes were characterized by scanning electron microscopy (SEM). The results indicate that they had a well-defined morphology, a uniform diameter of about 1.7μm (as shown in figure1).
The TiO_2 hollow spheres shows very strong photocatalytic activity for the degradation of Rhodamine B with high photochemical stability under UV light irradiation (as shown in figure2).
This newly designed TiO_2 hollow spheres offering the ability to uniformly control the shape, offers a high-performance photocatalysts for degradation of Rhodamine B.

Keywords: TiO_2, LPD, Polystyrene, Photocatalyst.

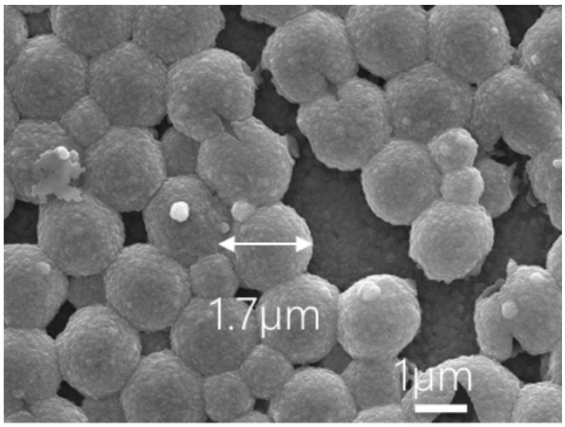

Figure 1 SEM micrograph of TiO_2 hollow spheres.

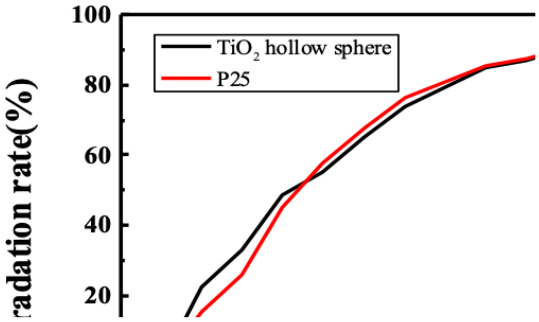

Figure 2 The degradation of Rhodamine B by TiO_2 hollow spheres and P25 TiO_2 thin films.

References:

1. Hamed E., Meisam Z., Arkaye K., Alireza A. (2018) Shape-controlled fabrication of TiO_2 hollow shells toward photocatalytic application, Appl. Catal. B-Environ., 227, 519-529.
2. Qianqian J., Li L., Jinhong B., Shijing L., Minghua L. (2017), Design and Synthesis of TiO_2 Hollow Spheres with Spatially Separated Dual Cocatalysts for Efficient Photocatalytic Hydrogen Production, Nanomaterials 7, 24.

Micro-alloys precipitation in NiO- and CoO-bearing enamel coatings and their effect on adherence of enamel/steel

K. Chen,[1,2,*] M. Chen[3], S. Zhu[2], F, Wang[3]

[1] Laboratory for Corrosion and Protection, Institute of Metal Research, Chinese Academy of Sciences, Shenyang 110819, China
[2] School of Material Science and Engineering, University of Science and Technology of China, Hefei 230000, China
[3] Key Laboratory for Anisotropy and Texture of Materials (Ministry of Education), School of Materials Science and Engineering, Northeastern University, Shenyang, China 110819, China

Abstract:
The effect of CoO and NiO on the adherence between enamel coating and steel is investigated experimentally in this study. Enamel coatings are applied to the steel using a wet process with slurries. A total of five enamels were prepared including three single layer enamels: blank enamel (BL), NiO bearing enamel (MTNi3), CoO bearing enamel (MTCo3), and two double layer enamels: BL-MTNi3, BL-MTCo3, which consisted an inner layer of BL and an outer layer of MTNi3 or MTCo3. Falling-weights tests were performed and the cross-sections at the enamel/steel interface were analyzed with a scanning electron microscopy (SEM) coupled with an energy dispersive spectroscopy (EDS) and electron probe microanalysis (EPMA). Results show that the increases of adherence for MTCo3 and MTNi3 coated steel are attributed to the micro-alloys precipitation at the enamel/steel interface. These micro-alloy precipitations grow parallel to the steel/enamel interface for MTNi3, while they are dendritic and perpendicular for MTCo3. Compared with MTCo3, the negative reaction energy between NiO and FeO for MTNi3 causes micro-alloy precipitations formed far away from the enamel/steel interface, resulting in different morphology and adherence.

Keywords: enamel coating, steel, interface reaction, adherence.

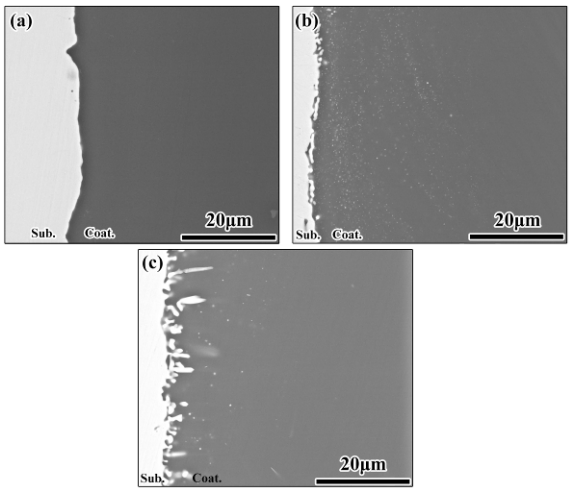

Figure 1: Three different enamel/steel interface morphologies after firing: (a) Blank enamel, (b) NiO bearing enamel and (c) CoO bearing enamel.

References:

1. King BW, Tripp H, Duckworth WH. Nature of adherence of porcelain enamels to metals. J Am Ceram Soc. 1959;42:504-525
2. Donald IW, Metcalfe BL, Gerrard LA. Interfacial reactions in glass-ceramic-to-metal seals. J Am Ceram Soc. 2008;91:15-20.

Effects of Process Parameters on the Properties of Ga-doped SnO_x Thin Films

H. I. Bang,[1] B. S. Bae,[2] E.-J. Yun,[1,*]

[1] Hoseo University, Department of ICT Automotive Engineering, Dangjin, Chungnam, South Korea
[2] Hoseo University, Department of Display Engineering, Asan, Chungnam, South Korea

Abstract:
Sputter-deposited tin oxide (SnO_x) thin films are one of the most attractive bipolar oxide semiconductor (OS), in which both n- or p-type carrier doping are possible in the same material. Therefore, they have been applied as the channel layer in the fabrication of flexible n- or p-type TFTs with reasonably high mobility. However, SnO_x has a high carrier concentration, which makes TFTs difficult to turn OFF, and can be easily crystallized, which causes non-uniformity in the display. These problems can be solved by doping with suitable cations acting as carrier supressors and crystallization stoppers because SnO_x is a bipolar OS. To date, various doping elements have been reported to improve the performance of SnO_x-based TFTs, such as aluminum, nitrogen, antimony, indium, and fluorine. Nevertheless, there are no reports showing the effects of gallium (Ga) doping and process parameters on the properties of SnO_x films deposited using a SnO-Ga ceramic target. Hence, this study examined systematically the effects of the sample temperature on the properties of Ga-doped SnO_x thin films using a SnO (90 at.%)-Ga (10 at.%) ceramic target. Ga-doped SnO_x thin films were deposited at an oxygen ratio of 4 % by RF magnetron sputtering as a function of the sample temperature. X-ray photoelectron spectroscopy (XPS) was conducted to monitor the contents (at. %) and the Sn, O, and Ga chemical bonding states in the Ga-doped SnO_x thin films (Figure 1). To investigate the changes in the depth profiles of O, Sn, and Ga in the samples, secondary ion mass spectroscopy analyses were also performed. The surface roughness and electrical property of the Ga-doped SnO_x films were analyzed by atomic force microscope and Hall measurement, respectively.

Keywords: process parameters, Ga-doped tin-oxide, sputtering, bipolar semiconductor.

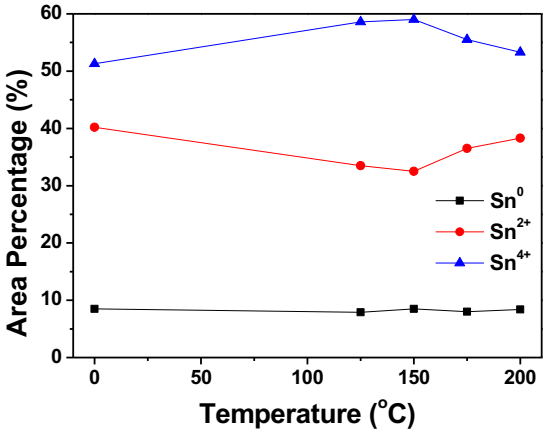

Figure 1: Figure illustrating the percentage area characteristics of three Gaussian peaks as a function of the sample temperature obtained from the Sn $3d_{5/2}$ narrow scan XPS spectra of Ga-doped SnO_x thin films prepared at various sample temperature. This result was obtained after fitting the $3d_{5/2}$ peaks using the three Sn^0, Sn^{2+}, and Sn^{4+} Gaussian peaks. It indicates that there is a larger amount of SnO_2 phase in the sample than SnO.

References:

1. Yang, J., Pi, S., Han, Y., Fu, R., Meng, T., Zhang, Q. (2016) Characteristic of bismuth-doped tin oxide thin-film transistors, *IEEE Trans. Electron Devices*, 63, 1904-1909.
2. Ammari, A., Trari, M., Zebbar, N. (2019), Transport properties in Sb-doped SnO_2 thin films: Effect of UV illumination and temperature dependence, *Mater. Sci. in Semicond. Proc.*, 89, 97-104.

Development and Evaluation of Self-polishing Copolymer (SPC) resins and antifouling paints based on silyl acrylate

Rahui Park,[1*] Hyun Park[1,2]

[1] Pusan National University, Department of Naval Architecture and Ocean Engineering, Pusan, Korea
[2] Pusan National University, Global Core Research Center for Ships and Offshore Plants (GCRC-SOP), Pusan, Korea

Abstract:
Silyl acrylate which are used in the development of environmentally friendly antifouling paints, can give the coatings self-smoothing properties. However, it has a low erosion rate in a static environment. In this study, we compared two different types of silyl acrylate, and then synthesized SPC resins using silyl acrylate with better performance. The experiment was carried out in three stages. First experiment, we synthesized SPC resins using the silyl acrylate, ethyl acrylate, and methyl methacrylate and modified the Si-acrylate SPC resins by using other acrylate monomers to determine the effect of monomers on silyl acrylate. Second experiment, we need to improve the hardness and polishing ability of Si-acrylate SPC resins. So, we synthesized Si-acrylate SPC resins and analyzed the characteristics of each resins using Taguchi method, one of the experimental design methods. The SPC structures of the synthesized polymers were confirmed using FT-IR spectroscopy. As a result of the image analysis, it was showed that PSM-T7 had a fouling area of 25.96%, which is lower than that of Zn-based PRD3-1 with a fouling area of 36.47%, showing better antifouling performance. Third experiment, we developed antifouling paints using four type resins including the optimum condition of monomers obtained by Taguchi method. We investigated the basic properties test, polishing rate test and immersion test of the developed paints. As a result of the image analysis by the immersion test of the developed paints, PSM-T7P and PSM-T8P showed a fouling area of 31.55 and 33.37%, which is similar to that of the Zn-based commercial paint. Through this, the antifouling performance of the Si-based antifouling paint was confirmed.

Keywords: antifouling, silyl acrylate, Self-polishing copolymer, environmentally friendly,

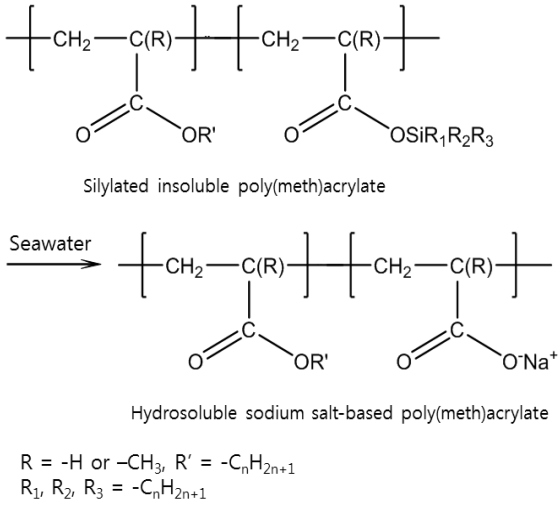

Figure 1: Mechanism of Si-acrylate SPC resin.

References:

1. Elisabete Almeida, Teresa C. Diamantin, Orlando de Sousa (2007), Marine paints: The particular case of antifouling paints, *Progress in Organic Coatings*, 59, 2-20.
2. Chambers L.D., Stokes K.R., Walsh F.C., Wood R.J.K. (2006), Modern approaches to marine antifouling coatings, *Surface & Coatings Technology*, 201, 3642-3652.
3. Bressy C., Hellio C., Ngocet M. (2014), Optimized silyl ester diblock methacryliccopolymers: A new class of binders for chemically active antifouling coatings, *Prog. Coat.*, 77, 665-673.
4. Jaharah A. (2013), Philosophy of Taguchi approach and method in design of experiment, *Asian journal of scientific research,* 6, 27-37.

General Electrical Characteristics of an Impulse Magnetron Discharge in Target Material Vapor

A.V. Kaziev[1], K.A. Leonova[1,*], M.M. Kharkov[1], A.V. Tumarkin[1], D.V. Kolodko[1,2], D.G. Ageychenkov[1]

[1] National Research Nuclear University MEPhI (Moscow Engineering Physics Institute), Moscow, Russia
[2] Kotel'nikov Institute of Radio Engineering and Electronics, Fryazino Branch, Russian Academy of Sciences, Fryazino, Russia

Abstract:
Magnetron sputtering is among the main tools for deposition of thin-film coatings. Despite the wide application of magnetron sputtering systems (MSS), in this area there is demand in improving both the quality of films and the efficiency of their preparation process. In the past 10 years, special attention of researchers and innovative industries dealing with thin-film technologies has been focused on impulse regimes of magnetron operation: high-current impulse magnetron discharge (HCIMD) and high-power impulse magnetron sputtering (HiPIMS). They provide an increase in the density and adhesion of films, and also allow tailoring the film structure within a wide range due to outstandingly high degree of plasma ionization [1].
Our main goal is to investigate impulse magnetron discharges formed in target material vapor, with or without an inert working gas, and to study the relationships between plasma parameters and characteristics of deposited coatings. In the studied regimes, high plasma ionization levels are achieved, the deposition rates are greatly enhanced as compared to any of existing modifications of MSSs, and the energy efficiency of the process is increased due to optimized utilization of power that heats up the magnetron target. A distinctive feature of the discharge form under study is its quasistationary behavior, that is, maintaining constant high values of discharge current and voltage, and ion concentration, throughout the discharge pulse (up to tens of ms).
In present contribution we report on the voltage-current characteristics of an impulse magnetron discharge in target material vapor operated with Cu, Cr, and Si targets. These materials are extensively utilized in thin-film industries, e.g. for creation of protective wear and corrosion-resistant Cr-based coatings in automotive field; Cu metallization of VLSI in microelectronics, as well as preparation of corrosion-resistant coatings based on Si.
The *I–V* curves have been measured depending on the magnetic field strength to reveal the most promising regimes of operation in terms of enhanced sputtering flux coupled with high ionization degree of material.
The dynamics of discharge evolution have also been studied by measuring relation between current and voltage during a single impulse.
This work is supported by the Russian Science Foundation under grant no. 18-79-10242.

Keywords: magnetron discharge, hot target, self-sputtering, ionization degree, discharge in metal vapor, chromium, copper, silicon.

References:

1. Gudmundsson J.T., Brenning N., Lundin D., and Helmersson U. (2012) High power impulse magnetron sputtering discharge, *J. Vac. Sci. Technol.,* 30(3).
2. Tumarkin A.V., Kaziev A.V., Kharkov M.M., Kolodko D.V., Ilychev I.V., Khodachenko G.V. (2016) High-current impulse magnetron discharge with liquid target, *Surface and Coatings Technology*, 293, 42–47.

Highly stable robust superhydrophobic coating deposited on glass substrate using atmospheric pressure plasma jet

Md. Mokter Hossain, Quang Hung Trinh, Duc Ba Nguyen, M.S.P. Sudhakaran,Young Sun Mok*

Department of Chemical and Biological Engineering, Jeju National University, Jeju 63243, Korea
*Corresponding author, Tel: (+82)64-754-3680, Fax: (+82)64-755-3670, E-mail: smokie@jejunu.ac.kr

Abstract:
Plasma polymerization by atmospheric pressure plasma was successfully used to obtain highly stable robust superhydrophobic coating onto glass substrates. Noble gas argon was used to generate argon plasma by dielectric barrier discharge (DBD) configure reactor for the this study. Hexamethyldisiloxane (HMDSO) and 3-Aminopropyl(diethoxy)methylsilane (APDMES) were used as precursors where HMDSO was used to promote hydrophobicity and APDMES to promote robustness of the thin film. The main objective of this work is to find an optimum mixture of these two precursors that will make highly stable robust superhydrophobic thin film on the glass surface. A high voltage alternating current (AC) (operating frequency: 11.5 kHz) was used to generate argon plasma for making a coating layer onto the soda-lime glass sample. Water contact angle (WCA) of 164° and a stable mechanical strength were achieved with an optimal APDMES/HMDSO ratio of 1.4 (Figure 1). Atomic force microscopy (AFM), Scanning electron microscopy (SEM), X-ray photoelectron spectroscopy (XPS), Fourier transform infrared spectroscopy (FTIR), static water contact angle (WCA), and scratch test were done to examine the coating.

Keywords: robust coating, scratch test, plasma jet, thin film, superhydrophobic, APDMES, HMDSO.

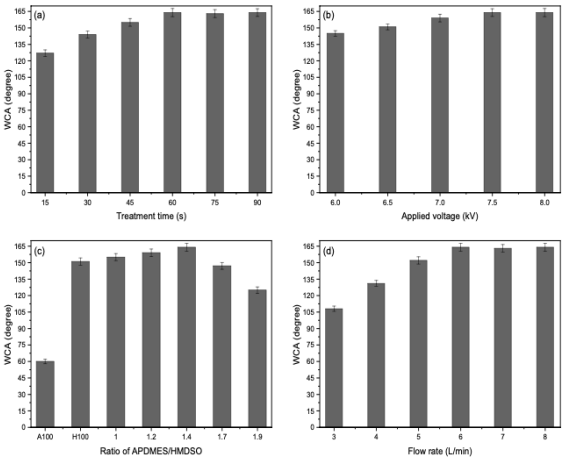

Figure 1: Dependence of WCA on (a) the treatment time, (b) the applied voltage, (c) the H/A ratio and (d) the gas flow rate.

Reference:

1. Hossain MM, Trinh QH, Nguyen DB, et al. Robust hydrophobic coating on glass surface by an atmospheric-pressure plasma jet for plasma-polymerisation of hexamethyldisiloxane conjugated with (3-aminopropyl) triethoxysilane. *Surf. Eng*. 2018;1–10.
2. Hossain MM, Trinh QH, Sudhakaran MSP, et al. Improvement of mechanical strength of hydrophobic coating on glass surfaces by an atmospheric pressure plasma jet. *Surf. Coatings Technol*. 2019;357:12–22.

SurfCoat Korea 2019 / Graphene Korea 2019
Joint Posters Session II: Surfaces and Coatings applications / Graphene synthesis and applications

Growth of $MnSi_{1.7}$ Thermoelectric Coating on Si Substrate by Pack Cementation

A. Teknetzi, E. Tarani, D. Kourtidou, D. Karfaridis, E. Pavlidou, K. Chrissafis, G. Vourlias, E. K. Polychroniadis

Aristotle University of Thessaloniki, Department of Physics, Thesssaloniki, Greece

Abstract:
Thermoelectric materials are of great scientific interest since they convert heat to electric power and vice versa directly. They find application on refrigeration systems and devices for waste heat recovery. Nowadays, some of the most effective thermoelectric materials face problems that impede a wider use, such as high cost, complex preparation methods, and toxic or rare element content. Higher manganese silicides, $MnSi_{\sim 1.7}$, are very attractive materials for thermoelectric applications, combining good thermoelectric properties (figure of merit ZT=0.7 for the undoped material [1], ZT~1 for the doped one [2]), mechanical and chemical stability, low cost and non-toxicity. In the current work we report on the growth of $MnSi_{1.7}$ coatings on Si substrates. The method used is pack cementation, which is characterized by its simplicity, eco-friendliness and cost-effectiveness. The effect of different experimental parameters (initial composition, deposition time, tempereature) on the structure, the phase formation and some of the properties of the $MnSi_{1.7}$ coatings is studied. The structural study and the phase identification were performed by X-Ray diffraction analysis, while the morphology and the chemical composition were determined by a Scanning Electron Microscope equipped with an EDS analyzer (Figure 1). Chemical analysis and formulation of the coatings were confimed by X-ray Photoelectron Spectroscopy. The oxidation resistance of the coatings was tested by exposing the samples to high-temperature air environment using a Thermogravimetric setup. Finally, we attempted dopping the $MnSi_{1.7}$ coatings with elements reported to enhance the thermoelectric efficiency using pack cementation, and the experimental results are discussed.

Keywords: thermoelectric materials, higher manganese silicides, pack cementation, oxidation resistance.

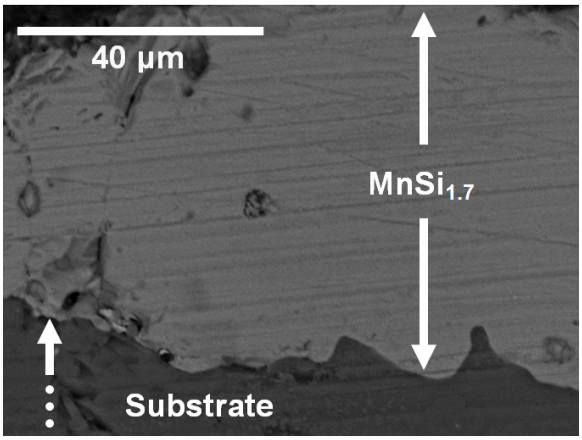

Figure 1: Cross sectional SEM micrograph of the $MnSi_{1.7}$ thermoelectric coating formed on the silicon substrate.

References:

1. Fedorov, M. I., Zaitsev, V. K. (2006) Thermoelectrics of Transition Metal Silicides, in Thermoelectrics Handbook: Macro to Nano, ed. by Rowe, D. M., *CRC Press*, 31-1 – 31-19.
2. Yamamoto, A., Ghodke, S., Miyazaki, H., Inukai, M., Nishino, Y., Matsunami, M., Takeuchi, T. (2016), Thermoelectric properties of supersaturated Re solid solution of higher manganese silicides, *Jpn. J. Appl. Phys.*, 55(2), 020301-20304.

Aknowledgement:
The implementation of this research was co-funded through the action "SUPPORTING THE RESEARCH HUMAN RESOURCES VIA THE DOCTORAL RESEARCH IMPLEMENTATION" by funds of the Operation Program "Human Resources Development, Education and Lifelong Learning", 2014-2020 and partially by EU in the framework of the NetFISiC project (Grant No PITN-GA-2010-264613).

Electron Beam annealing method for realization of High Mobility Oxide Semiconductor Thin-film transistor

Yu-Jung Cha, Moon Uk Cho, Joon Seop kwak*

Department of Printed Electronics Engineering, Sunchon National University, Jeonnam 540-742, Korea

Abstract:
Displays are required such as high resolution, various shape, larger, flexable. Therefore, various field of light emitting diodes (LEDs) as light source had been studing. As LEDs had high performace, thin film transistor (TFT) also required development for driving LED display. Over the last several years, there has been great interest in TFT made of transparent oxide semiconductor. The amorphous state oxide semiconductor TFT showed high carrier mobility, excellent large-area uniformity and optical transparency. However, oxide semiconductor TFT was required an annealing process at high temperature (>350) for channel activation, which has prevented to use polymer substrate in flexible electronics.[1] In most manufacture, channel was activatied by furnace, dry oven, hot plate, rapid thermal annealing system, etc. Here we report novel method for forming stable oxide semiconductors TFT at low temperature by electron beam irradiation annealing (EBA). We fabricated bottom-gate a-IGZO TFT on hydrothermal SiO2 (100 nm)/Si wafer and on the Al_2O_3 gate insulator by ALD with polimide substrate. A-IGZO TFT were irradiated as time and DC power then fixed RF power of EBA. The mobility of a-IGZO TFT were changed according to time and DC power of EBA. At all DC power, mobility were saturated after irradiated time of 3 min. the mobility was more slowly increased and saturated at low DC power. It means that mobility is able to control by time and DC power of EBA. Thus, we suggest that EBA method is good candidate to replace high temperature annealing method.

Keywords: a-IGZO, TFT, electron beam annealing, channel activation

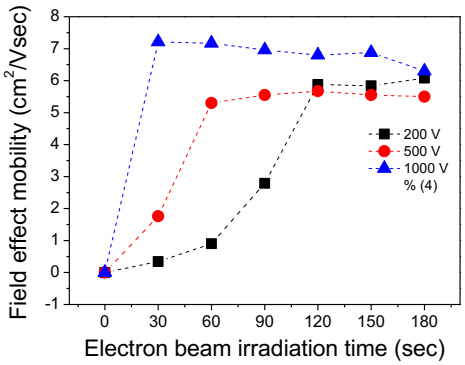

Figure 1: The variation of field effect mobility as irradiated time with DC power by electron beam

References:

1. Kim, M. G., Kanatzidis, M. G., Facchetti, A. & Marks, T. J. (2011), Low-temperature fabrication of high-performance metal oxide thin-film electronics via combustion processing. *Nature Mater.* 10, 382–388.

Anti-corrosion and Anti-oxidation Effects of Aluminum Metal Substrate by Inorganic-Organic Binder / Graphene NanoComposite Film Coating

Han Kim,[1,†] Hyemin Lee,[1,†] Hong-Baek Cho,[1] Yong-Ho Choa,[1,*]

[1] Hanyang University, Department of Materials Science and Chemical Engineering, Ansan, Republic of Korea

*choa15@hanyang.ac.kr, [†] these authors contributed equally to this work

Abstract:

Aluminum (Al) and its alloys have been widely used and investigated in various industrial fields from small scale (electronics, batteries, etc.,) to large scale (aerospace, building, machinery, aviation, automobile) because of own valuable properties such as ductility, light weight, high strength, high electrical and thermal conductivities. Even though Al and its alloys are well known about anti-corrosive material through creation of the protective native oxide layer from air, they are very easily degraded by moisture and harsh condition such as strong acids and high temperature, it critically reduces the applicable boundary in various industrial sectors. Fabricating shielding layer on the surface of this metal and alloy materials is regarded as the solution to overcome this limitation. Organic polymer or its composites coating was traditionally used for this strategy. However, some additives in this coating such as isocyanate cross-linking agents or the additives which can generate volatile organic carbon (VOC) are harmful in environment, and their structure collapses rapidly at high temperature because of low melting and glass transition temperatures. Inorganic polymer matrix with eco-friendly and dense film formation due to siloxane (-Si-O-Si-) network including silane-based resin is one of alternative methods comparing to organic polymer. Nonetheless, they are suffered from micropores arising from the poor crosslinking density. In terms of this weakness, incorporating the nano-sized filler into polymer could be an excellent breakthrough. Graphene and its derivatives such as graphene oxide, reduced graphene oxide, edge-oxidized graphene are attractive materials in this purpose with processibility of fabricating nanocomposite film including densely layered structure and chemical inertness.

In this research, inorganic-organic binder/graphene nanocomposite coating on a Al foil was investigated. polysiloxane (PSX) is used as a main polymer matrix, graphene (G) is selected as an additional supporting agent in this composite system. PSX is good enough as a main structure of this nanocomposite system with dense siloxane bonding network and functional group which is possible to cover the graphene-induced defect. Graphene is also excellent assistant in this system which can improve mechanical stability and flexibility and chemical stability. PSX-G nanocomposite coating film is fabricated on Al foil substrate by simple bar coating using mayor rod followed by drying and hot-pressing for the fabrication of dense film structure. The changes of morphologies, anti-corrosion, and anti-oxidation properties were measured by scanning electron microscopy, energy dispersive spectrometer, and various electrochemical analysis such as polarization curves and electrical impedance spectroscopy. PSX-G nanocomposite coated-Al foil shows no significant change in surface structure after thermal shock experiment and after exposure to surfuric acid (H_2SO_4) or seawater which is comparable to pristine Al. Furthermore, enhanced corrosion inhibiting property of the PSX-G nanocomposite coated Al foil in H_2SO_4 solution is observed in polarization curves by decreasing of current density. With result of this study, the graphene-polymer nanocomposite coating layer exhibits a possibility as an anti-corrosion and anti-oxidation barrier with the complementary effect between inorganic-organic binder and graphene. PSX-G nanocomposite coating system has the potential to broaden the area of application such as thermal interface material as well as industrial fields as mentioned above, with optimizing coating process, modifying the graphene-polymer composite system, and so on.

Keywords: graphene, graphene-polymer composites coating, anti-corrosion, electrical conductivity, thermal conductivity

A Synergistic Combination of Au-coated Ag Nanowire and WO_3 Nanofiber for Enhanced Electrochromic Application

Yeong-Been Oh,* Jimin Lee, Hong-Baek Cho, Yong-Ho Choa

Hanyang University, Department of Material Science and Chemical Engineering, Ansan, Korea

Abstract:
Electrochomic (EC) materials are able to reversibly tune their optical properties including a transmittance, an absorbance and a reflectance during insertion/desertion of mediums (e.g., electron, H^+ and Li^+ ions) under external electric field. In recent years, EC devices have attracted attention in energy-saving and various display application such as smart window, optical display and rear-view mirror. Among the EC materials, tungsten oxide (WO_3) has been extensively studied as one of the promising materials having excellent EC properties. The crystalline WO_3 exhibits a superior long-term stability when they are applied as practical products such as the smart window. But until now, the low diffusion coefficient and long diffusion length of the mediums (especially H^+ and Li^+ ions) to the crystalline WO_3 remain a critical point to solve, leading to inferior optical modulation and response time.
With this regard, applying one-dimensional (1-D) WO_3 structure, which provides a path favorable to charge transfer as well as enlarged active-sites area, results in more activating electrochemical reaction. Electrospinning process is an effective way to fabricate fibers in nano- to submicron-scale.
Unlike dense WO_3 film, the WO_3 fiber-based EC layer has a porous structure with low proximity to electrodes as well as fiber-to-fiber. In this regard, conventional flat transparent electrodes such as fluorine- and indium-doped tin oxide are difficult to appropriately transfer electrons to the EC layer. Thus, introduction of highly conductive gold (Au)-coated silver nanowires (Ag NWs) in the fiber-based EC layer, which is affording an additional electron transfer pathway, is one way to solve this problem.
Pristine Ag NWs are, however, vulnerable to humidity and electrochemical reaction; when they are exposed to the ambient condition or electrochemical reaction, Ag NW networks become collapsed, leading to drastic performance degradation. It is expected that Au coating on Ag NWs is able to overcome the weakness by complementing reduction potential of Ag in redox system.
Herein, we prepared the polycrystalline WO_3 nanofibers (NFs) *via* electrospinning and subsequent calcination process. Au-coated Ag NWs are synthesized using a solution process then are combinated with the electrospun WO_3. The morphology, corresponding microstructures, crystallinity and electrochromic behavior of the NWs & NFs-based EC composites were characterized by means of scanning electron microscope, transmission electro microscope, X-ray diffractometer, UV-vis spectroscopy and Potentiostat/Galvanostat analyzer.

Keywords: electrochromism, tungsten oxide, nanowire, electrospinning, silver nanowire, galvanic-free coating

References:

1. Lee, H.; Hong, S.; Lee, J.; Suh, Y. D.; Kwon, J.; Moon, H.; Kim, H.; Yeo, J.; Ko, S. H., Highly stretchable and transparent supercapacitor by Ag–Au core–shell nanowire network with high electrochemical stability. ACS applied materials & interfaces 2016, 8 (24), 15449-15458.
2. Shim, H.-S.; Kim, J. W.; Sung, Y.-E.; Kim, W. B., Electrochromic properties of tungsten oxide nanowires fabricated by electrospinning method. Solar Energy Materials and Solar Cells 2009, 93 (12), 2062-2068.

Preparation of one dimensional Co_3O_2-NiO@AgNWs nanowire for the thin film electrodes of supercapacitor

Jian-Yang Lin[1], Yu-Xuan Zhang[1], Yui-Qi Wu[2], Jung-Jie Huang[2,*]

[1]Department of Electronic Engineering, National Yunlin University of Science and Technology, Yunlin 640, Taiwan, ROC.
[2]Department of Electrical Engineering, Da-Yeh University, Changhua 515, Taiwan, R.O.C.

Abstract:
The experimental results that of the activated carbon thin film electrode doped with silver nanowires as conductive material can improve the electrochemical performance of the supercapacitor. The specific capacitance increases as the diameter of silver nanowires increasing. The optimal diameter of silver nanowires was 500 nm.
In order to further improve the capacitance of electric double layer capacitor, the NiO and Co_3O_2 were deposited outer of the silver nanowires surface by hydrothermal process to form Co_3O_2-NiO@AgNWs core-shell nanomaterial. It can shows the pseudo-capacitors characteristic after the activated carbon doping with Co_3O_2-NiO@AgNWs. In the experiment, 0.1 g silver nanowires were dispersed in 40 ml deionized water, and then 10 mM $Ni(NO_3)_2{\cdot}6H_2O$, 5 mM $Co(NO_3)_2{\cdot}6H_2O$ and 0.04 M urea were mixed together. Finally, the container was heated at 95 °C for 24 hours to form the Co_3O_2-NiO@AgNWs nanomaterial.
Figure 1(a) shows the synthesized Co_3O_2-NiO@AgNWs image by transmission electron microscope. The flake structure of Co_3O_2-NiO composite oxide was deposited on AgNWs surface unifromly. Energy dispersive X-ray spectroscopy was used to identify the composition and distribution as shown in Fig. 1(b). Moreover, the different solid content of Co_3O_2-NiO@AgNWs was doped into the activated carbon paste to improve the electrochemical performance. The pseudo-capacitors characteristic can be seen as the thin film electrode doping with Co_3O_2-NiO@AgNWs nanomaterial as shown in Fig. 2. The optimal doping condition is 25 wt% and the specific capacitance can be increased by 36%.

Keywords: AgNWs, NiO, CoO, Co_3O_2-NiO@AgNWs, hydrothermal method, ultrasonic spray.

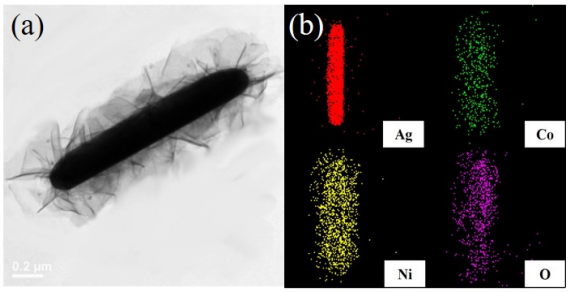

Fig. 1.(a) TEM images of Co_3O_2-NiO@AgNWs nanocomposites and (b) elemental maps of Ag, Ni, and Co in the Co_3O_2-NiO@AgNWs.

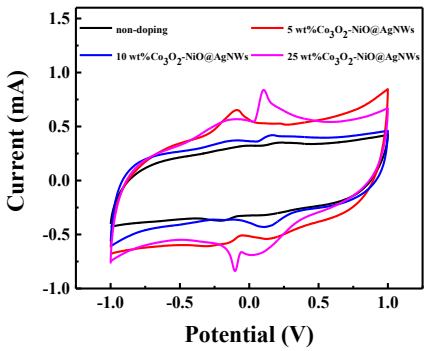

Fig. 2. The specific capacitance of Co_3O_2-NiO@AgNWs doped with 25 wt% increased by 36%.

References:

1. J. Xu, X. Qiao, M. Arsalan, N. Cheng, W. Cao, T. Yue, Q. Sheng, J. Zheng (2018) Preparation of one dimensional silver nanowire/nickel-cobalt layereddouble hydroxide and its electrocatalysis of glucose, J. Electroanal. Chem. 823, 315-321.
2. J.-Y. Lin, J.-J. Huang, Y.-L. Hsueh, Y.-X. Zhang (2018) Diameter effect of silver nanowire doped in activated carbon as thin film electrode for high performance supercapacitor, Applied Surface Science., (in press)

Low–temperature Encapsulating perovskite solar cells by RF Sputtering

Maro kim[1], Sangmo kim[2], He Rui[2], and Chung Wung Bark[*]

[1,2]Gachon University , Department of Electrical Engineering, Seongnam, KOREA

1. Introduction

In recent years Perovskite solar cells (PSCs) have received a great deal of attention owing to ease for fabricating, low manufacturing cost, flexibility. Especially, efficiencies have rapidly increased for the last several years, reaching up to 22.7% for single junction devices.[1]

However, Degradation of perovskite materials caused by water, humidity, and heat is the biggest obstacle to the commercialization of PSCs.

In this work, we introduce an encapsulation in which Al_2O_3 layer is deposited as a thin film through low temperature (under 95°C) RF sputtering which allows uniform films over a large area.

In order to find the optimum low temperature, we have conducted the experiment at low temperature (under 95°C).

2. Experimental process and Measurment

We used two-step[2] spin-coating method for PSCs layer, Electron Transporting Layer (ETL), (Hole Transporting Layer (HTL) and thermal evaporation for Au electrode.

Firstly, Lab-made TiO_2 paste were used for compact layer (C-L) and mesoporous layer (M-L)TiO_2 paste was prepared with a titanium dioxide powder.

Secondly, perovskite layer ($CH_3NH_3PbI_3$) was prepared. And hole transport layer, spiro-MeOTAD deposited on the perovskite layer. Before fabrication of solar cells, fluorine-doped tin oxide (FTO) coated glass substrates (Sheet resistance: 8 Ohm/sq, Films thickness: 400 nm) were cleaned.

Finally, 60 nm of Al_2O_3 was deposited by RF sputtering at low temperature. The structure and morphology of prepared samples was observed using field-emission scanning electron microscopy (FE-SEM, Hitachi S-4500) and X-ray diffraction (XRD, Rigaku RINT2100) using Cu-Kα radiation (λ = 1.54056 Å, 40 kV, 40 mA) in the 2-theta range of 20-80°. The conversion efficiency of prepared solar cell devices were measured by using current-voltage (J-V) solar simulator (K3400, McScience Company) adjusted to AM 1.5G.

Keywords: perovskite solar cell, RF sputtering, encapsulation, electron transporting layer, hole transporting layer.

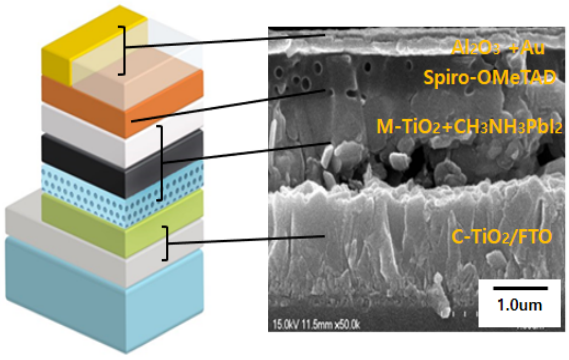

Fig. 1 Cross-sectional SEM image of PSCs fabricated with Lab-made Encapsulation

3. Summary

Applied at low temperature Encapsulation (under 95°C) to the PSC, the efficiency retained over 80% of the initial efficiency over a certain period of time, and the color of the black perovskite layer did not change for 300h in room temperature. And It has been found that the encapsulation method at 65°C is thicker than the lower temperatures (under 95°C) and the duration of the perovskite layer (65°C) is relatively longer.

References:

1. W. S. Yang, B.-W. Park, E. H. Jung, N. J. Jeon, Y. C. Kim, D. U. Lee, S. S. Shin, J. Seo, E. K. Kim, J. H. Noh and S. Il Seok, Science. 356, 1376-1379 (2017).
2. J.H Im, H.S Kim, N.G Park, Apl Materials, (2014),

Molybdenum Disulfide/Carbon Hybrid Thin Films as High Performance cathode for Reverse Electrodialysis

N. Jeong,[1,*] H. Kim,[1] J. Choi,[1] J. Nam,[1] K. Hwang,[1] S. Yang,[1] J. Han,[1] E. Jwa,[1] S. Park,[2]

[1] Korea Institute of Energy Research, Marine Energy Convergence & Integration Laboratary, Jeju-do, Republic of Korea
[2] Korea Institute of Energy Research, Jeju Global Research Center, Jeju-do, Republic of Korea

Abstract:
Reverse electrodialysis (RED) is an electrochemical method using ion transport phenomenon through ion exchange membrane (IEM) to generate electrical energy from the difference in concentration between salt water and fresh water.[1] The typical RED stack is composed of IEM, spacer, gasket, and electrode. The cation and anion exchange membrnaes are alternally arranged between anode and cathode. The spacer are generally palced between two membrnaes to secure the flow path for feeding waters. Up to now, most studies have been focused on the enhancement of IEM characteristics in order to impove RED performace: reduction of resistance and increase of perselectivity and ion exchange capacity. Despite the importance of electrode part in RED stack as an electrochemical system, on the other hand, only a few researches have shown the effect of types of electrodes and rinse solution on RED performace. Therefore, search for new electrodes is very important for optimization of RED stack.
Two demetional molybdenum disulfide (2D-MoS_2) is a very interesting materials for various applications, such as electrochemical catalyst, gas sensing, lubricant, field emission, and solar cell. In particular, the majority of MoS_2 research have focused on the hydrogen evolution reaction. Herein, we explore the use of 2D-MoS_2 thin films as a potential elctrocatalysts for cathodic reaction of RED. For this purpose, the 2D-MoS_2 thin films was directrly coated on the surface of 2D-carbon structure, such as graphene and graphite paper. Our previous study reported the direct synthesis of MoS_2 on the surface of 1D-carbon structure, such as carbon nanotube and carbon fiber paper, and its RED application.[2] The 2D-MoS_2/carbon hybrid electrodes shows higher power density than as-received carbon electrodes, and their performance was similar to that of Pt-based carbon electrodes.

Keywords: Molybdenium disulfide, reverse electrodialysis, graphene, graphite thin film,

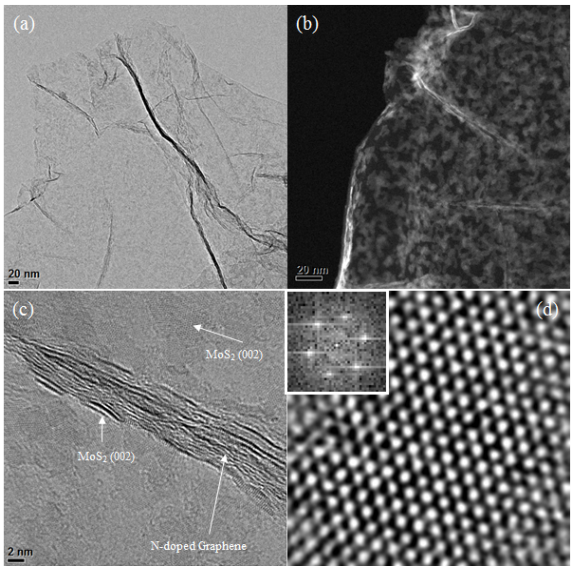

Figure 1: (a) TEM, (b) STEM, (c and d) HRTEM images of 2D-MoS_2/graphene hybrid structures. The inset of (d) is the FFT parrten of 2D-MoS_2.

References:

1. Tufa, R. A., Pawlowski, S., Veerman, J., Bouzek, K., Fontananova, E., Profio, G., Velizarov, S., Grespo, J. G., Nijmeijer, K., Curcio, E. (2018) Progress and prospects in reverse electrodialysis for salinity gradient energy conversion and storage, *Appl.Energy*, 225, 290-331.
2. Jeong, N., Kim, H., Kim, W., Choi, J., Han, J., Nam, J., Hwang, K., Yang, S., Jwa, E., Kim, T., Park, S., Seo, Y., Kim, S. (2019), Uniform coating of molybdenum disulfide over carbon substrates and its electrochemical application, *Chem. Eng. J.*, 356, 292-302.

Adlayer-free, single crystal graphene grown on large-area Cu(111) foil

Meihui Wang,[1,2] Da Luo,[1] Youngwoo Kwon,[1] Rodney S. Ruoff[1,2,3,4*]

[1] Center for Multidimensional Carbon Materials (CMCM), Institute for Basic Science (IBS), Ulsan, Rep. of Korea
[2] Department of Chemistry, Ulsan National Institute of Science and Technology (UNIST), Ulsan, Rep. of Korea
[3] School of Materials Science and Engineering, Ulsan National Institute of Science and Technology (UNIST), Ulsan, Rep. of Korea
[4] School of Energy and Chemical Engineering, Ulsan National Institute of Science and Technology (UNIST), Ulsan, Rep. of Korea

Abstract:
We have grown single crystal graphene that is 'adlayer-free single layer' (the graphene film is pure single layer without any adlayer patches at all) on home-made Cu(111) foils, in a relatively wide synthesis window of H_2/CH_4 ratios and CVD pressures. The graphene has long parallel "fold" regions that have an average width of about ~80-100 nm and are up to a centimeter or so in length, and that are separated by about ~20-50 μm, and is everywhere epitaxial with the Cu(111) substrate. We studied the structure of these folds and also their influence on electron and hole transport in graphene field-effect transistors (GFETs).
In contrast, on as-received commercial polycrystalline Cu foils under the same growth conditions, graphene films with adlayers are always obtained. Through time-of-flight secondary ion mass spectrometry depth-profiling and combustion anaylysis of the Cu foils, we discovered that it is the carbon contaminants inside the foils that lead to adlayers. After removing the carbon dissolved inside the polycrystalline Cu foils by annealing in a hydrogen atmosphere, adlayer-free polycrystalline graphene film was achieved on such polycrystalline Cu foils. The presence of adlayers and grain boundaries in the polycrystalline graphene, and graphene folds in the single crystal graphene, in the channel region of the GFETs (folds orthogonal to the long axis of the chanel region) were observed to significantly decrease the mobility of graphene. By patterning GFETs with the channel parallel to graphene folds, and specifically within the region lying between two adjacent folds in the single crystal graphene film (which eliminates the effect of adlayers, grain boundaries, and graphene folds), high performance devices with mobility values of around 1.0 x 10^4 $cm^2V^{-1}s^{-1}$ for both holes and electrons were obtained.

Keywords: monolayer graphene, CVD, Cu(111) foil, single crystal, adlayer-free, folds.

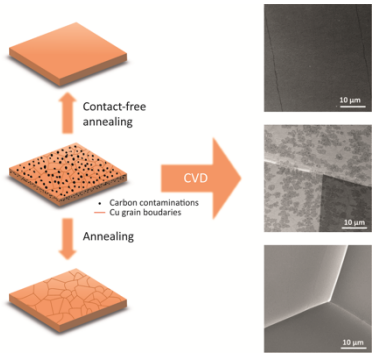

Figure 1: Graphene films grown on Cu foils (top—Cu(111); middle and bottom—polycrystalline copper foil). Adlayers do not appear if there is no carbon inside the Cu foil.

References:

1. Jin, S., Huang, M., Kwon, Y., Zhang, L., Li B., Oh, S., Dong, J., Luo, D., Biswal, M., Cunning, B., Bakharev, P., Moon, I., Yoo, W., Camacho-Mojica, D., Kim, Y., Lee, S., Wang, B., Seong, W., Saxena, M., Ding F., Shin, H., Ruoff, R. (2018), Colossal grain growth yields single-crystal metal foils by contact-free annealing. *Science.*, 362 (6418), 1021-1025.
2. Huang, M., Biswal, M., Park, H., Jin, S., Qu, D., Hong, S., Zhu, Z., Qiu, L., Luo, D., Liu, X., Yang, Z., Liu, Z., Huang, Y., Lim, H., Yoo, W., Ding, F., Wang, Y., Lee, Z., Ruoff, R. (2018), Highly oriented monolayer graphene grown on a Cu/Ni(111) alloy foil, *ACS Nano*., 12 (6), 6117-6127.

Acknowledgement

This work was supported by the Institute for Basic Science (IBS-R019-D1).

Crystalline and Uniform ZrO_2 by Atomic Layer Deposition on Atmospheric Plasma Treated Graphene

Jeong Woo Shin[1,*], Myung Hoon Kang[2], Seongkook Oh[1], Byung Chan Yang[1], Dohyun Go[1], Tae Hoon Lee[2], and Jihwan An[1]

[1] Department of Manufacturing Systems and Design Engineering (MSDE), Seoul National University of Science and Technology (SeoulTech), Seoul 01811, Republic of Korea
[2] Department of Electrical Engineering, Kwangwoon University, Seoul 01897, Republic of Korea

Abstract:
Graphene has the advantages of excellent electrical properties, thermal and mechanical properties. It is important to deposit a uniform high-k dielectric film on the graphene surface in order to fabricate a graphene based device. However, atomic layer deposited (ALD) dielectric films deposited on the graphen surface have noncontinous and noncrystalline film properties owing to the inert surface of graphene. Therefore the functionalization technique on the graphene surface while minimizing degration of the graphene surface is needed. Here, we demonstrate the crystalline and uniform high-k dielectric film (ZrO_2) deposition on the surface of graphene by atmospheric oxygen plasma treatment at the relatively low temperature of 150℃. The damages of graphene surface is minimized and a uniform thin film is deposited without additional seed layer by using atmospheric plasma with low ion energy. Based on the Raman analysis, defects on functionalized graphene surface are considered to be defects of dangling bond type. Also, the surface XPS analysis of functionalized graphene shows that C-O and C(O)O bonds are formed on the graphene surface. As a result, the ZrO_2 thin films on functionalized graphene is covered with fine grains forming a dense layer. Also, the ZrO_2 thin films with relatively high crystallinity of the tetragonal phase are deposited on the plasma treated graphene despite the deposition at a low temperature of 150 ℃.

Keywords: Graphene, Atmospheric Plasma Treatment, ZrO_2, Functionalization, Atomic Layer Deposition

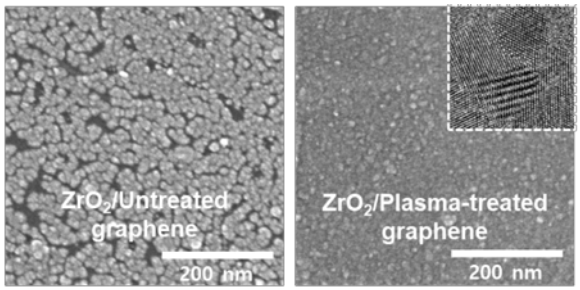

Figure 1: SEM and TEM images of ZrO_2 films on the untreated and plasma treated graphene (10passes).

References:

1. Schwierz F,Nat. Nanotechnol (2010) 5,487–96.
2. Lee C et al., Science (2008) 321, 385–8
3. Yan F et al., Adv. Healthc Mater (2014) 3, 313–31
4. Eckmann et al., Nano Lett (2012) 12, 3925–30
5. Kukli K et al., Journal of Applied Physics (2002) 92, 1833-40

Temperature Dependence of optical properties of WS_2 by Spectroscopic Ellipsometry

H. T. Nguyen[1], T. J. Kim[1], H. G. Park[1], V. L. Le[1], X. A. Nguyen[1], W. Lee[1], D. H. Koo[2], C.-H. Lee[2], Y. D. Kim[1,*]

[1] Kyung Hee University, Department of Physics, Seoul, Korea
[2] Korea University, KU-KIST Graduate School of Converging Science & Technology, Seoul, Korea

Abstract:
Transition-metal dichalcogenide (TMDC); MX_2 (M= Mo, W; X=S, Se) materials have emerged as a new class of semiconductors that display distinctive properties related to their low dimensionality. Among these TMDC materials, WS_2 has been a subject of great interest. Besides common characteristics of TMDC family ie. van der Waals layered structure, indirect-to-direct bandgap transition in the monolayer regime, spin-valley coupling, WS_2 also constitutes a high quantum yield in 2D system, and can be synthesized on a large area by chemical vapor deposition, opening various potential applications [1,2]. To properly design and understand 2D optoelectric device's function correctly, the optical constants of monolayer WS_2 are needed. Although there are a few studies on the dielectric functions, systematic study on temperature dependence of critical points (CPs) of monolayer WS_2 has not been reported so far.
In this work, we determined ε of monolayer WS_2 from 0.8 to 6.42 eV at temperatures from 41 to 325 K using spectroscopic ellipsometry. The CP energies were determined from standard lineshape analysis of numerically calculated second derivatives of ε with respect to energy. A lot of novel CPs are distinguished at low temperature. Especially, by carefully examining the region near 2 eV, the existence of another new CP at the shoulder of the A-exciton peak was diagnosed. The B-exciton structure also shows a significantly asymmetric lineshape, indicating contributions of two CP structures. At low temperature, blue shifts and sharpening of the CPs structure in WS_2 are also shown as results of the reduced lattice constant and electron-phonon interaction (Fig. 1). These results will be useful for physical understanding and application for the device based on WS_2.

Keywords: Transition metal dichacolgenide, Tungsten disulfide, Spectroscopic Ellipsometry, Dielectric function, Critical points, Temperature dependence

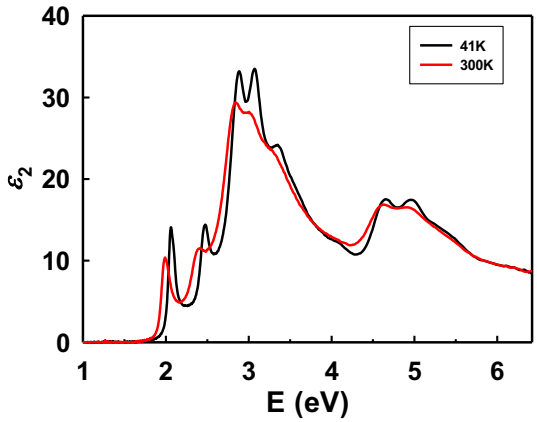

Figure 1: Imaginary parts of the ε spectra of WS_2 at 41 (solid line) and 300 K (dashed line)

References:

1. Zhang, Y., et al. (2013), Controlled Growth of High-Quality Monolayer WS2 Layers on Sapphire and Imaging Its Grain Boundary, *ACS Nano,* 7, 8963-8971.
2. Kim, M. S., et al. (2016), Biexciton Emission from Edges and Grain Boundaries of Triangular WS_2 Monolayers, *ACS Nano*, 10, 2399-2405.

A Graphene-Gated Carbon Nanotube Electron Emitter for Digital X-ray Tubes with High-Spatial Resolution

H. Jeon[1,2], E. Go[1,2], J.-W. Lee[1,2], Y. Ahn[1,2], S. Park[2], J.-W. Kim[2], J.-T. Kang[2], J.-W. Jeong[2], K.N. Yun[2], J.-W. Yeon[2], S. Kim[2], and Y.-H. Song[1,2*]

[1]ETRI ICT School, University of Science & Technology, Daejeon, Korea
[2]Emerging Devices Research Group, ETRI, Daejeon, Korea

Abstract:
Graphene, an ultrathin two-dimensional carbon-material, has been received huge attention to various applications due to a great electrical- and thermal-conductivity, high electron transmittance, and a good mechanical strength [1]. One of the applications of recent interest is the use as an electron-transparent gate electrode in a field emission triode structure [2]. The graphene electrode can suppress the electric potential distortion between a cathode and a gate electrode and provides focused electron-beams (E-beams) for x-ray tubes, enhancing x-ray spatial resolution. We fabricated a graphene gate using multilayer graphene and applied it to carbon nanotube (CNT) field emission devices and analyzed converging of E-beams reaching at the phosphor plate [3]. In this study, we present a fully vacuum-sealed digital x-ray tube based on the graphene-gated CNT electron emitter. To optimize the geometric parameters of the x-ray tube, a finite element method was used to simulate the E-beam trajectories for a given structure. The vacuum-sealed digital x-ray tube consisted of metal electrodes and ceramic spacers and was fabricated through a high temperature brazing process. It is noted that thermal durability of graphene was attentively considered for vacuum sealing. The graphene gate was well preserved even after the high-temperature sealing, which is confirmed by its field emission characteristics, as shown in Fig. 1. The evaluation results of additional field emission properties and x-ray imaging will be reported at the conference.

Keywords: graphene, carbon nanotube, field electron emitter, gate, x-ray tube

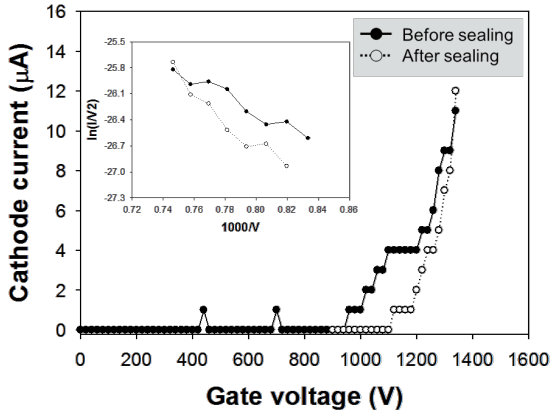

Figure 1: Field emission characteristics of the multilayer graphene-gated CNT emitters before and after the vacuum-sealing process of x-ray tube. The inset is their Fowler-Nordheim plots.

References:

1. Geim, A. K., Novoselov, K. S. (2007) The rise of graphene, *Nat. Mater.,* 6, 183-191.
2. Li, C., Cole, M. T., Lei, W., Qu, K., Ying, K., Zhang, Y., Robertson, A. R., Warner, J. H., Ding, S., Zhang, X., Wang, B., Milne, W. I. (2014), Highly Electron Transparent Graphene for Field emission Triode Gates, *Adv. Funct. Mater*., 24, 1218-1227.
3. Jeon, H., Choi, Y. C., Park, S., Kang, J.-T., Go, E., Lee, J.-W., Kim, J.-W., Jeong, J.-W., Song, Y.-H. (2017), Very large suspended graphene as an efficient electron-transparent gate electrode, *Carbon.*, 119, 371-377.

Comparison of Cytotoxicity of Black Phosphorus Particles against Three Different Types of Fibroblastic Cells

S.J. Song[1] , Y.B. Lee[1], M.S. Kang[1], Y.C. Shin[2], H.U. Lee[3], D.W. Han[1*]

[1] Pusan National University, Department of Cogno-Mechatronics Engineering, Busan, Republic of Korea
[2]Yonsei University, Department of Medical Engineering, Seoul, Republic of Korea
[3]Korea Basic Science Institute (KBSI), Advanced Nano-Surface Research Group, Daejeon, Republic of Korea
*nanohan@pusan.ac.kr

Abstract:
Black phosphorus (BP) as a two-dimensional (2D) material has recently emerged as novel nanomaterial. Biomedical applications such as imaging, optical and electronic using BP have been introduced through many studies, but there is not much research about biological safety. In this study, BP particles were prepared and their physicochemical properties were characterized by Fourier transform infrared spectroscopy (FTIR), Atomic Force Microscopy (AFM), and Zetasizer. The cytotoxicity of BP particles against three types of cells (i.e. NIH3T3 fibroblast cell line, primary cultured normal Human Dermal Fibroblasts and HT1080 fibrosarcoma cell) was evaluated by CCK-8 and LDH assay for metabilic activity and plasma membrane integrity, respectively. After treatment of BP, cell morphology was confirmed by optical microscopy. The BP particles did not observed cytotoxicity at low concentration. Therefore, it is expected that BP particles can be widely used in the biomedical applications, although further comprehensive studies must be conducted to evaluate the biocompatibility and biological effects of BP.

Keywords: 2D material, black phosphorus, cytotoxicity, CCK-8, LDH

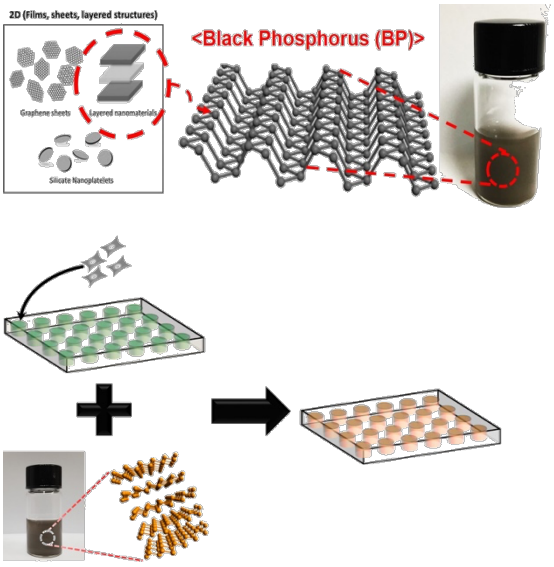

Figure 1: BP particles were prepared using a modified ultrasonication-assisted solution method. Three types of cells were treated with various concentrations of BP particles in culture medium (0 to 125 μg/mL) and then evaluated by CCK-8 and LDH assay.

References:

1. Lee, H. U., Park, S. Y., Lee, S. C., Choi, S., Seo, S., Kim, H., ... & Kim, H. S. (2016). Black phosphorus (BP) nanodots for potential biomedical applications. Small, 12(2), 214-219.
2. Latiff, N. M., Teo, W. Z., Sofer, Z., Fisher, A. C., & Pumera, M. (2015). The cytotoxicity of layered black phosphorus. Chemistry–A European Journal, 21(40), 13991-13995.

Structure-directing effect of single crystal graphene film on polymer carbonization and graphitization

Benjamin V. Cunning,[1] Bin Wang[1], Tae Joo Shin[2], Rodney S. Ruoff[13]

[1] Center for Multidimensional Carbon Materials, Institute for Basic Science (IBS), Ulsan 44919, Republic of Korea
[2] UNIST Central Research Facilities & School of Natural Science, Ulsan National Institute of Science and Technology (UNIST), Ulsan 44919, Republic of Korea
[3]Department of Chemistry, School of Materials Science and Engineering, School of Energy and Chemical Engineering, UNIST, Ulsan 44919, Republic of Korea

Abstract:
'Templating' (including epitaxial growth on crystal substrates and seeds) is used in the synthesis of well-ordered materials, yet has never been used to make high-quality graphite films. Current syntheses of graphite films have drawbacks, requiring either a combination of high temperatures and pressures ('highly oriented pyrolytic graphite', HOPG) or suffering from severe wrinkling and buckling of films due to thermal contraction mismatch between growth substrates and graphite (catalytic growth on metals). By incorporating large area single-crystal graphene in the interior of a polymer film, we discovered that heat-treatment results in 'structure-directing' by the graphene during polymer carbonization and graphitization. Electron microscopy reveals that at the early stages of carbonization, graphene induces the carbon atoms in its near vicinity to form oriented layers parallel to the graphene layer. At elevated temperatures, these layers develop further to form extended graphitic (002) planes parallel to the graphene surface. For the samples which were heat treated and graphitized, grazing incidence X-ray scattering reveals that graphene narrows the distribution of graphite grain orientations. Based on these results, we propose that graphene can act as a structure directing agent in both the carbonization and graphitization of polymer thin films, and may provide an approach to realize single crystal graphite films, perhaps in combination with established techniques such as stress recrystallization.

Keywords: structure directing, graphite, graphene, SU-8, polymer

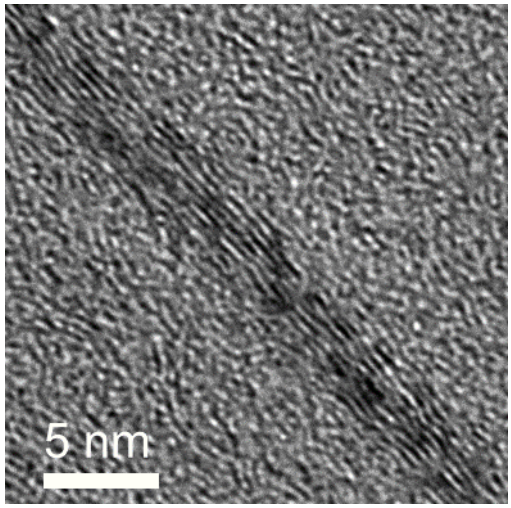

Figure 1: Cross-sectional transmission electron micrograph of bi-layer graphene embedded inside an SU-8 film heated to 1000 °C. There are additional graphitic lattice fringes present than the 2 expected for bi-layer graphene.

References:

1. Benjamin V. Cunning, Bin Wang, Tae Joo Shin and Rodney S. Ruoff, *Mater. Horiz.*, 2019, Advance Article. DOI: 10.1039/C8MH01507D

Aknowlegment:
This work was supported by IBS-R019-D1. Experiments at PLS-II 6D UNIST-PAL beamline were supported in part by the Ministry of Science and Technology (MSIT), Pohang University of Science and Technology (POSTECH), and UNIST Central Research Facilities (UCRF) in the Ulsan National Institute of Science and Technology (UNIST).

Mass produed high quality and large area CVD Graphene using Roll to Roll process

Jinwoo Sung,[1*] Youn-Su Kim,[1] Jin San Moon,[1] Won Bae Park,[1] Jonghyun Rho,[1] Myung Hee Jung[1]

[1] LG electronics, Materials and Production Engineering Research Institute, Seoul, Korea

Abstract:
Mass production of large area graphene grown on copper foil has been achieved using roll-to-roll chemical vapor deposition (CVD) system. The large area graphene of 400 mm in width were synthesized over rolling speed of 30 m/hr and double roll-to-rolls aligned in parallel were introduced to increase through-put, allowing high throughput (25 m^2 /hr). High quality of single-layered graphene was synthesized on Cu (111) surface rendered by the homogeneous tension in vertically loaded Cu film [1, 2]. The large area graphene having a uniform quality of mono-layer coverage in the manner of suppressed multi-dots and controlled grain size (5 ~ 200 um^2) demonstrated a sheet resistance of 240 Ω/ □ (without intentional doping) on plastic films. Moreover, the CVD grown graphene consisted of large grain (200 um^2) and minimized number of multi-dots (10 - 30 / 100 X 100 um^2) exhibited as high as 2500 cm^2 V/ s in mobility by Hall measurement under ambient condition [3].

Keywords: Thermal Chemical Vapor Deposition, Carbon, Graphene, Roll-to-Roll process, Hall measurement, Mobility, Sheet resistance, Raman Spectrum, Mass production, Quality control, Large area graphene.

Figure 1: Roll-to-roll CVD system for graphene mass production.

References:

1. Deng, B., Liu, Z., Peng, H. (2018), Toward mass production of CVD graphene films, *Adv. Mater.,* 30, 1800996.
2. Jo, I. et al. (2018), Tension-controlled single-crystallization of copper foils for roll-to-roll synthesis of high-quality graphene films, *2D materials,* 5, 024002.
3. Chen, J.-H., Jang, C., Xiao, S., Ishigami, M., & Fuhrer, M. S. (2008), Intrinsic and extrinsic performance limits of graphene devices on SiO2, *Nat. Nanotech.*, 3, 206-209.

SURFCOAT KOREA 2019

SURFCOAT KOREA 2019

GRAPHENE KOREA 2019

Book of Abstracts

March 27th – 29th, 2019
Songdo Convensia, Incheon, Korea

Organizers

SETCOR Conferences & Exhibitions

MESSE ESANG